CHARACTERISTICS OF MELTING HEAT TRANSFER IN HYBRID NANOFLUID FLOW WITH JOULE HEATING

By

Rabia Aftab

NATIONAL UNIVERSITY OF MODERN LANGUAGES
ISLAMABAD

June, 2023

Characteristics of Melting Heat Transfer in Hybrid Nanofluid Flow with Joule Heating

By

Rabia Aftab

A THESIS SUBMITED IN PARTIAL FULLFILMENT OF
THE REQUIREMENT FORTHE DEGREE OF

MASTER OF SCIENCE

In **Mathematics**

To

FACULITY OF ENGINEERING & COMPUTER SCIENCES

NATIONAL UNIVERSITY OF MODERN LANGUAGES ISLAMABAD

THESIS AND DEFENSE APPROVAL FORM

The undersigned certify that they have read the following thesis, examined the defense, are satisfied with overall exam performance and recommend the thesis to the Faculty of Engineering and Computer Sciences for acceptance.

Thesis Title: Characteristics of Melting Heat Transfer in Hybrid Nanofluid Flow with Joule Heating

Submitted By: Rabia Aftab

Registration # : 5/MS/Maths/S20

Master of Science in Mathematics (MS Maths)
Title of the Degree

Mathematics
Name of Discipline

Dr. Anum Naseem
Name of Research Supervisor

Signature of Research Supervisor

Dr. Sadia Riaz
Name of HOD (MATH)

Signature of HOD (MATH)

Dr. Muhammad Noman Malik
Name of Dean (FE&CS)

Signature of Dean (FE&CS)

Date: 13th June,2023

AUTHOR'S DECLARATION

I Rabia Aftab

Daughter of Aftab Alam

Registration #5/MS/MATH/S20

Discipline Mathematics

Candidate of **Master of Science in Mathematics** at National University of Modern Languages do here by declare that the thesis **Characteristics of Melting Heat transfer in Hybrid Nanofluid Flow with Joule Heating** submitted by me in fractional fulfillment of **MS Mathematics** degree, is my original work, and has not been submitted or published earlier. I also solemnly declare that it shall not, in future, be submitted by me for obtaining any other degree from this or any other university or institution. I also understand that if evidence of plagiarism is found in my thesis/dissertation at any stage, even after the award of a degree, the work may be cancelled and degree revoked.

Signature of Candidate: _____

Name of Candidate: Rabia Aftab

Date: 13th June, 2023

ABSTRACT

Title: Characteristics of Melting Heat Transfer in Hybrid Nanofluid Flow with Joule Heating

Hybrid nanofluids are accepted as more useful fluids than traditional nanofluids. There is no doubt that the hybrid nanofluids' mixed properties of two or more nanoparticles respond to better thermal conductivity. The concept is beneficial for improving the properties of the advanced kind of nanofluids than those made out of a single nanoparticle. The present study examines the magnetohydrodynamic hybrid nanofluid flow near a stagnation point over a stretching sheet of variable thickness. The heat transfer phenomenon is analyzed in the presence of Joule heating, melting heat transfer, viscous dissipation and heat generation/absorption. The fluid model is presented in the form of partial differential equations and in order to convert these partial differential equations into ordinary differential equations, appropriate similarity transformations are used. Bvp4c method, a numerical technique is employed to solve the ordinary differential equations and through this method, the effects of influential parameters on velocity, skin friction coefficient, temperature and Nusselt number are examined. A graphical comparison of basefluid (Gasoline oil), nanofluid (SWCNTs, gasoline oil), and hybrid nanofluid (SWCNTs, Ag and gasoline oil) is also carried out which provides the evidence of hybrid nanofluids' improved performance.

TABLE OF CONTENTS

LIST OF FIGURES

LIST OF TABLES

NOMENCLATURE

Symbols

x, y	Cartesian coordinates
u, v	Components of velocity
m	Flow behavior index parameter
μ_f	Dynamic viscosity of Gasoline Oil
v_f	Kinematic viscosity of Gasoline Oil
ρ_f	Density of Gasoline Oil
q_w	Wall heat flux
κ_f	Thermal conductivity of Gasoline Oil
α_f	Thermal diffusivity of Gasoline Oil
f'	Non-dimensional velocity
A	Velocity ratio parameter
θ	Non-dimensional temperature
T_w	Wall temperature
ϕ_1	SWCNT volume fraction
ϕ_2	Ag volume fraction
C_s	Heat capacity of solid surface

τ_w	Wall shear stress
U_o	Arbitrary constant
U_e	Free stream velocity
M	Melting parameter
CNTs	Carbon nanotubes
$SWCNTs$	Single wall CNTs
κ_{swcnt}	Thermal conductivity of SWCNTs
κ_{Ag}	Thermal conductivity of Gasoline oil
Ec	Eckert number
Ag	Silver
Nu_x	Nusselt number
C_{f_x}	Skin fraction coefficient
Ag	Silver
T_m	Surface temperature
U_w	Stretching velocity
δ	Heat generation and absorption
α	Wall thickness parameter
T_∞	Ambient temperature
$(C_p)_f$	Specific heat capacity

ACKNOWLEDGEMENT

I am thankful to Almighty ALLAH who has enabled me to learn and to achieve milestones towards my destination and His beloved Prophet Hazrat Muhammad (PBUH) who is forever a constant source of guidance, a source of knowledge and blessing for the entire creation. His teaching shows us a way to live with dignity, stand with honor and learn to be humble.

My acknowledgment is to my kind, diligent and highly zealous supervisor, Dr. Anum Naseem who supported me with her valued opinions and inspirational discussions. Her expertise, suggestions, comments and instructions greatly improved the worth of this research work. I am placing my earnest thanks to Dr. Anum Naseem. I am so grateful to work under the supervision of such a great person. My gratitude is to my honorable supervisor who took me to the apex of my academia with their guidance. In particular, Dr. Anum Naseem has always been supportive during all of my course work and kept encouraging me throughout the session at the National University of Modern Languages.

My strong gratitude is to my parents and my adored siblings who have been always real pillars for my encouragement and showered their everlasting love, care and support throughout my life. Humble prayers, continuing support and encouragement from my family are always highly appreciated.

Consequently, my plea is to Allah, the Almighty, the beneficial to keep showering His blessings upon me and strengthen my wisdom and knowledge.

DEDICATION

Dedicated to my exceptional family, friends and teachers whose tremendous support and cooperation led to this wonderful accomplishment.

Chapter 1

Introduction

The frequent classification of fluids (materials) in engineering and industries has sparked recent interest of analysts in their thermal properties. Owing to their inadequate thermal conductivity, common fluids, such as water, motor oil, kerosene, ethylene, fuel oil and others have a limited capacity to transfer heat. In order to raise thermal conductivity of ordinary fluids, nanosized particles with sizes ranging from 1 to 100 nm can be suspended in the fluid. Some examples of nanoparticles include metals, carbides, oxides and nitrides etc. Nanoparticles, nanofibers, nanotubes, nanowires, nanorods, nanosheets, or droplets can be dispersed in base fluids to produce nanofluids, a new class of fluids. To look at it in another way, condensed nanomaterials are dissolved in nanoscale colloidal solutions. When compared to conventional fluids including water or oil, nanofluids have been found to possess better convective heat transfer, thermal conductivity, thermal diffusivity and other thermophysical features. Nanofluids have special characteristics that render them potentially valuable in various heat transfer purposes, including microelectronics, engine cooling/vehicle thermal dissipation, household refrigerator, fuel cells and in heat exchangers. By combining two kinds of nanoparticles with a base fluid, one can produce an advanced type of nanofluid known as a hybrid nanofluid. Hybrid nanofluid is the one that simultaneously combines the thermal and physical properties of different materials. Better thermal conductivity than isolated nanofluids is the primary objective of hybrid nanofluids. They are designed to replace nanofluids due to a number of advantages, including a larger absorption range, a low pressure drop, a high thermal conductivity, smaller frictional losses and more pumping power. Hybrid nanofluids have been investigated for use in a variety

of applications, including solar collectors, photovoltaic thermal applications, electronic component thermal management, engine applications and car cooling and many others. The discovery of nanofluids [1] was modified by Turcu [2] and Jana [3] by laying the foundations for hybrid nanofluids. Suresh *et al.* [4] carried out the experiments, through an evenly heated circular tube containing a hybrid nanofluid, whereas laminar forced convection transfer and pressure drop properties were inspected. As a result of dispersing manufactured hybrid particles in deionized water or alumina-copper/water, hybrid nanofluids were prepared. Labib *et al.* [5] used the two-phase mixture model to examine the hydrodynamic and thermal performance of laminar forced convection hybrid nanofluid inside a tube that was uniformly heated. The two oxides with basefluid investigated were Al_2O_3/water and Al_2O_3/Ethylene glycol. Convective heat transfer performance has been evaluated in relation to the impact of using base fluids. Madhesh *et al.* [6] investigated the behavior of a hybrid nanofluid moving through a tubular heat exchanger in terms of heat transmission. In this study, the effects of forced convection's thermal characteristics, thermal conductivity and heat transfer coefficient were examined. The creation of energy-efficient heat-transfer machinery depends on the thermo fluid's ability to transport heat. However, conventional working fluids with low heat transfer properties include water, ethylene glycol and engine oil. In this context, enhanced heat transfer fluids are highly sought out due to their improved heat transfer properties. Major steps were taken by Esfe *et al.* [7] in introducing hybrid nanofluid. They concentrated on improving basefluid's thermal conductivity. Despite the advances made in the study of hybrid nanofluids, no reliable model has been put out that can anticipate how well these nanofluids conduct heat. Innovative fluids, i.e., hybrid nanofluids have quickly succeeded conventional heat transfer fluids in recent years due to their improved heat transfer and flow properties. The use of nanofluids in thermal management systems improves heat transmission while simultaneously reducing heat exchanger size. Several scientists recently explored the performance of heat exchangers using hybrid nanofluids. The thermal conductivity of nanofluids is one of the factors contributing to better heat transfer. In light of this, Yaseen *et al.* [8] explored the heat transfer properties of both the hybrid nanofluid and MHD squeezing flow between the parallel plates. The thermal radiation, magnetic field, heat source/sink, porous medium and suction/injection factors were used to evaluate the heat transport phenomenon. The upper plate was considered to be moving and the bottom plate

was stretching with a linear velocity. Huminic *et al.* [9] developed new hybrid nanoparticle clusters with various iron-based and silicon nanophases to boost the thermal conductivity of the base fluid. Using a sinusoidal hairpin heat exchanger and induced convection, Li *et al.* [10] chose to study the hydrothermal and irreversibility characteristics of a hybrid nanofluid. XRD, TEM and HR-TEM analyses were performed on the liquid aggregates that were produced utilizing the pyrolysis laser technique. Through the use of artificial neural networks, Rostami [11] examined the thermal properties of hybrid nanofluid. Shoaib *et al.* [12] computed the MHD hybrid nanofluid flow caused by rotating disc with the effects of heat generation/absorption and thermal slip.

Magnetohydrodynamics is an intriguing subfield of physics in which fluid dynamics using magnetic influences is analyze. The term magnetohydrodynamics is derived from the words magneto (which suggests a magnetic field), hydro (which means water) and dynamics (which means movement). The study of magnetic characteristics and behavior of electrically conducting fluids is commonly known as magneto fluid dynamics or hydromagnetics. Plasma, liquid metal (such as mercury), seawater and electrolytes are all examples of magnetic fluids. The core assumption behind MHD is that the magnetic field can induce a current in a moving conducting fluid, polarizing the fluid and hence changing the magnetic field. Parsa *et al.* [13] investigated the steady and two-dimensional magnetohydrodynamic boundary-layer flow through a stretching surface with internal heat generation or absorption for an electrically conductive fluid. In the transverse direction, a steady magnetic field was also applied. Ashorynejad *et al.* [14] used the lattice Boltzmann method to study the natural convection heat transport of an Al_2O_3, CuO and water based hybrid nanofluid inside an open curved space due to a constant magnetic field. The continuous flow and heat transmission of a hybrid nanofluid across a penetrable elongating wedge with magnetic field and radiation effects were studied by Waini *et al.* in [15]. Mabooda *et al.* [16] studied the flow of an unstable three dimensional, MHD stagnation point flow for hybrid nanoliquid exhibiting nonlinear radiation and also uneven heat generation. Naqvi *et al.* [17] investigated the properties of magnetohydrodynamic flow of nanofluids caused by radially stretching/extended disc with heat source/sink, chemical reaction and radiation which was considered non-uniform. In order to further study about the stability analysis, Zainal *et al.* [18] looked at an unsteady three-dimensional flow with magnetohydrodynamics and non-regular

Homann stagnation point. Yashkun *et al.* [19] examined the heat transfer characteristics of MHD hybrid nanofluid flow over the stretching sheet which is linear and contracting under the impact of thermal radiation.

The process by which electric current moves through a conductor and converts a portion of its energy into heat is known as Joule heating. In particular, when electric current flows through a solid or liquid with finite conductivity, electrical energy is transformed to heat via depletion layer inside the materials. Khan *et al.* [20] studied the heat transfer analysis on steady, MHD and axi-symmetric flow between two infinite stretching discs in the presence of viscous dissipation and Joule heating. The focus has been on acquiring the equations' similarity solutions for the flow field. An electrically conducting hybrid nanofluid's flow and thermal conduction above a horizontal penetrable stretching sheet with velocity slip were studied by Aziz *et al.* [21] . A uniform magnetic field is applied at an angle to the flow and the mathematical model of Maxwell non-Newtonian fluid was used to describe the hybrid nanofluid. The streamlined model considered the effects of thermal radiation with Joule heating. The two-dimensional, MHD fluid flow of a copper plus alumina/water hybrid nanofluid on an exponentially stretchable surface saturated within a porous media was explored by Yan et al. [22] in relation to the parameters of thermal slip, Joule heating and velocity slip. Khashi *et al.* [23] explored the flow properties with heat transmission of hybrid nanofluid caused by an axially stretchable surface involving the interactions of Joule heating, suction and MHD. To facilitate fluid suction from the wall bulk, the surface is permeable. Khan *et al.* [24] looked at the MHD and incompressible flow in two dimensions toward a translucent extended sheet with the existence of Joule heating, slip conditions and viscous dissipation. The impacts of convective conditions, mass suction and heat source/sink were additional factors taken into account. Mostafa *et al.* [25] analyzed how Joule heating affected hybrid nanofluid mixed convection flow and heat transport occur via an exponentially expanding/contracting surface. Xia *et al.* [26] explored the incompressible, viscous hybrid nanofluid flow in three dimensions with in a rotating frame. The base liquid was ethylene glycol and the nanoparticles were copper and silver. Between two parallel surfaces, with the bottom surface extending linearly, a constant magnetic field is applied. The important effects of viscous dissipation, Joule heating and nonlinear thermal radiation were taken into account.

Melting heat transfer is of enormous interest to scientists and engineers because of its significance in industrial processes. Melting phenomenon in flow of stretched surfaces is more essential because of its numerous uses in industrial processes such as magma solidification, semi-conductor preparation, thawing frozen ground procedure and so on. In this context, Hayat *et al.* [27] studied the melting heat transfer for Powell-Eyring fluid near the region of stagnation point and in the direction of a stretched linear sheet. Kumar *et al.* [28] talked about the analysis of heated, laminar liquid flow of a nanofluid towards a stretched sheet with the existence of melting heat transfer. Hayat *et al.* [29] studied the flow of Jeffrey material toward a nonlinear stretching surface with changing surface thickness with the occurrence of magnetohydrodynamic (MHD) and stagnation point. Melting heat transfer, viscous dissipation and internal heat generation were used to study the properties of heat transport. A Jefrey fluid flow was considered by Hayat *et al.* [30] using magnetohydrodynamics and a stagnation point flow towards a nonlinear stretching surface. With the already applied factors, internal heat generation, viscous dissipation and the melting heat transfer process were employed to evaluate the heat transfer qualities. The thermal properties were investigated using the melting boundary condition for homogeneous-heterogeneous reactions in hybrid nanofluid flow by Hussain *et al.* [31] under the influence of temperature-dependent stiffness, magnetohydrodynamics and mixed convection. A flexible cylinder is what causes the flow of fluid. Thermal radiation, a heat source and viscous dissipation were used to examine the processes of heat transfer. The study employed a straightforward isothermal model to regulate solute concentration.

The stagnation point is a point at which fluid velocity approaches to zero on the surface of a material which has been plunged in a flowing fluid. Stagnation point flow has its plentiful applications including wire drawing, cooling of electronic devices by fans, polymer extrusion, cooling of nuclear reactors, drawing of plastic sheets and several hydrodynamic procedures that are carried out in engineering applications. The stagnation point flow of nanofluids due to its extensive applications in local cooling/heating processes has gained the interest of many academics, especially in the nuclear and electrical device sectors. Yousefi *et al.* [32] studied the continuous generic stagnation-point flow of an aquatic titania-copper hybrid nanofluid past a rotating disk with sinusoidal variations. Nadeem *et al.* [33]. looked at the motion of a hybrid nanofluid around a cylinder in three dimensions near its stagnation point. Fluid flow was

considered in the presence of thermal slip effects. Rostamia *et al.* [34] used a hybrid nanofluid containing aluminium oxide and silicon dioxide nanoparticles with water as the base fluid to analytically model the stable linear motion. MHD boundary layer mixed convection flow of a hybrid nanofluid at the stagnation point on a stretchable flat plate was studied. Waini *et al.* examined the stagnation point flow flowing towards a squeezing cylinder for a nanofluid [35]. Water is employed as the base fluid and hybrid nanoparticles made of copper and alumina were utilized.

Heat transfer rates are influenced by viscous dissipation, which acts as an energy source and alters temperature distributions. Depending on whether the sheet is being heated or cooled, viscous dissipation has different effects. To be more precise, a few real-world uses for flow across a stretching sheet include cooling of metallic sheets or electronic chips, cooling of heat-treated materials moving between feed rolls and wind-up rolls, or materials made via extrusion. Arafa *et al.* [36] investigated the effect of viscous dissipation on the mixed convection flow of a micropolar fluid over an exponentially stretching sheet. Micropolar boundary-layer flow and the characteristics of heat transfer for a heated exponential stretching sheet being cooled by the mixed convection flow were examined. Megahed. *at al.* [37] studied the cumulative impact of viscous dissipation and Newtonian heating on boundary layer flow over a moving flat plate for a kind of water-based Newtonian nanofluids comprised of metallic or nonmetallic nanoparticles such as titania and copper. An incompressible third-grade nanofluid's flow over a stretching surface in two dimensions was studied by Sabi *et al.* [38]. When Newtonian heating and viscous dissipation were present, the influence of thermophoresis and Brownian motion was taken into account. Johnson *et al.* [39] examined the findings of the numerical analysis of forced convection between parallel plate channels during steady-state thermal development under the impact of viscous dissipation. For the momentum equation, the Darcy-Forchheimer-Brinkman model is employed.

Significant heat generation or absorption effects could change the temperature distribution, thus heat transfer rate in specific contexts involving semiconductors, electronic devices and nuclear reactors, so it is studied by many researchers. Chu *et al.* [40] analyzed continuous, laminar free convection flow across a vertical porous surface in the presence of a magnetic field, along with heat generation or absorption. In another study, Chu *et al.* [41] studied unsteady

heat and mass transfer and mixed convection flow over a vertical permeable rotating cone with a time-dependent angular velocity in the presence of a magnetic field and heat generation or absorption effects. On the surface of the cone, fluid suction or injection is thought to happen. An implicit, iterative finite-difference method was used to numerically solve the coupled nonlinear partial differential equations. Saleem *et al.* [42] presented the effects of changing viscosity, thermophoresis and heat generation or absorption on hydromagnetic flow and analysis of heat and mass transfer was performed over a stretching surface. Tahar *et al.* [43] researched on boundary layer flow in two dimensions along a moving semi-infinite vertical plate. The plate was moving in the direction of the flow at a constant speed. The analysis took into account the impact of internal heat generation or absorption.

1.1 Thesis Organization

In this thesis, our study in six chapters is summarize..

Chapter 1 is an introductory chapter in which the foundations of different concepts are discussed.

A detailed and comprehensive literature review based on the recent carried out research is presented in chapter. 2.

Chapter. 3, includes all the basic definitions and concepts that are inevitable for the investigation of the proposed work.

In chapter. 4, the stagnation point fluid flow of hybrid nanofluid flowing over a variable thicked sheet is discussed. The stretching of the variably thickened sheet induces the flow. The melting heat transfer and the significant impact of viscous dissipation also control the heat transfer process. The problem is modelled as partial differential equations system that are transformed into a system of ordinary differential equations via similarity transformations. A numerical method, bvp4c technique assists to solve these resultant equations. The temperature, velocity and in addition, Nusselt number and skin friction coefficient are examined through plots.

Though chapter. 5, hybrid nanofluid (SWCNTs, Ag and gasoline oil) flow near a stagnation region when magnetohydrodynamics is involved was investigated. A variable thickened

stretching sheet is considered to maintain the fluid flow. Additionally studied are the effects of viscous dissipation, melting heat phenomenon, Joule heating and heat generation/absorption. The momentum and energy equations are reconstructed as ordinary differential equations with the aid of appropriate transformations. Then using bvp4c technique, this system of ordinary differential equations is solved. The impacts of key parameters for velocity, temperature, skin friction coefficient and Nusselt number are explored graphically. Furthermore, a comparison study with basefluid, nanofluid and also hybrid nanofluid is also carried out to highlight the hybrid nanofluid effectiveness.

The last chapter gives the conclusions of the research work carried out and provides few proposed studies.

Chapter 2

Literature Review

To improve thermophysical features of nanofluids, hybrid nanofluids are created by combining basefluid with two distinct kinds of nanoparticles. When the deformable sheet is stretched in its own plane at a velocity proportionate to the distance from the stagnation-point, Muneerah *et al.* [44] studies steady two-dimensional stagnation-point flow of an incompressible viscous electrically conducting fluid over the flat sheet. It is demonstrated that when the free stream velocity is less than or larger than the stretching velocity, the velocity at a place reduces or increases with an increase in the magnetic field. When the surface is maintained at a constant temperature, the temperature distribution in the flow is obtained. Jakeer investigates whether entropy is produced in an EMHD hybrid nanofluid at a stagnation point when slippage, heat, and viscous dissipation are present. Water with hybrid Ag-Cu nanoparticles is the fluid in the container. Safdar *et al.* [45] outlines current research on the synthesis, thermophysical properties, heat transport, pressure drop characteristics, potential applications, and difficulties of hybrid nanofluids. The results of the review indicated that correct hybridization might make hybrid nanofluids very promising for enhancing heat transfer, but many more studies are still required in the areas of preparation and stability, characterization, and applications to solve the difficulties. The nonlinear differential systems are converted into an ordinary differential system using the homotopy perturbation approach by using the appropriate self-similarity variables. Khan *et al.* [46] examined how buoyancy forces influence a hybrid nanofluid's behavior close to an area of stagnation in a saturated porous medium as it approaches a vertical plate. The effects of thermal radiation, nonlinear and unique activation energy on the axisymmetric rotating stag-

nation point flow of hybrid nanofluid were examined by Abbasi *et al.* [47]. Involving the base fluid and nanoparticles, the thermophysical characteristics of water and SWCNT/MWCNT were investigated. In order to manage energy costs, Muhammad *et al.* [48] examined the thermal efficiency of ethylene with Fe_3O_4 and SWCNT as hybrid nanoparticles and used an artificial neural network experimental data to model and investigate the temperature with nanoparticle volume fraction. Zainal *et al.* [49] examined the suction and buoyancy forces' effects to determine a hybrid nanofluid's squeezing flow and heat transfer across an elevated stretching sheet. Magnesium oxide and silver were two hybrid nanoparticles that were suspended in water to create a hybrid nanofluid. Hybrid nanofluids were inspected for their potential to improve heat transmission by Muneeshwaran et al. [50]. Khan *et al.* [51] studied the tiny stirring needle to analyze the flow of a bio-convective and chemically reactive hybrid nanofluid with viscous dissipation where the flow model was modified and dissipation and chemical reaction were both present. Ali *et al.* [52] explored the impact of a Cu-Al_2O_3, hybrid nanofluid for heat transfer and flow through a pore-sized opening with heat flux and viscous dissipation effects. The investigation of diverse hybrid composites and hybrid nanofluids, including their development and synthesis were discussed and in many thermal management applications, including heat pipes, heat sinks, heat exchangers and solar panels, the hydrothermal behavior of hybrid nanofluids were examined. Chu *et al.* [53] presented model-based comparative research of particle shape effects in the flow of an unstable hybrid nanofluid affected by magnetohydrodynamics among two infinite parallel plates. Waini *et al.* [54] investigated the hybrid nanofluid stagnation-point flow through a porous medium. The heat exchange properties and stagnation point flow of a second-grade hybrid magnetohydrodynamic nanofluid travelling through a convectively heated permeable shrinking/stretching sheet were investigated by Nadeem *et al.* [55]. For the MHD flow of Cu-Ag/H_2O-$C_2H_6O_2$ hybrid nanofluid across a stretchy Darcy-Forchheimer porous media, the effects of heat radiation and suction/blowing were taken into consideration by Jyothi *et al.* [56]. In order to increase the pace of heat transmission, hybrid nanofluid has been developed by Sulochana *et al.* [57] as a new class of nanofluid, distinguished by its thermal characteristics and prospective applications. The major objective of the current analysis is to compare the behaviour of conventional nanofluid and newly developed hybrid nanofluid in the presence of rotation, porous medium, and an exponentially stretched surface while taking into account

the micropolar fluid theory. Salam *et al.* [58] describes microscale that have improved heat transfer. This analysis takes into account earlier research that sought to enhance heat transmission both with and without hybrid nanofluids. Results from experiments and computations using hybrid nanofluids. Additionally, multiple flow regimes and working fluids are used with backward-facing steps (BFS), forward-facing steps (FFS), and microscale steps. His research shows that using hybrid nanofluids as a working fluid results in an increase in heat transfer and that the coefficient of heat transfer improves as hybrid nanofluid nanoparticle quantities and concentrations rise. This study highlights research on hybrid nanofluids over BFS and FFS, describes different nanoparticles employed in thermal conductivity, and illustrates an increase in heat transfer rate. Rostami *et al.* [59] examined the usage of a two-stage approach for creating water-based (Al_2O_3-SiC-TiO_2) hybrid nanofluids. For this investigation, Al_2O_3-SiC-TiO_2 nanoparticles make up an equal volume fraction of each sample of hybrid nanofluids. A 35–40 °C temperature range and a volume fraction range of (0.01-0.1%) were used to analyze the results for the dynamic viscosity of ternary hybrid nanofluids. The examination was expanded to include an EDX analysis and a study of morphological characterization using SEM images for ternary hybrid nanofluid with a volume fraction of 0.1%. Additionally, based on the validated results, a novel correlation was predicted for the dynamic viscosity of ternary hybrid nanofluid and also compared with the pertinent literatures. The findings showed that low vol. fractions have little effect on the viscosity of ternary hybrid nanofluids and that rising vol. fractions play a significant role in raising the internal resistance of fluid. In accordance with the obtained data, the margin of deviation within the intervals of 2.6% was found to have the best relative consistency within 0.1% vol. fraction. The thermal conductivity of nanofluids is one of the factors contributing to better heat transfer. In light of this, Yaseen *et al.* [60] explored the heat transfer properties of both the hybrid nanofluid and MHD squeezing flow between the parallel plates. The thermal radiation, magnetic field, heat source/sink, porous medium and suction/injection factors were used to evaluate the heat transport phenomenon. The upper plate was considered to be moving and the bottom plate was stretching with a linear velocity.

The physical-mathematical framework of the evolution of magnetic fields within fluids that conduct electricity is the subject of magnetohydrodynamics (MHD). The essential idea behind MHD is that magnetic fields have the ability to create currents in moving conductive

fluids. Hayat *et al.* [61] studied the flow of Jeffrey material toward a nonlinear stretching surface with changing surface thickness at the magnetohydrodynamic (MHD) stagnation point. Melting, viscous dissipation, and internal heat generation are used to study the properties of heat transport. Considered is an applied magnetic field that is not uniform. The problem formulation uses boundary-layer and low magnetic Reynolds number approximations. Using the proper transformations, the momentum and energy equations are both transformed into the non-linear ordinary differential system. For the ensuing issues, convergent solutions are computed. The effects of several relevant parameters on the distributions of velocity and temperature are carefully examined. Additionally, the rate of heat transfer is calculated and examined. Hussain *et al.* [62] evaluated the features of hybrid nanofluid flow involving heat exchanges with thermal radiations in the context of magnetohydrodynamics. The bvp4c approach was used to numerically solve the flow problem under consideration. Multiple regression model was used by Neethu *et al.* [63] to analyze the flow of an evolvable MHD hybrid nanofluid across an exponentially stretched sheet with radiation and dissipation effects. Wahid *et al.* [64] explored the magnetohydrodynamic hybrid nanofluid flows on a transparent porous plate with mixed convection and radiation. The numerical analysis of the highly ionized MHD Williamson hybrid nanofluid's with non-Fourier mass and heat transfer was presented by Salmi et al. [65]. For a moving flat plate, a hybrid nanofluid was studied by Mehdi *et al.* [66] with the occurrence of magnetohydrodynamic and spatial fractional heat transport. For an incompressible and hydromagnetic hybrid nanofluid with heat and mass transport close to a nonlinearly permeable stretching sheet, Kayalvizhi *et al.* [67] looked into nonlinear radiation, Ohmic dissipation and velocity slip. Additionally, consideration is given to the impacts of heat generation and absorption, chemical processes, convective mass and heat condition. Naqvi *et al.* [68] investigated the dynamics of bio convective, MHD hybrid nanofluid flow across an exponentially growing surface with in a saturated porous media. Chemical reaction, thermal radiation, heat generation/absorption and porosity of the surface have all been considered as significant factors. Vijatha *et al.* [69] discussed the MHD boundary layer phenomenon of Casson and Williamson hybrid nanofluids on a stretching cylindrical surface using ethylene glycol and water as the base fluids and Cu-Al_2O_3 as the nanoparticles. Azam *et al.* [70] investigated the enhancement in thermal properties of hybrid nanofluid by studying the magnetohydrodynamic, three dimensional flow

of hybrid nanofluids that are only partly ionized across a stretched sheet. The heat and mass flux model of Cattaneo- Christov heat flux was used in the flow model. Magnetohydrodynamic Darcy-Forchheimer flow of a nanofluid in a hybrid form across an extended permeable sheet with viscous dissipation was studied by Johnson *et al.* [71]. Sequential radiation's effect on a revolving tiny needle in a MHD and Al-Cu/methanol hybrid nanofluid were investigated by Sulochana *et al.* [72]. By extending an inclined surface, Somroo *et al.* [73] looked at the performance of heat transmission and hybrid nanofluid flow. The impact of a magnetic field has been taken into account when studing the stretching surface. Khan *et al.* [74] studied the influence of viscous dissipation, Joule heating with heat generation and absorption for a slip flow of a nanofluid with inclined MHD and numerically analyzed the frictional drag and heat transfer

The practice of Joule heating plays chief role in many areas involving in industry and engineering. Gangadhara *et al.* [75] examined the impact of Joule heating on the relationship between the properties of conventional and hybrid nanofluids. The viscous dissipation across an increasingly stretched surface was explained by the micropolar theory. Zainal *et al.* [76] analyzed the impact of heat generation and absorption on the magnetohydrodynamics (MHD) flow towards the bidirectional exponentially stretching/shrinking hybrid nanofluid sheet. Jyoth et al. [77] studied the results of Joules heating on the flow of a Casson hybrid nanofluid squeezed between two parallel plates. Sulochana *et al.* [78] observed the boundary layer properties of MHD flow of hybrid nanoliquids across a stagnation region with thermal radiation and heat source/sink effects. Khan *et al.* [79] looked at the MHD, incompressible flow in two dimensions towards a translucent extended sheet in the context of Joule heating, slip condition and viscous dissipation. The impacts of convective conditions, mass suction and heat source/sink were additional factors taken into account. Mostafa *et al.* [80] analyzed how a hybrid nanofluid's mixed convection flow and heat transport occur via an exponentially expanding/contracting surface. Ali *et al.* [81] analyzed to demonstrate heterogeneous-homogeneous chemical processes and magnetic field features of Al_2O_3, Cu-water based hybrid nanofluid flow across a stretching or stretching cylinder with Joule heating. Numerical research was conducted by Yang. *et al.* [82] for a hybrid nanofluid flow in three dimensions across a sheet that is stretching and shrinking. The investigation was done to determine how the Joule heating and magnetic field affect the velocity and temperature profiles. Additionally, the effects of suction were also scrutinized.

Khashie *et al.* [83] studied the MHD hybrid nanofluid flow and heat transmission for a rotating plate utilizing Joule heating. The base fluid for the analysis was water and a mixture of metal (Cu) and metal oxide Al_2O_3 nanoparticles was also utilized. Wahid *et al.* [84] provided an illustration of the magnetohydrodynamic, radiative hybrid nanofluid flow through slip effects and Joule heating for a cylinder with permeability and is being stretched. Wahid *et al.* [85] investigated the roles of viscous dissipation, melting heat phenomena and Joule heating in the magnetohydrodynamic (MHD) flow of an alumina-water nanofluid that were being forced by a shrinking sheet towards a stagnation point. Khan *et al.* [86] studied the influence of viscous dissipation, Joule heating with heat generation and absorption for a slip flow of a nanofluid with inclined MHD and numerically analyzed the frictional drag and heat transfer. Eid *et al.* [87] examined the impact of magnetic field, Joule heating, Hall current and nonlinear thermal radiation for a spinning hybrid Fe_3O_4/Al_2O_3 nanofluid over a stretched plate.

Due to numerous applications of melting heat transfer in various fields, it is emphasized in many studies. Features of heat transfer are usually described by the melting effect and viscous dissipation. Hayat *et al.* (2019) noticed the chemically reacting flow of carbon nanotubes (CNTs) over a stretchable curved sheet. The flow is initialized due to a stretched surface and a heat source was present. The vital interest of work was the heat phenomenon via melting heat transfer. Arshad *et al.* [88] reported the melting heat transfer and flow of carbon nanotubes (CNTs) undergoing chemical reaction over a flexible curved sheet while the flow was initiated due to a stretched surface. Song *et al.* [89] explained solutal Marangoni flow and thermal analysis of the Sutterby nanofluid that contains gyrotactic microorganisms and melting phenomenon were also taken into account. The flow was initialized by a stretched cylinder. The stagnation point flow of a water based hybrid nanofluid with heat transfer over a contracting/expanding wedge was explored by Kakar *et al.* [90] under the influence of melting heat exchange. The hybrid nanofluid stagnation point flow across a permeable stretchable sheet in case of melting heat transfer under the influence of thermal radiation was solved numerically by Kayalvizhi *et al.* [91]. Labib *et al.* [92] explored the problem involving melting heat phenomenon for a hybrid nanofluid flow exposed to a stretching wedge near a stagnation point. The use of a curved stretched sheet with a hybrid nanomatel (SWCNTs+CuO + Engine oil) was discussed by Muhammad *et al.* [93] where the melting phenomenon and flow features for

heat transfer were elaborated. Huminic *et al.* [94] examined the hybrid nanomaterial flowing through a porous Darcy-Forchheimer (D-C) medium that is confined by two infinite parallel walls .The upper wall presses down on the lower wall while the lower wall is fixed and flexible. Instead of using the conventional Fourier's heat flux, Cattaneo-Christov (C-C) heat flux is discussed. Nalivela *et al.* [95] considered melting heat transfer for a hybrid nanofluid flowing due to a stretching surface with magnetohydrodynamics and OHAM was employed to solve the approach for the analysis.

The study of stagnation point flow is beneficial in a variety of processes, including hydrodynamic processes, wire drawing, chilling of electronic devices, utilizing fans, polymers extrusion, chilling of nuclear reactors, etc. Mah *et al.* [96] Studied on the impact of viscous dissipation on entropy formation in water-alumina nanofluid forced convection in circular microchannels is described. For models with and without a viscous dissipation term in the energy equation, closed form solutions of the temperature distributions in the radial direction are derived using the first-law approach. The findings demonstrate that, when the viscous dissipation effect is taken into consideration, the heat transfer coefficient substantially decreases with nanoparticle volume fraction in the laminar regime of nanofluid flow in microchannel. In the second-law analysis, the relative entropy generation deviations of the two models for various Reynolds numbers and nanoparticle volume fractions are compared. The temperature distribution is considerably impacted when viscous dissipation is taken into account, and as a result, the formation of entropy associated with irreversible heat transfer is significantly increased. The rise in thermal conductivity and viscosity of the nanofluid, which results in an increase in heat transfer and fluid friction irreversibilities, respectively, is blamed for the increase in entropy generation caused by the increase in nanoparticle volume fraction. Contrary to common belief, which holds that nanofluids have an advantage over pure fluid and are associated with higher overall effectiveness from the aspects of first- and second-law of thermodynamics, the viscous dissipation effect shows that both thermal performance and energetic effectiveness for forced convection of nanofluid. Yousefi *et al.* [97] studied the continuous generic stagnation-point flow of an aquatic titania-copper hybrid nanofluid past a rotating disk with sinusoidal variations. Nadeem *et al.* [98]. looked at the motion of a hybrid nanofluid around a cylinder in three dimensions near its stagnation point. Fluid flow was considered in the presence of thermal slip

effects. Rostamia *et al.* [99] used a hybrid nanofluid containing aluminium oxide and silicon dioxide nanoparticles with water as the base fluid to analytically model the stable linear motion. MHD boundary layer mixed convection flow of a hybrid nanofluid at the stagnation point on a stretchable flat plate was studied. For relatively homogenous reactions, Zainal *et al.* [100] investigated the stagnation point flow of a Cu-Al_2O_3/water hybrid nanofluid caused by a stretching or contracting sheet with convective boundary conditions and magnetohydrodynamics. The flow and heat exchange over a stretching/shrinking surface at the constant magnetohydrodynamic stagnation point were theoretically and numerically explored in a hybrid nanofluid flow involving partial slip and viscous dissipation by Emad *et al.* [101]. Waini et al. [102] examined the stagnation point flow flowing towards a squeezing cylinder for a nanofluid.Water is employed as the base fluid and hybrid nanoparticles made of copper and alumina were utilized. The temperature-dependent circulation of a viscoelastic nanofluid through an extending cylinder in its stagnation zone was investigated by Adigun *et al.* [103]. The temperature-dependent circulation of a viscoelastic nanofluid through an extending cylinder in its stagnation zone was investigated by Adigun et al. [104]. Alphonsa et al. [105] looked at the effects of multiple slip in the presence of an effective magnetic field for flow of silver-blood nanofluid close to its stagnation point. Zainal *et al.* [106] investigated the heat transfer efficiency of Cu-Al_2O_3/H_2O in a stagnation point flow towards a surface that stretches/shrinks exponentially with viscous dissipation effect and with magnetohydrodynamics. Using proper similarity transformations, the differential equations involving the partial derivatives of dimensional functions were converted to a set of ordinary differential equations. Alphonsa *et al.* [107] looked at the effects of multiple slip in the presence of an effective magnetic field for flow of silver-blood nanofluid close to its stagnation point. Towards a vertically extended sheet, the stagnation point flow of an unstable compressible Casson hybrid nanofluid was examined by Abbas *et al.* [108]. Normal flow directions were applied to implement the Lorentz force where nonlinear radiation's impact was studied. Hybrid nanofluid unsteady flow across a horizontal cylinder that was extending or contracting near a stagnation point was studied by Zainal *et al.* [109]. Additionally, magnetic field implications on boundary layer flows are analyzed. In their study of the hybrid nanofluid flow at the stagnation point in a magnetic field, Ohmic dissipation and convective conditions over a disc that is radially shrinking, Yahaya *et al.* [110] analyzed the results. Towards a ver-

tical sheet, the stagnation point flow of an unstable compressible Casson hybrid nanofluid was examined by Abbas *et al.* [111]. Normal flow directions were applied to implement the Lorentz force where nonlinear radiation's impact was studied. Hybrid nanofluid unsteady flow across a horizontal cylinder that is extending or contracting near a stagnation point was studied by Zainal *et al.* [112].

Due to the significant temperature variations that are observed during high-speed polymer processing flows like injection molding or extrusion, viscous dissipation is of importance for a range of applications. Industrial applications like polymer processing flows and aerodynamic heating highlight the significance of the impact of viscous dissipation in hybrid nanofluids. Farooq *et al.* [113] investigated the suction and injection impact with viscous dissipation on entropy formation in a hybrid nanofluid (Cu-Al_2O_3-H_2O) boundary layer flow across a nonlinear radially expanding porous disc. The energy dissipation is introduced into the energy equation to account for the effects of viscous dissipation. This work employs the Tiwari and Das model. The flow and heat transfer analysis was carried out with the use of a modified version of the Maxwell Garnett (MG) and Brinkman nanofluid models. Emad *et al.* [114] theoretically and quantitatively explored the steady, magnetohydrodynamic, stagnation point flow and heat transfer of a hybrid nanofluid with partial slip and viscous dissipation over a stretching/shrinking surface. Roy *et al.* [115] investigated that the thermal radiation with viscous dissipation have an effect on heat transport and assisting and opposing flows of a hybrid nanofluid (Cu-Al_2O_3/water) around a circular cylinder. The convex and concave shape effects on the flow of a radiative hybrid nanofluid were being studied by Yaseen *et a*l. [116]. Additionally, the injection and suction of a hybrid nanofluid towards the surface of a sheet that was stretching or contracting was investigated. Aziz *et al.* [117] studied that in comparison to standard nanofluids, hybrid nanofluids have improved surface stability, diffusion and dispersion characteristics. The simplified model accounts for linear thermal radiation and viscous dissipation. In their research, Venkateswarlu *et al.* [118] found that hybrid nanofluids outperform regular nanofluids due to their superior thermal properties. His research examined the effects of hybrid nanofluid and radiative heating on a stretched porous sheet when viscous dissipation was involved. Nanoparticles of copper (Cu) and alumina oxide (Al_2O_3) were mixed in water to form a hybrid nanoliquid in this model. Fluid viscosity, together with natural convection

and viscous dissipation were introduced to the momentum and energy equations. Zainal *et al.* [119] investigated the heat transfer efficiency of Cu-Al_2O_3/H_2O in a stagnation point flow towards a surface that stretches/shrinks exponentially with viscous dissipation effect and with magnetohydrodynamics. Using proper similarity transformations, the differential equations involving the partial derivatives of multi-dimensional functions were converted to a set of ordinary differential equations. Magnetohydrodynamic (MHD) flow of hybrid nanofluid created by a nonlinear shrinking/stretching surface was demonstrated by Lund *et al.* [120], along with heat transfer features and a stability investigation. The porosity factor and energy dissipation were added to the momentum and energy equations to investigate how high temperature affects the porous surface. Famakinwa *et al.* [121] examined the viscous dissipation implications and heat radiation on a compressible, unstable flow that squeezes between two aligned edges.

Heat generation or absorption phenomenon is of immense interest to many researchers. Hayat *et al.* [122] inspected the outcomes of heat generation and absorption, magnetohydrodynamics (MHD) and the influence of nanoparticle volume fraction for the behavior of hybrid nanofluid past a stretched surface. Another model of thermophysical characteristics was engaged by Tayebi *et al.* [123] to explore the effects of the Lorentz force on a three-dimensionalized flow for a stretched sheet. Natural convection, internal heat generation or absorption and entropy formation in a circular elliptic cylinder packed with a hybrid nanofluid were examined. Yaseen *et al.* [124] explored the heat transfer properties of both the hybrid nanofluid and MHD squeezing nanofluid flow between the parallel plates. The thermal radiation, magnetic field, heat source/sink, porous medium and suction/injection action were used to evaluate the heat transport phenomenon. In the current model, the upper plate is moving and the bottom plate was stretching with a linear velocity. Naqvi *et al.* [125] investigated the properties of magnetohydrodynamic flow of nanofluids caused by radially stretching/extended disc with heat source/sink, chemical reaction and radiation which is non-uniform. Shoaib *et al.* [126] computed the MHD hybrid nanofluid flow caused by rotating disc with the ability to absorb heat and undergo thermal slip. Zainal *et al.* [127] analyzed the impact of heat generation and absorption on the magnetohydrodynamics (MHD) flow towards the bidirectional exponentially stretching/shrinking hybrid nanofluid sheet. Jyoth *et al.* [128] studied the results of source/sink on the flow of a Casson hybrid nanofluid squeezed between two parallel plates. Sulochana *et*

al. [129] observed the boundary layer properties of MHD flow of hybrid nanoliquids across a stagnation region with thermal radiation and heat source/sink effects. Khan *et al.* [130] studied the influence of viscous dissipation, Joule heating with heat generation and absorption for a slip flow of a nanofluid with inclined MHD and numerically analyzed the frictional drag and heat transfer. Krishna *et al.* [131] explored the Newtonian heating, heat generation/absorption and chemical reaction on free convective Casson hybrid nanofluid through permeable vertical plate with oscillations. Hameed *et al.* [132] analyzed the significance of viscous dissipation, heat generation or absorption and magnetic field for a Casson hybrid nanofluid flowing towards a nonlinear stretching surface. When studying the effects of viscous dispersion and heat sink on the free convection flow with unstable MHD on the radiating as well as chemical reactive Casson hybrid nanofluid through a vertical plate that oscillates indefinitely immersed in porous material, Khrishna *et al.* [133] explored useful results. Unyong *et al.* [134] examined the hybrid nanofluid flow across a stretching sheet subjected to a magnetic field at an angle, partial slip and thermal radiations.

The earlier works and importance of magnetohydrodynamic hybrid nanofluid flow provides inspiration for the researchers to further analyze the fluid properties under different assumptions. To the best of author's knowledge, no work has been carried out on the magnetohydrodynamic stagnation point flow of a hybrid nanofluid under the effects of Joule heating and viscous dissipation, where the flow is induced due to a variable thicked stretching sheet. With the use of similarity transformations, the governing equations are simplified into nonlinear ODEs and bvp4c method is incorporated to solve the fluid problem. The plots for velocity, temperature and also concentration profiles are exhibited through the same method. It is assumed that the existing analysis will lead to useful results that can be applied in engineering and industrial purposes.

Chapter 3

Basic definations and equations

The current chapter covers some standard definitions and related laws to develop understanding of the analysis of next chapters.

3.1 Fluid [135]

When an external force is applied, a fluid (can be either a liquid or a gas) slightly resists the external shearing force and then continues to move and deform or in other words the substances that are incapable of sustaining shear forces. Its examples include liquid, gases and plasmas.

3.2 Fluid mechanics [135]

The part of applied mechanics that deals with the characteristics and behavior of fluids as well as the forces that affect them. There are two primary branches.

3.2.1 Fluid statics [135]

The branch of fluid mechanics that elucidates the properties of fluids while they are at rest.

3.2.2 Fluid dynamics [135]

The field of fluid mechanics that examines how forces affect the characteristics of fluids in motion.

3.3 Nanofluid [135]

A fluid containing nanoparticles is referred to as a nanofluid. Engineered colloidal suspensions comprising of nanoparticles added in a base fluid make up these fluids. Typically, oxides, metals, carbides or carbon nanotubes are considered to be the nanoparticles for nanofluids. Oil, water or ethylene glycol are examples of typical base fluids. Compared to basefluid, nanofluids are known to have better thermal conductivity.

3.4 Hybrid Nanofluid [136]

The most advanced kind of nanofluids are called hybrid nanofluids and they are created by mixing two nanoparticles with in a suitable base fluid. The introduction of hybrid nanofluids is intended to upgrade the thermal conductivity of the relative conventional fluids as well as simple nanofluids. Hybrid nanofluids offer a wide range of uses in heat transmission, including automobile cooling systems, heat pipes and refrigeration etc.

3.5 Stress [137]

Stress is described as the average force exerted per unit of afflicted body surface area.

$$\text{Stress} = \frac{\text{Force}}{\text{Area}}. \tag{3.1}$$

The stress is expressed in the SI system as Nm^{-2} or $kg/m.s^2$ and has dimensions $\left[\frac{M}{LT^2}\right]$. Stress has two different parts.

3.5.1 Shear stress [137]

Shear stress can be defined as a type of stress where the force acts parallel to the material's cross sectional area.

3.5.2 Normal stress [137]

A type of stress called normal stress occurs when a force works normally on the cross section of a material.

3.6 Strain [137]

When a force is applied to a material, strain is the measurement of the substance's relative deformation. It possesses no dimensions.

3.7 Viscosity [137]

The internal frictional force between adjacent fluid layers that are moving relative to one another is associated to viscosity. The state of a fluid, including pressure, temperature and rate of deformation, generally affects viscosity. Following are the two approaches to define viscosity:

3.7.1 Dynamic viscosity (μ) [137]

Absolute viscosity, also known as dynamic viscosity, is the ratio of shear stress to velocity gradient.

$$\text{Viscosity}\,(\mu) = \frac{\text{Shear stress}}{\text{Velocity gradient}}. \tag{3.2}$$

Dynamic viscosity is measured in SI units of Ns/m^2 or $kg/m.s$ and its dimensions are $\left[\frac{M}{LT}\right]$.

3.7.2 Kinematic viscosity (ν) [137]

The ratio among dynamic viscosity and fluid density determines kinematic viscosity. Mathematically this concept can be elaborated as

$$\nu = \frac{\mu}{\rho}. \tag{3.3}$$

Kinematic viscosity is evaluated in $\left[\frac{L^2}{T}\right]$ and has units of m^2/s.

3.8 Newton's law of viscosity [137]

It indicates that the fluid's shear stress is linearly and directly related to the velocity gradient. Mathematically it can be written as

$$\tau_{yx} \propto \frac{du}{dy}, \tag{3.4}$$

or

$$\tau_{yx} = \mu \frac{du}{dy}, \tag{3.5}$$

where τ_{yx} stands for the fluid element's applied shear stress.

3.9 Newtonian fluids [137]

Newtonian fluids are those that follow Newton's law of viscosity or those for which there exists a linear relationship among rate of strain ($\frac{du}{dy}$) and shear stress (τ_{yx}). Its examples include water, air and alcohol.

3.10 Non-Newtonian fluids [137]

Non-Newtonian fluids are those that deviate from Newton's law of viscosity or those for which the correlation between shear stress and strain rate is nonlinear. Mathematically it can be written as

$$\tau_{yx} \propto \left(\frac{du}{dy}\right)^n, \quad n \neq 1, \tag{3.6}$$

or

$$\tau_{yx} = \eta \frac{du}{dy}, \quad \eta = k \left(\frac{du}{dy}\right)^{n-1}, \tag{3.7}$$

where k stands for consistency index, n for flow behavior index and η stands for apparent viscosity.

3.11 Flow [137]

Flow is defined as the amount of fluid that passes a region in a unit of time.

3.11.1 Incompressible flow [137]

Incompressible flow is defined as a flow where the fluid element's density remains constant throughout the flow.

3.11.2 Compressible flow [137]

A type of flow known as compressible flow occurs when the density of the fluid flowing changes.

3.11.3 Laminar flow [137]

When fluid particles move in parallel layers or along predetermined pathways without crossing one another, this is known as laminar flow.

3.11.4 Turbulent flow [137]

The term "turbulent flow" describes a flow in which the fluid particles move randomly and follow no set patterns.

3.11.5 Steady flow [137]

When the point fluid's properties (such as pressure, density, velocity, etc.) are not dependent or independent of time, the flow is said to be steady.

$$\frac{\partial \Psi}{\partial t} = 0. \tag{3.8}$$

where Ψ represent fluid's property.

3.11.6 Unsteady flow [137]

Unsteady flow is when the properties of the fluid (such as pressure, density and velocity) at a given point change with time.

$$\frac{\partial \Psi}{\partial t} \neq 0. \tag{3.9}$$

3.12 Density [137]

The measurement of a quantity or mass per unit volume for a given substance is termed as density. Mathematically, it is defined as

$$\rho = \frac{m}{v}. \tag{3.10}$$

The SI units of density is kg/m^3 and the dimensions are $[ML^{-3}]$.

3.13 Pressure [137]

The ratio of force per unit area is known as pressure. The physical force applied to an object is referred to as pressure and the stress will be developed because of the pressure. Mathematically, it is defined as

$$P = \frac{F}{A}. \tag{3.11}$$

The SI units of pressure is N/m^2.

3.14 Thermal Conductivity [137]

Thermal conductivity is the study of the capacity of a material to transfer heat. Radiation, convection and conduction are the three ways that heat can transfer. Specifically, we can show this mathematically as

$$\text{Thermal conductivity} = \frac{\text{heat} \times \text{distance}}{\text{area} \times \text{temperature gradient}}, \tag{3.12}$$

so

$$k = \frac{QL}{A\triangle T}, \tag{3.13}$$

where A is noted to be the cross-sectional area, k is the thermal conductivity, Q stands for the heat flow per unit time and $\triangle T$ characterizes temperature difference. Its units are W/mK or $kg.m/s^3K$ with dimensions $\left[\frac{ML}{T^3\theta}\right]$.

3.15 Thermal diffusivity [137]

The ratio of thermal diffusivity per unit density and specific heat is known as thermal diffusivity. Mathematically, it is written as

$$\alpha = \frac{k}{\rho C_p}, \tag{3.14}$$

where k represents thermal conductivity, ρ represents density and C_p represents heat capacity.

3.16 Stagnation Point [138]

In flow field, stagnation point is a point where the fluid has zero velocity. Consider the surface of an object in the flow field, when the fluid is brought to rest by an object, then a stagnation point exists. For instance, when air is passing around an aeroplane wing, there is frequently a stagnation point right in front of the wing where the airflow is stopped.

3.17 Magnetohydrodynamic (MHD) [138]

Magnetohydrodynamics studies the motion of fluids that conduct electricity in the presence of a magnetic field. The term magneto-hydro-dynamics (MHD) comes from the terms "magneto" which stands for magnetic field, "hydro" related to liquid and "dynamics" which represents movement.

3.18 Joule Heating [138]

When electric current is passed by the conductor, it emits heat and this is described as Joule heating, also called as resistive heating or ohmic heating. By using electric current movement, Joule heating refines the heat transfer process to reduce dynamic viscosity leading to boost in electrical conductivity.

3.19 Viscous Dissipation [138]

During a viscous fluid flow, the motion of fluid generates kinetic energy which is taken by viscosity of the fluid and is turned into internal energy of the fluid. This phenomena is learned as viscous dissipation and is considered irreversible.

3.20 Heat generation/absorption [138]

In heat generation or absorption, Q is non-dimensional variable which depends on how much heat is absorbed or generated per unit volume. Its general representation is $Q\left(T - T_{\infty}\right)$. When $Q > 0$, heat is generated and when $Q < 0$, heat is absorbed.

3.21 Dimensionless numbers [138]

3.21.1 Reynolds number [138]

In fluid flow, Reynolds number is regarded as the most important dimensionless number. It is described as the ratio of inertial to the effective viscous forces.

$$\mathrm{Re} = \frac{\text{Inertial force}}{\text{Viscous force}}, \tag{3.15}$$

i.e.,

$$\mathrm{Re} = \frac{\rho v^2/L}{\mu v^*/L^2} = \frac{vL}{v^*}, \tag{3.16}$$

where density is denoted by ρ, velocity by v^*, characteristic length by L, dynamic viscosity as μ and kinematic viscosity v. Viscous terms vanish from the equation if Re is large in value. Inviscid flows are therefore associated with high Reynolds number values. Significant Reynolds numbers also indicate turbulent flow where inertial forces predominate, while low Reynolds numbers indicate high viscous forces and laminar flow.

3.21.2 Prandtl number [138]

The Prandtl number has no dimensions and determines the relation among momentum and thermal diffusivity. The following is the mathematical expression for the Prandtl number:

$$\mathrm{Pr} = \frac{\text{Viscous diffusion rate}}{\text{Thermal diffusion rate}}, \tag{3.17}$$

i.e.,

$$\mathrm{Pr} = \frac{\upsilon}{\alpha^*} = \frac{\mu/\rho}{k/\rho c_p} = \frac{c_p \mu}{k}, \tag{3.18}$$

where α^* stands for thermal diffusivity, k for thermal conductivity, υ for kinematic viscosity (momentum diffusivity) and c_p for specific heat at constant pressure. Thermal diffusivity predominates for $Pr << 1$ and momentum diffusivity for $Pr >> 1$.

3.21.3 Eckert number [138]

The Eckert number reported as a dimensionless number quantifies the relationship between kinetic energy and heat flow enthalpy. It can be write as

$$Ec = \frac{\text{Kinetic energy}}{\text{Enthalpy}} = \frac{V^2}{c_p \triangle T}, \tag{3.19}$$

where V denotes flow velocity, c_p denotes specific heat and $\triangle T$ denotes temperature difference.

The kinetic energy of the flow and its enthalpy are directly related by the Eckert number. It is used to determine heat dissipation occurring for high-speed flows where the fluid experience enormous viscous dissipation.

3.21.4 Skin friction [138]

Skin friction is the term used to describe the sort of friction caused by a fluid moving relative to a solid surface. Mathematically, the skin friction coefficient is expressed as

$$C_f = \frac{\tau_w}{\frac{1}{2}\rho U^2}, \tag{3.20}$$

where ρ signifies density, U is velocity and τ_w is the shear stress at the wall.

The friction drag is assumed as an aerodynamic or sometimes hydrodynamic drag. It behaves as a resistant force acted by the fluid on the subject. It originates due to fluid's viscosity and it progresses from laminar drag turbulent drag with the flowing fluid.

3.21.5 Nusselt number [138]

The Nusselt number, a dimensionless quantity that quantifies the link between convective and conductive heat transfer through the boundary. In terms of mathematics

$$Nu_L = \frac{\text{Convective heat transfer}}{\text{Conductive heat transfer}}. \tag{3.21}$$

Newton's law of cooling gives us the following

$$q' = h \triangle T, \tag{3.22}$$

where h stands for the coefficient of heat transfer and q' represents flux per unit area. Heat flow for the convectional process is defined as

$$q' = h(T_w - T_\infty). \tag{3.23}$$

Additionally, if the fluid layer is not moving, the heat flux for the conduction process is provided by.

$$q' = k(T_w - T_\infty)/L, \tag{3.24}$$

where k is thermal conductivity of fluid and L is characteristic length. Using the Nusselt number's definition, we can

$$Nu_L = \frac{h(T_w - T_\infty)}{k(T_w - T_\infty)/L} = \frac{hL}{k}. \tag{3.25}$$

If the value of Nusselt number is one, it will show a sluggish motion which is considered useful when compared to pure fluid conduction and it corresponds to laminar flow. If a large value of Nusselt number is taken, then an efficient convection is encountered which is obvious to turbulent pipe flow yielding Nu with order ranging from 100 to 1000.

Chapter 4

Stagnation point flow of Hybrid Nanofluid over a Variable Thicked Surface in the presence of Melting Heat Transfer

Hybrid nanofluids are identified as an advanced group of fluids that have suitable thermal conductivity. The flow of hybrid nanofluid over a stretched plate with varying thickness near a stagnation point is examined in this chapter. The study of heat transfer is performed in the presence of melting heat conditions and viscous dissipation. By using the appropriate similarity practice, the governing equations for the given model is simplified as a system of ODEs. Bvp4c technique is applied to graphically analyze temperature and velocity, thus Nusselt number and skin friction coefficient. A comparison study for basefluid, nanofluid and hybrid nanofluid is also carried out to point towards the refinement of nanofluids in terms of hybrid nanofluids.

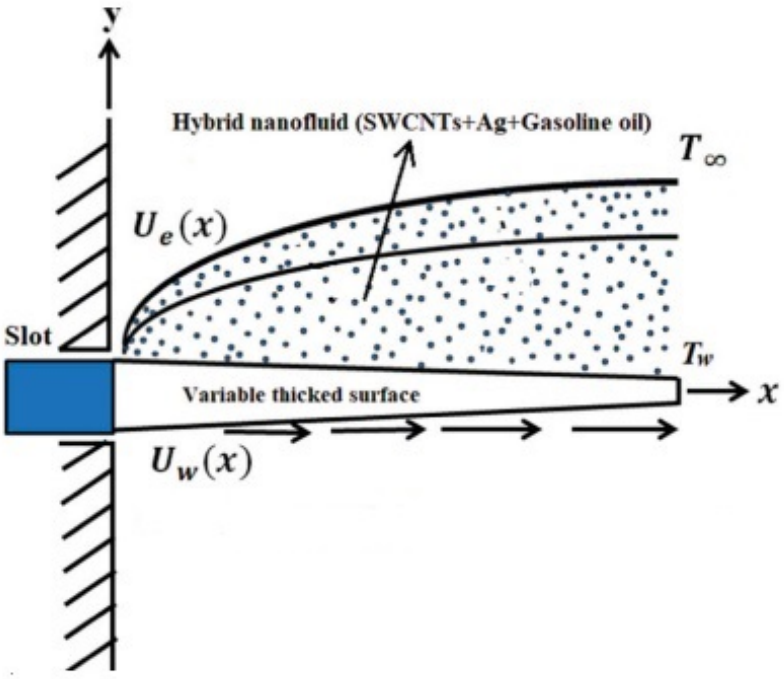

Fig. 4.1. Geometry of the problem

4.1 Mathematical Formulation

The present model is based on the stagnation point flow of hybrid nanofluid that is composed of SWCNTs, Ag and the base fluid is gasoline oil. The flow is maintained because of a variable thicked sheet stretching in the x-direction with velocity $U_w = U_o\,(x+b)^m$. The varying thickness of the stretching sheet is given by $y = b^*\,(x+b)^{\frac{1-m}{2}}$. The phenomenon of melting heat transfer is taken into account along with viscous dissipation.

The governing equations for the fluid flow are presented in the form of continuity, momentum and energy equations

The considered velocity field for this model is given by

$$\overrightarrow{\mathrm{V}} = [u\,(x,y)\,,\ v(x,y),\ 0]. \tag{4.1}$$

The governing equations for the fluid flow are presented in the form of continuity, momentum and energy equations.

$$\frac{\partial \rho}{\partial t} + \overrightarrow{\nabla}.\left(\rho\ \overrightarrow{\mathrm{V}}.\right) = 0, \tag{4.2}$$

$$\rho_{hnf}\left(\frac{\partial \overrightarrow{\mathrm{V}}}{\partial t} + \left(\ \overrightarrow{\mathrm{V}}\ .\overrightarrow{\nabla}\right)\overrightarrow{\mathrm{V}}\right) = \overrightarrow{\nabla}.\overrightarrow{\tau} + \rho_{hnf}\,\overrightarrow{\mathrm{b}}, \tag{4.3}$$

$$(\rho C_p)_{hnf}\left(\frac{\partial T}{\partial t} + \left(\overrightarrow{\mathrm{V}}.\overrightarrow{\nabla}\right)T\right) = -\overrightarrow{\nabla}.\overrightarrow{\mathrm{q}} + Tr\left(\overrightarrow{\tau}.\overrightarrow{\mathrm{L}}\right), \tag{4.4}$$

$$\overrightarrow{\mathrm{q}} = -k\,\mathrm{grad}\,T,$$

in which ρ is noted for density, $\overrightarrow{\mathrm{V}}$ designated as velocity field, ρ_{hnf} indicates density of hybrid nanofluid, T symbolizes temperature of fluid, $\overrightarrow{\mathrm{q}}$ stands for the heat flux, $\overrightarrow{\tau}$ characterizes Cauchy stress tensor, k represents thermal conductivity.

After applying boundary layer assumptions, we acquire the following equations.

$$\frac{\partial u}{\partial x} + \frac{\partial v}{\partial y} = 0, \tag{4.5}$$

$$u\frac{\partial u}{\partial x} + v\frac{\partial u}{\partial y} = U_e\frac{dU_e}{dx} + \upsilon_{hnf}\frac{\partial^2 u}{\partial y^2}, \tag{4.6}$$

$$u\frac{\partial T}{\partial x} + v\frac{\partial T}{\partial y} = \alpha_{hnf}\frac{\partial^2 T}{\partial y^2} + \frac{\mu_{hnf}}{(\rho \mathrm{c}_p)_{hnf}}(\frac{\partial u}{\partial y})^2. \tag{4.7}$$

The present model proposes the following boundary conditions.

$$\begin{aligned} u &= U_w(x) = U_0(x+b)^m \ \text{ and } \ v = 0,\ \mathrm{T} = \mathrm{T}_m \ \text{ at } \ y{=}b^*(x{+}b)^{\frac{1-m}{2}}, \\ u &\rightarrow U_e(x) = U_\infty(x+b)^m, \ \ T \rightarrow T_\infty \text{ as } y \rightarrow \infty, \end{aligned} \tag{4.8}$$

where u, v represents the velocity components, U_0 , U_∞ are arbitrary constants, U_w is stretching velocity, U_e be the free stream velocity and T_m is surface temperature. Condition for melting

heat is defined as:

$$\kappa_{hnf}\left(\frac{\partial T}{\partial y}\right)_{y=b^*(x+b)\frac{1-m}{2}} = \rho_{hnf}\left[\lambda + C_s\left(T_m - T_0\right)\right] v_{y=b^*(x+b)\frac{1-m}{2}}, \tag{4.9}$$

where λ is referred to as latent heat.

The similarity transformations for the considered flow are

$$\begin{aligned}
\eta &= \sqrt{\frac{m+1}{2\upsilon_f}U_0\left(x+b\right)^{m-1}}y, \quad \Psi = \sqrt{\frac{2\upsilon_f}{m+1}U_0\left(x+b\right)^{m+1}}f^*(\eta), \quad \theta^*\left(\eta\right) = \frac{\mathrm{T}-T_m}{T_\infty - T_m}, \\
u &= U_0\left(x+b\right)^m f^{*'}(\eta), \quad v = -\sqrt{\frac{(m+1)\upsilon_f}{2}U_0\left(x+b\right)^{m-1}}\left(f^*(\eta) + \eta f^{*'}(\eta)\frac{m\text{-}1}{m+1}\right),
\end{aligned} \tag{4.10}$$

where f^* shows non dimensional velocity, θ^* represents non dimensional temperature, m is flow behavior index parameter and υ_f is kinematic viscosity. From Eqs. (4.6) to (4.8), we have

$$\frac{A_{11}}{(1-\varphi_1)^{2.5}(1-\varphi_2)^{2.5}}f^{*'''} + f^*f^{*''} - \frac{2m}{m+1}\left(f^{*'}\right)^2 + \frac{2m}{m+1}A^2 = 0, \tag{4.11}$$

$$\frac{\kappa_{hnf}}{\kappa_f}\theta^{*''} + B_{11}Prf^*\theta^{*'} + \frac{PrEc}{(1\text{-}\varphi_1)^{2.5}(1\text{-}\varphi_2)^{2.5}}\left(f^{*''}\right)^2 = 0, \tag{4.12}$$

$$\begin{gathered}
f^{*'}(\alpha) = 1, \quad \theta^*\left(\alpha\right) = 0, \\
\frac{k_{hnf}}{k_f}M_1\theta^{*'}\left(\alpha\right) + A_{11}(Prf^*\left(\alpha\right) + \frac{m\text{-}1}{m+1}\alpha) = 0 \quad \text{at } \alpha = b^*\sqrt{\frac{m+1}{2\upsilon_f}U_0}, \\
f^{*'}\left(\infty\right) \to A \ , \theta^*\left(\infty\right) \to 1 \text{ as } \alpha \to \infty.
\end{gathered} \tag{4.13}$$

Also we have

$$A_{11} = \frac{1}{(1-\varphi_2)\left((1-\varphi_1) + \varphi_1\frac{\rho_{SWCNTs}}{\rho_f}\right) + \varphi_2\frac{\rho_{Ag}}{\rho_f}}, \tag{4.14}$$

and

$$B_{11} = (1-\varphi_2)\left((1-\varphi_1) + \varphi_1\frac{(\rho c_p)_{SWCNTs}}{(\rho c_P)_f}\right) + \varphi_2\frac{(\rho c_p)_{Ag}}{(\rho c_p)_f}. \tag{4.15}$$

where φ_1 and φ_2 represent SWCNTs volume fraction, Ag volume fraction and k be the thermal conductivity of mentioned fluid.

In this case, prime indicates the derivative with reference to η. The wall thickness is given by $\alpha = b^* \sqrt{\frac{m+1}{2\nu_f}} U_0 = \eta$ which describe flat surface. Now $f^*(\eta) = f(\eta - \alpha) = f(\xi)$. From this, we reach at the following equations

$$\frac{A_{11}}{(1-\varphi_1)^{2.5}(1-\varphi_2)^{2.5}} f^{'''} + f f^{''} - \frac{2m}{m+1}\left(f^{'}\right)^2 + \frac{2m}{m+1} A^2 = 0 \ ,$$

$$\frac{\kappa_{hnf}}{\kappa_f}\theta^{''} + B_{11}\,\mathrm{Pr}\, f\theta^{'} + \frac{\mathrm{Pr}\, Ec}{(1-\varphi_1)^{2.5}(1-\varphi_2)^{2.5}}\left(f^{''}\right)^2 = 0 \ ,$$

$$\begin{aligned} f^{'}(0) &= 1,\ \theta(0) = 0\ ,\ \frac{k_{hnf}}{k_f} M_1 \theta^{'}(0) + A_{11}\left(Prf\ (0) + \frac{m-1}{m+1}\alpha\right) = 0, \\ f^{'}(\infty) &\to A,\ \theta(\infty) \to 1 \text{ as } \xi \to \infty. \end{aligned}$$

The dimensionless terms in equation are defined as:

$$\begin{aligned} A &= \frac{U_\infty}{U_0}\ ,\ \alpha = b^* \sqrt{\frac{m+1}{2\upsilon_f}} U_0,\ M_1 = \frac{C_{\rho f}(T_\infty - T_m)}{\lambda + C_s\,(T_m - T_0)}, \\ Pr &= \frac{\nu_f}{\alpha_f},\ Ec = \frac{(U_w(x))^2 \rho_f}{(\rho c_p)_f\,(T_\infty - T_m)}. \end{aligned}$$

In these terms, A is velocity ratio parameter, α is wall thickness parameter, parameter M_1 shows melting effect parameter, Pr be the Prandtl number and Ec is defined as Eckert number. Expressions for local Nusselt and surface friction coefficient number is described as.

$$C_f = \frac{\tau_w}{\rho_f\ U_w^2}, \tag{4.16}$$

where

$$\tau_w = \mu_{hnf}\left(\frac{\partial u}{\partial y}\right)_{y = b^*\sqrt{\frac{m+1}{2\upsilon_f}U_0}}. \tag{4.17}$$

We consider Nusselt number as :

$$Nu_x = \frac{(x+b)\,q_w}{k\,(T_\infty - T_m)}, \tag{4.18}$$

where

$$q_w = -k_{hnf}\left(\frac{\partial T}{\partial y}\right)_{y=b^*\sqrt{\frac{m+1}{2\upsilon_f}U_0}}. \tag{4.19}$$

We acquire non dimensional representations of C_f and Nu_x by substituting above equations.

$$C_f\sqrt{\mathrm{Re}_x} = \frac{1}{(1-\varphi_1)^{2.5}(1-\varphi_2)^{2.5}}\sqrt{\frac{m+1}{2}}f''(0), \tag{4.20}$$

$$\frac{Nu_x}{\sqrt{\mathrm{Re}_x}} = -\frac{\kappa_{hnf}}{\kappa_f}\sqrt{\frac{m+1}{2}}\theta'(0) \tag{4.21}$$

where the local Roynold number is presented as $\mathrm{Re}_x = \frac{U_0(x+b)}{\nu_f}$

Table. 4.1

From the Hamilton-Crosser model for Nanofluid (SWCNTs and gasoline oil).

Muhammad *et al.* [139].

Properties	Nanofluid
Dynamic viscosity	$\mu_{nf} = \frac{\mu_f}{(1-\varphi_1)^{2.5}}$
Kinematic viscosity	$\nu_{nf} = \frac{\mu_{nf}}{\rho_{nf}}$
Specific Heat	$(\rho c_p)_{nf} = (1-\varphi_1)(\rho c_p)_f + \varphi_1(\rho c_p)_{SWCNTs}$
Density	$\rho_{nf} = (1-\varphi_1)\rho_f + \varphi_1\rho_{SWCNTs}$
Thermal conductivity	$\frac{\kappa_{nf}}{\kappa_f} = \frac{\kappa_{SWCNTs}+(n-1)\kappa_f-(n-1)\varphi_1(\kappa_f-\kappa_{SWCNTs})}{\kappa_{SWCNTs}+(n-1)\kappa_f+\varphi_1(\kappa_f-\kappa_{SWCNTs})}$

Table. 4.2

For hybrid nanofluid (SWCNTs, Ag and gasoline oil). Muhammad *et al.* [139].

Properties	Hybrid Nanofluid
Dynamic viscosity	$\mu_{hnf} = \frac{\mu_f}{(1-\varphi_1)^{2.5}(1-\varphi_2)^{2.5}}$
Kinematic viscosity	$\nu_{hnf} = \frac{\mu_{hnf}}{\rho_{hnf}}$
Specific Heat	$\frac{(\rho c_p)_{hnf}}{(\rho c_p)_f} = (1-\varphi_2)\left[1-\varphi_1+\varphi_1(\frac{(\rho c_p)_{SWCNT}}{(\rho c_p)_f})\right]+\varphi_2(\frac{(\rho c_p)_{Ag}}{(\rho c_p)_f})$
Density	$\rho_{hnf} = (1-\varphi_2)((1-\varphi_1)\rho_f+\varphi_1\rho_{SWCNTs})+\varphi_2\rho_{Ag}$
Thermal conductivity	$\frac{\kappa_{hnf}}{\kappa_{nf}} = \frac{\kappa_{Ag}+(n-1)\kappa_{nf}-(n-1)\varphi_2(\kappa_{nf}-\kappa_{Ag})}{\kappa_{Ag}+(n-1)\kappa_{nf}+\varphi_2(\kappa_{nf}-\kappa_{Ag})}$ $\frac{\kappa_{nf}}{\kappa_f} = \frac{\kappa_{SWCNTs}+(n-1)\kappa_f-(n-1)\varphi_1(\kappa_f-\kappa_{SWCNTs})}{\kappa_{SWCNTs}+(n-1)\kappa_f+\varphi_1(\kappa_f-\kappa_{SWCNTs})}$

where n = 6 because of nanoparticles cylindrical shape.

Table. 4.3. Thermophysical properties of (SWCNT, Ag and Gasoline oil). Muhammad *et al.* [139].

Nanoparticle/Thermophysical properties	$\rho\left(\frac{kg}{m^3}\right)$	Pr	$c_p(\frac{J}{kgK})$	$\kappa(\frac{W}{mK})$
Ag	10490.0	-	235.0	429.0
SWCNTs	1600.0	-	796.0	3000.0
Gasoline oil	750.0	9.4	425.0	0.114.0

4.2 Numerical Stratagem:

The bvp4c package in MATLAB is used to create solutions for the governed flow equations (ODEs). The obtained equations are generally higher order differential equations. At an initial step, these differential equations are reduced to first order form and these first order differential equations use bvp4c as its implementation.

$$f_1 = f, \tag{4.22}$$

$$f_2 = f_1^{'} = f,^{'} \tag{4.23}$$

$$f_3 = f_2^{'} = f^{''}, \tag{4.24}$$

$$f_5 = \theta \quad , \quad f_6 = f_5^{'} = \theta^{'}, \tag{4.25}$$

$$f_4 = f_3^{'} = f^{'''} = -\frac{(1-\varphi_1)^{2.5}(1-\varphi_2)^{2.5}}{A_{11}}\left(f_1 f_3 - \frac{2m}{m+1}\left(f_2\right)^2 + \frac{2m}{m+1}A^2\right), \tag{4.26}$$

$$f_7 = f_6^{'} = \theta^{''} = -\frac{1}{\frac{\kappa_{hnf}}{\kappa_f}}\left(B_{11} Pr f_1 f_6 + \frac{PrE_c}{(1-\varphi_1)^{2.5}(1-\varphi_2)^{2.5}}\left(f_3\right)^2\right). \tag{4.27}$$

4.3 Graphical Analysis and Discussion

This section of the chapter highlights the graphical results of velocity, temperature, friction drag and Nusselt number with respect to the different parameters. Further, a comparison has been carried out for the relative research of hybrid nanofluid, nanofluid (SWCNT and gasoline oil) and basefluid (gasoline oil). Fig. 4.2. represents the impact of SWCNTs volume fraction φ_1 on $f^{'}(\eta)$. Increase in φ_1 causes augmentation in $f^{'}(\eta)$ whereas more ascendancy of hybrid nanofluid (SWCNT, Ag and gasoline oil) can be assessed as compared to nanofluid (SWCNT and gasoline oil). Fig. 4.3. is plotted to study the influence of Ag volume fraction φ_2 for velocity profile $f^{'}(\eta)$. It is monitored that with rise in φ_2, velocity profile enhances. Fig. 4.4. shows the rise in velocity profile $f^{'}(\eta)$ with the growing values of melting parameter M_1, in which $f^{'}(\eta)$ portrays direct relation with M_1. Elevated values of M_1 moves the fluid particles to drift through melting surface towards the fluid above it, resulting in an increased fluid velocity. Fig. 4.5. is plotted to observe the affect of flow behavior index parameter m relative to velocity

profile. Intensified choice of m results in respective growth of thickness of wall leading to decrease in the velocity whereas greater impact of hybrid nanofluid (SWCNT, Ag and gasoline oil) is shown if evaluated with nanofluid (SWCNT and gasoline oil). Fig. 4.6. shows increment in velocity distribution as α increases. The domination of hybrid nanofluid can be perceived from the figure. Fig. 4.7. examines the effects of velocity ratio parameter A on velocity profile, where $f^{'}(\eta)$ enhances as the value of A increases. It is also monitored that no boundary layer formation is seen when $A = 1$ while $A >1$ indicates thinning of the respective boundary layer formation and $A < 1$ exhibits the inverse trend. For the comparative study of hybrid nanofluid (SWCNT, Ag and gasoline oil) along with nanofluid (SWCNTs and gasoline oil) and basefluid (gasoline oil), Figs. 4.8. to 4.12. are plotted to evaluate the effects of variables such as $\varphi_1, \varphi_2,\ \alpha$, m and M_1 on $f^{'}(\eta)$ for hybrid nanofluid (SWCNT, Ag and gasoline oil), nanofluid (SWCNT, Ag and gasoline oil) and the base fluid (gasoline oil). The hybrid nanofluid's better performance is crystal clear from this graphical comparison which is in line with the recent developments in the field of nanotechnology. Fig. 4.13. depicts the analysis of temperature $\theta(\eta)$ for surging values of SWCNTs volume fraction φ_1. Decrease in $\theta(\eta)$ is resulted from the increase in φ_1. Even in case of temperature, the hybrid nanofluid sustains its superior stance. In Fig. 4.14. temperature profile $\theta(\eta)$ decreases through increment in Ag volume fraction φ_2. This outcome is obvious and there is no significant impact of φ_2 on temperature profile for nanofluid as it has no direct correspondence with nanofluid. Through Fig. 4.15., plotted to study the impact of melting parameter M_1 relative to the temperature profile $\theta(\eta)$, it can observe that when M_1 expands, the temperature profile diminishes. As M_1 rises, more cold particles of fluid travel from melting surface to fluid at increased temperature leading to low temperature profile. With amplified values of melting parameter, thermal layer thickness continues to decrease. For elevated values of melting parameter, cold particles are transferred into the hot fluid due to melting. Therefore temperature profile consequently decreases. Fig. 4.16. demonstrates the Eckert number Ec affecting the temperature profile. Due to the additional kinetic energy, an augmentation in Eckert number Ec results in an increased temperature profile and raises the temperature. Figs. 4.17. to 4.19. show a comparative analysis between hybrid nanofluid and nanofluid and in addition, the base fluid. From the figures, the importance of hybrid nanofluid exceeds than that of the considered nanofluid and also basefluid. The behavior of parameters like φ_1, φ_2, M_1

and A on skin friction coefficient C_{f_x} is shown in Figs. 4.20. and 4.21. It is obvious from the figures that enhanced values of A reduces the friction drag. Figs. 4.22. and 4.23. are drawn to assess the impact of φ_1, φ_2, M_1 and A for the Nusselt number Nu_x and the influence of these parameters can be easily determined from these results as Nu_x responds to φ_1, φ_2, M and A. Consequently, the variables can be utilized as cooling agents in a variety of modern technology. The last Figs. 4.24 to 4.27 give the comparative approach for the fluids under study and even these outcomes points towards the excellence of hybrid nanofluid

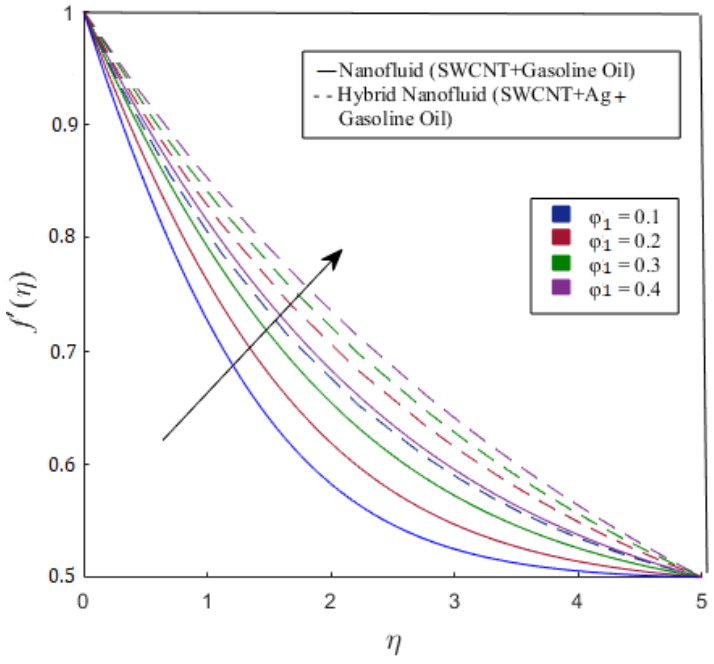

Fig. 4.2. Velocity distribution $f^{'}(\eta)$ for φ_1.

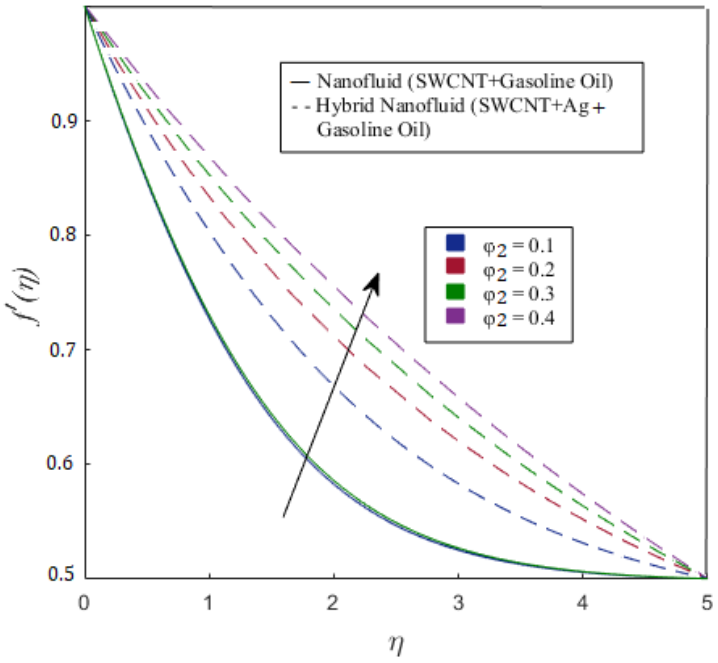

Fig. 4.3. Velocity distribution $f^{'}(\eta)$ for φ_2.

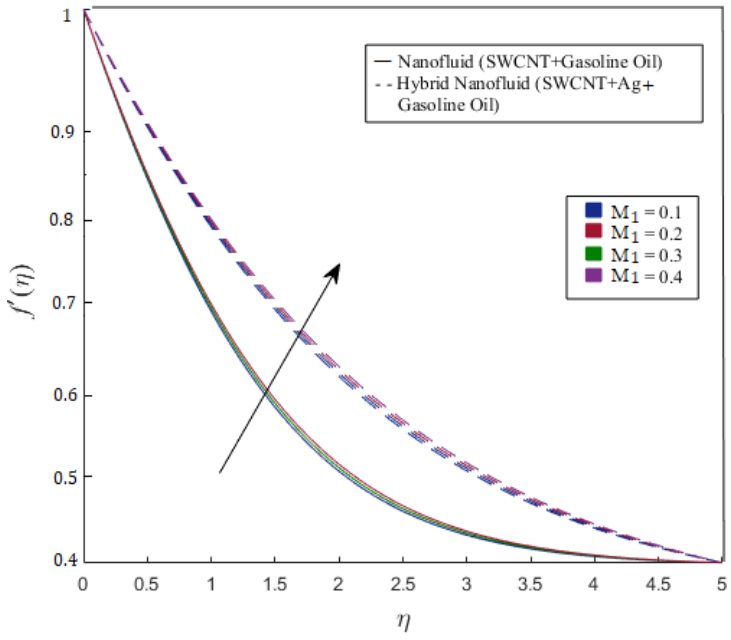

Fig. 4.4. Velocity distribution $f^{'}(\eta)$ for M_1.

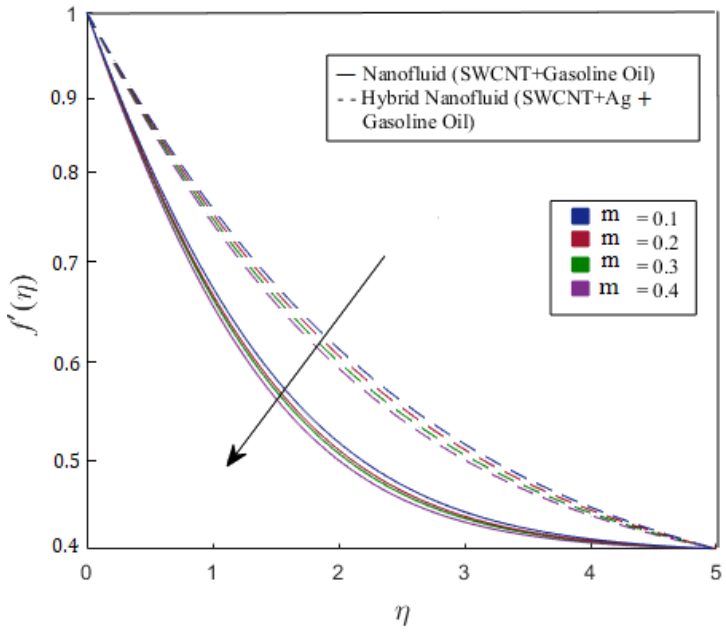

Fig. 4.5. Velocity distribution $f^{'}(\eta)$ for m.

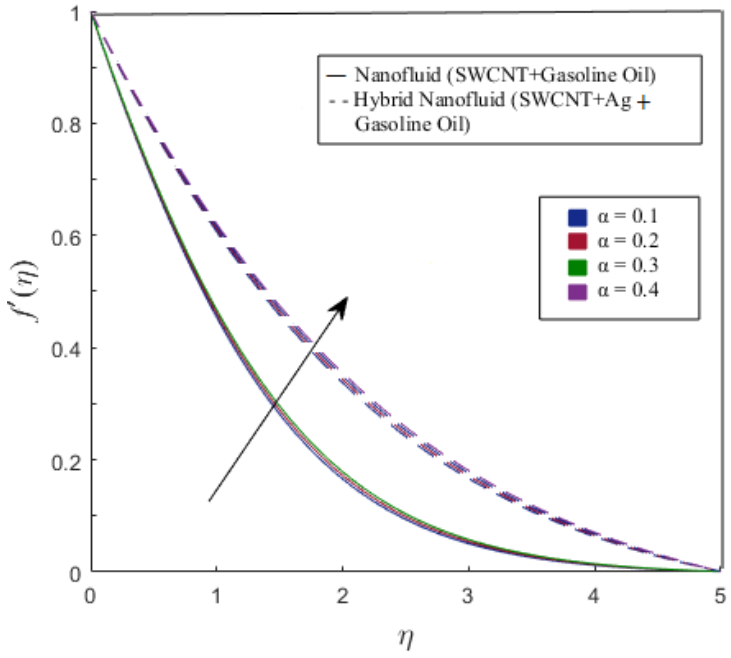

Fig. 4.6. Velocity distribution $f^{'}(\eta)$ for α.

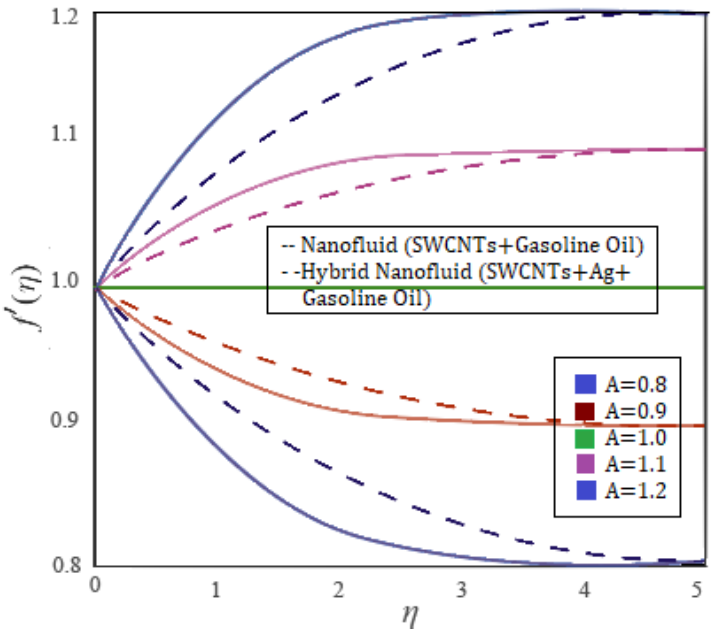

Fig. 4.7. Velocity distribution $f'(\eta)$ for A.

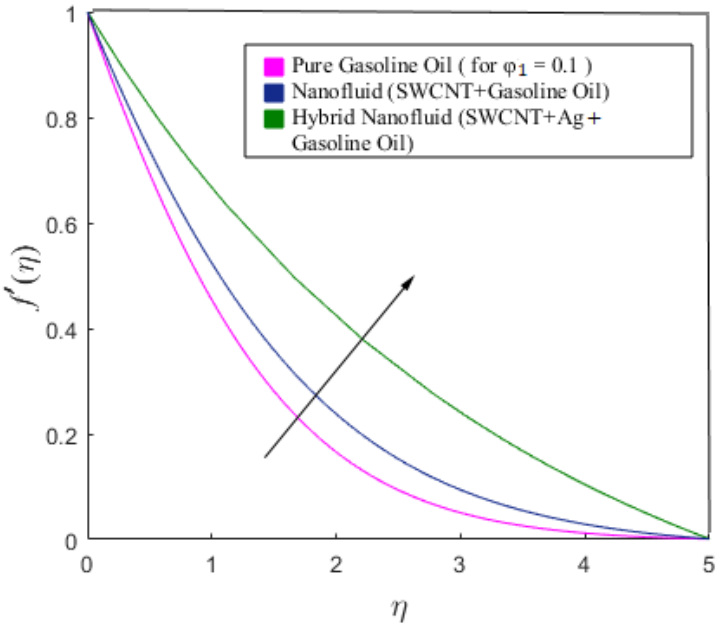

Fig. 4.8. Comparison of $f'(\eta)$ for φ_1.

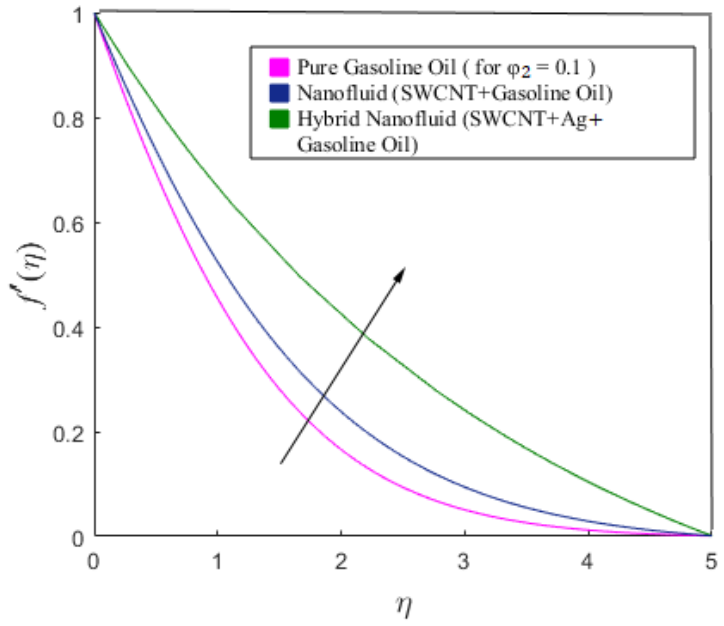

Fig. 4.9. Comparison of $f^{'}(\eta)$ for φ_2.

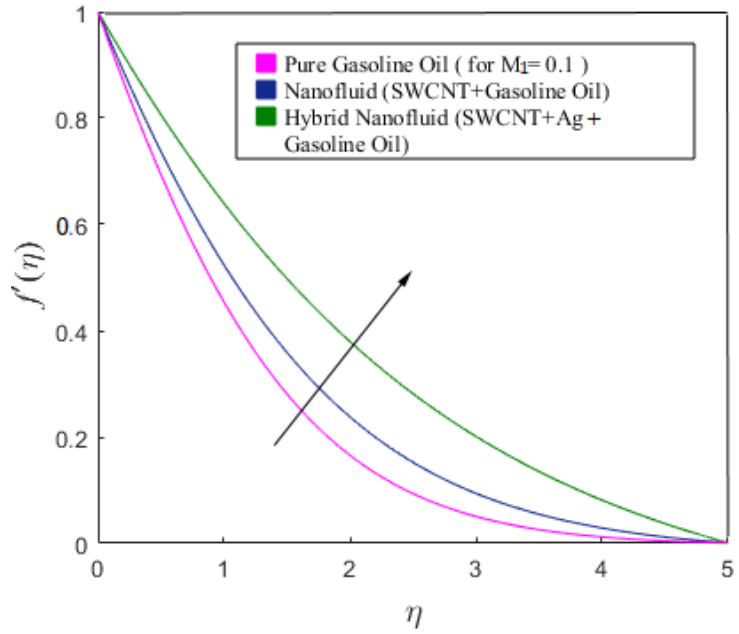

Fig. 4.10. Comparison of $f^{'}(\eta)$ for M_1.

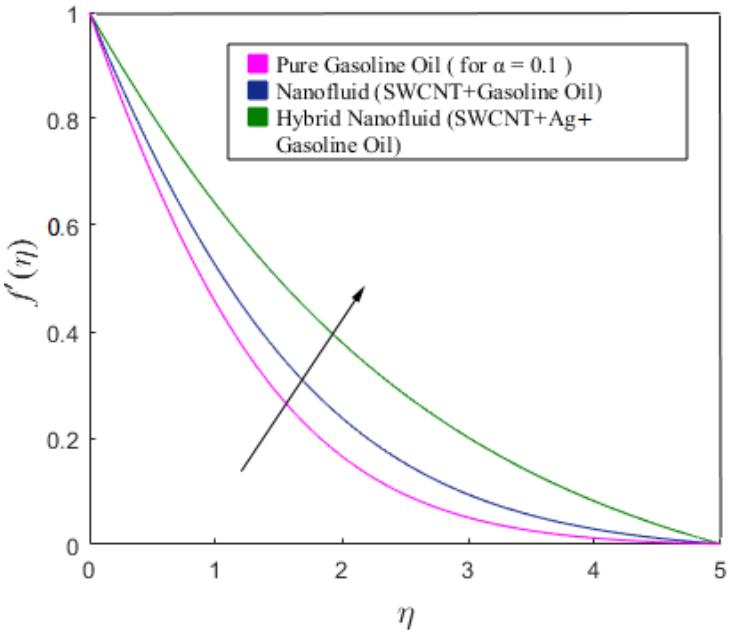

Fig. 4.11. Comparison of $f'(\eta)$ for α.

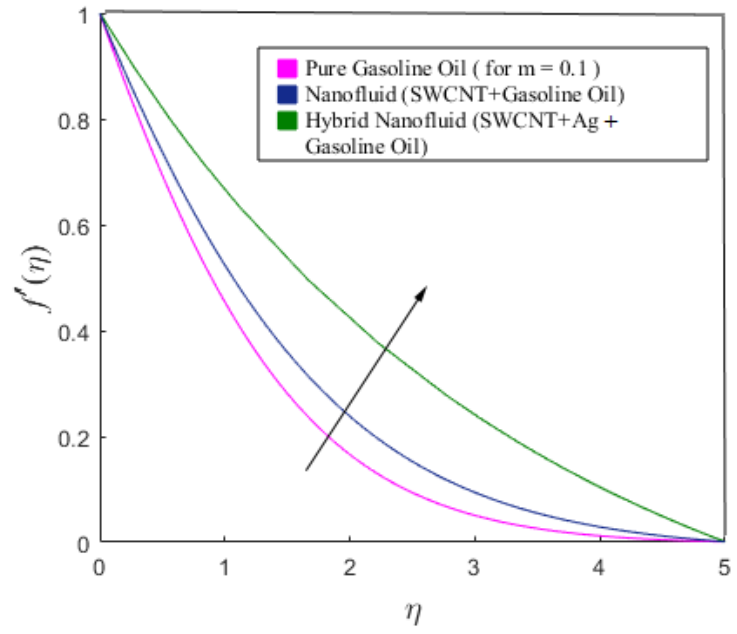

Fig. 4.12. Comparison of $f'(\eta)$ for m.

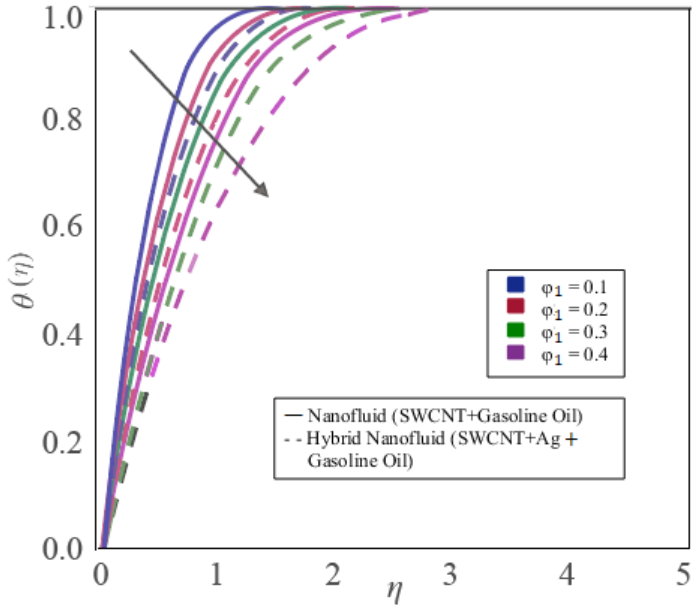

Fig. 4.13. Temperature distribution $\theta(\eta)$ for φ_1.

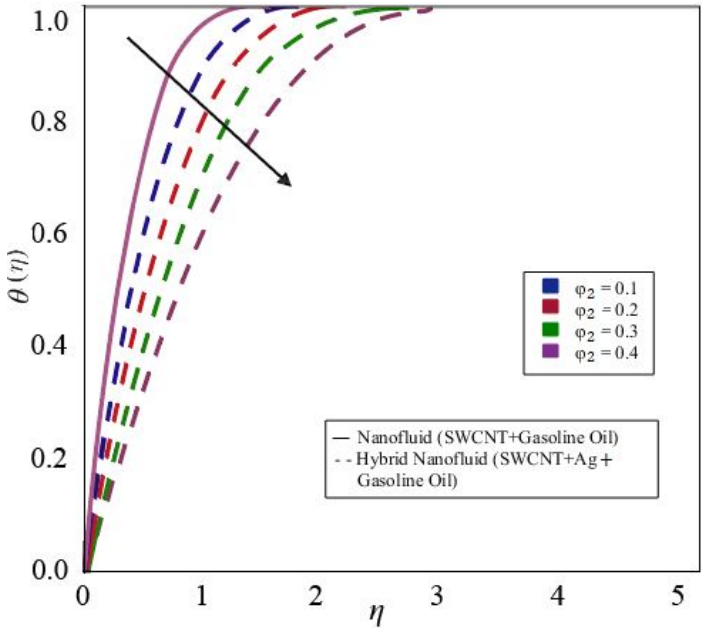

Fig. 4.14. Temperature distribution $\theta(\eta)$ for φ_2.

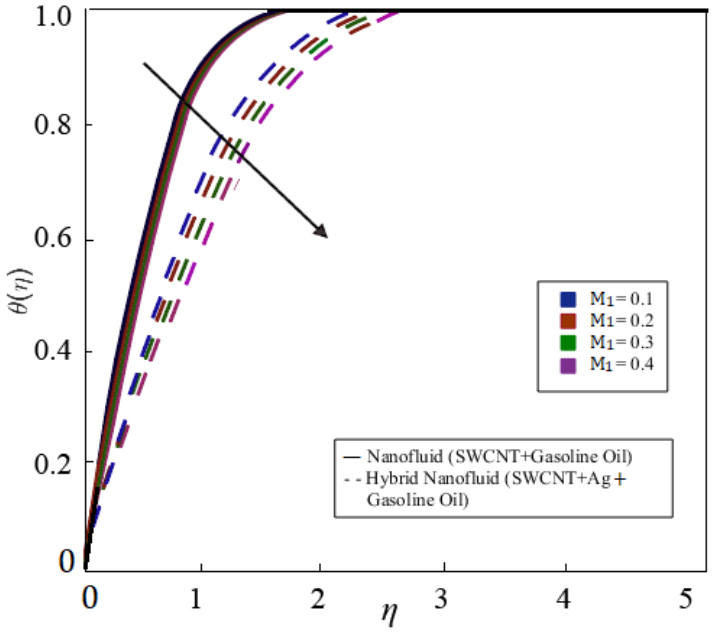

Fig. 4.15. Temperature distribution $\theta(\eta)$ for M_1.

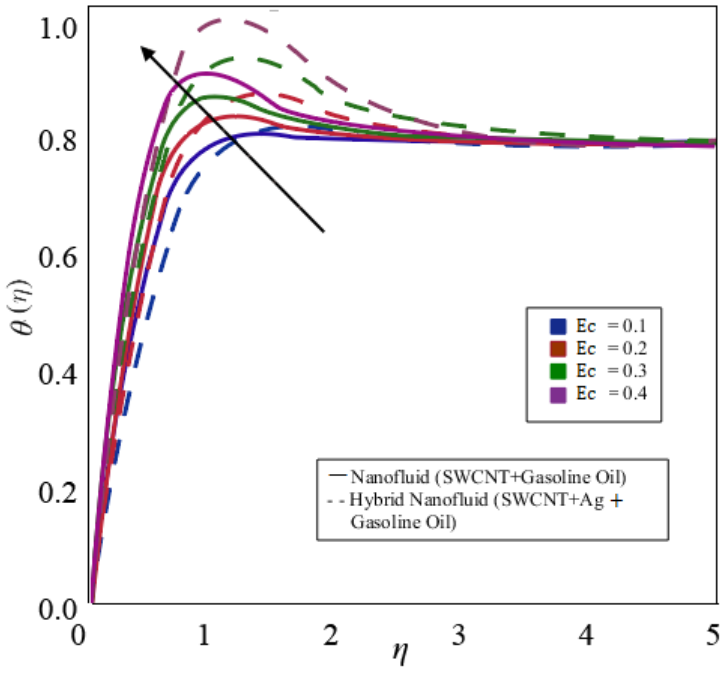

Fig. 4.16. Temperature distribution $\theta(\eta)$ for Ec.

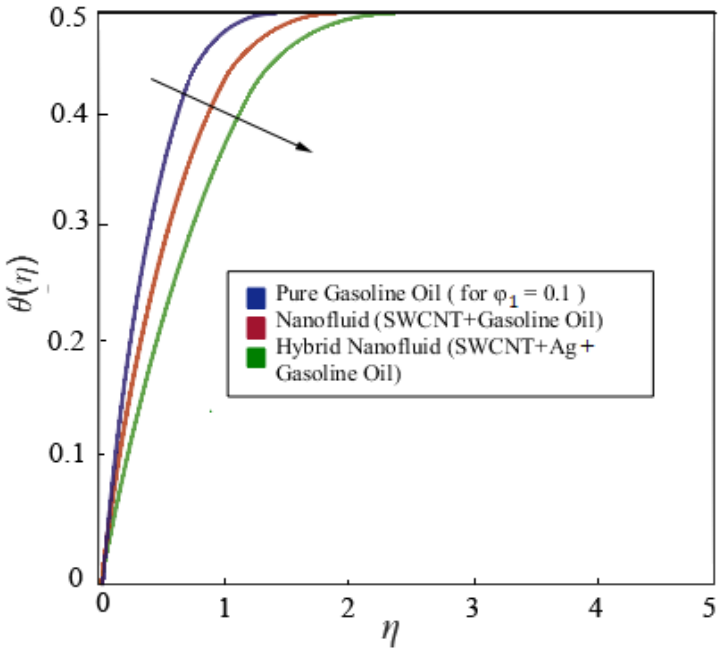

Fig. 4.17. Comparison of $\theta(\eta)$ for φ_1.

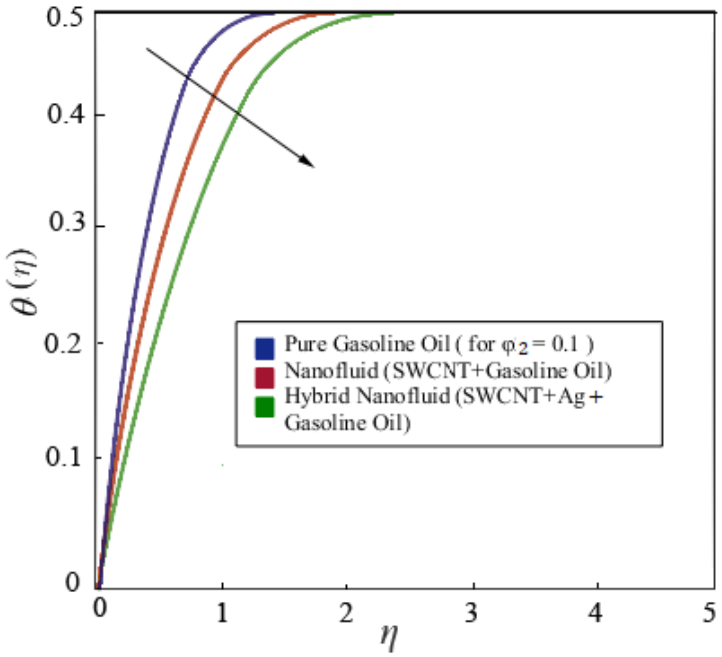

Fig. 4.18. Comparison of $\theta(\eta)$ for φ_2.

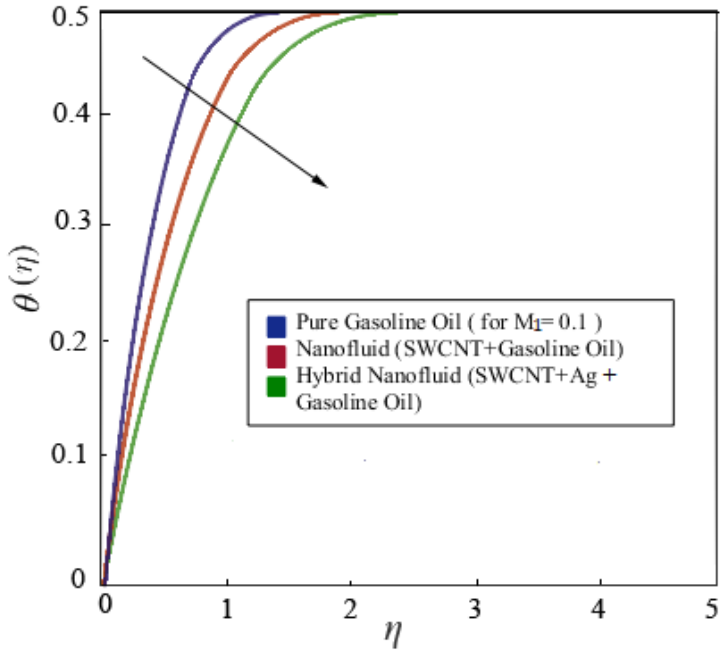

Fig. 4.19. Comparison of $\theta(\eta)$ for M_1.

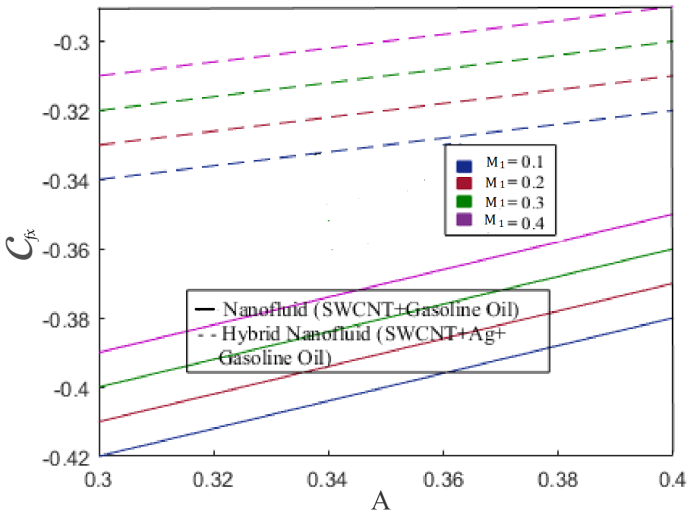

Fig. 4.20. Skin friction coefficient C_{fx} for M_1 and A.

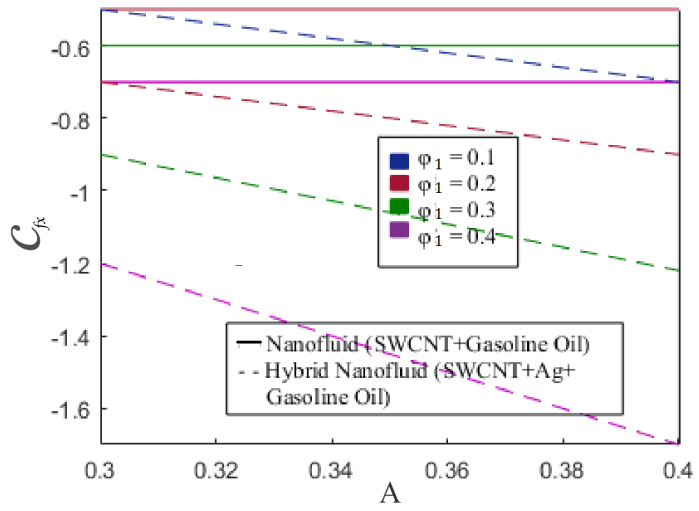

Fig. 4.21. Skin friction coefficient C_{fx} for φ_1 and φ_2.

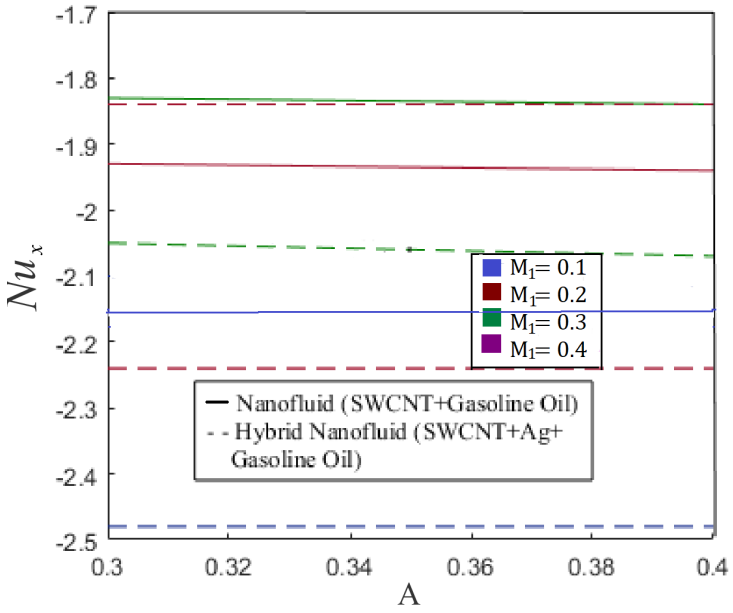

Fig. 4.22. Nusslt number Nu_x for M_1 and A.

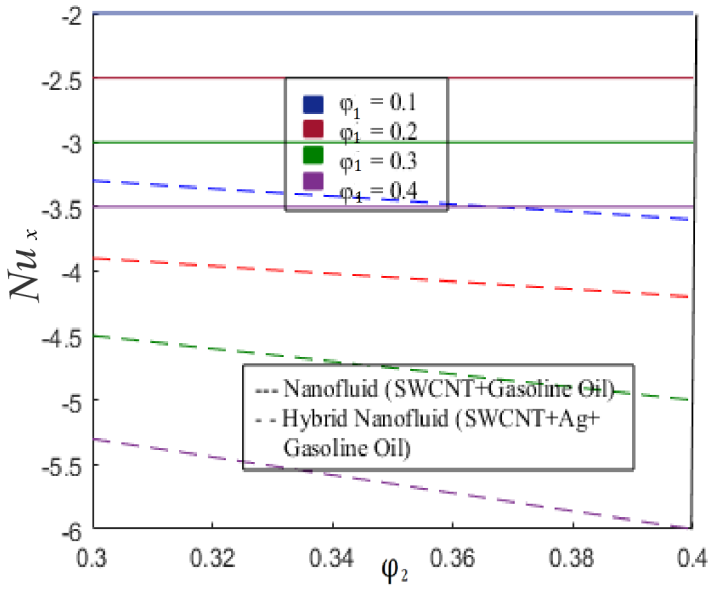

Fig. 4.23. Nusslt number Nu_x for φ_1 and φ_2.

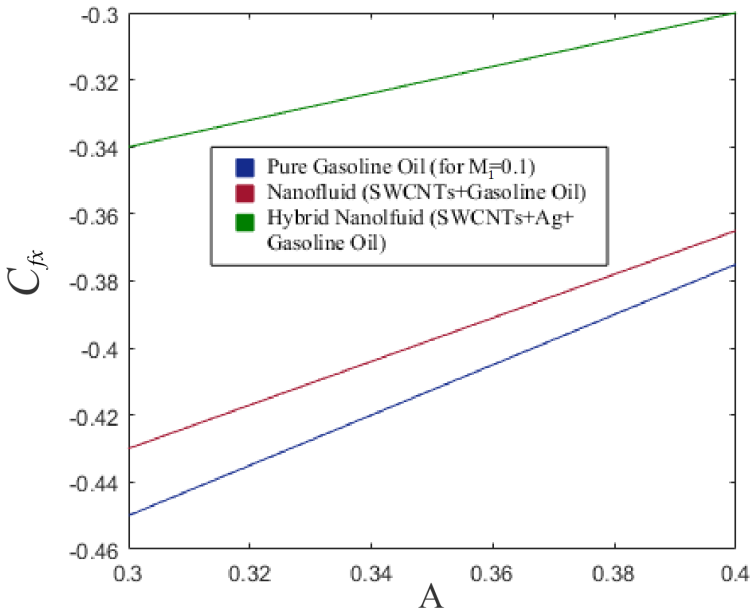

Fig. 4.24. Comparison of C_{fx} for M_1 and A.

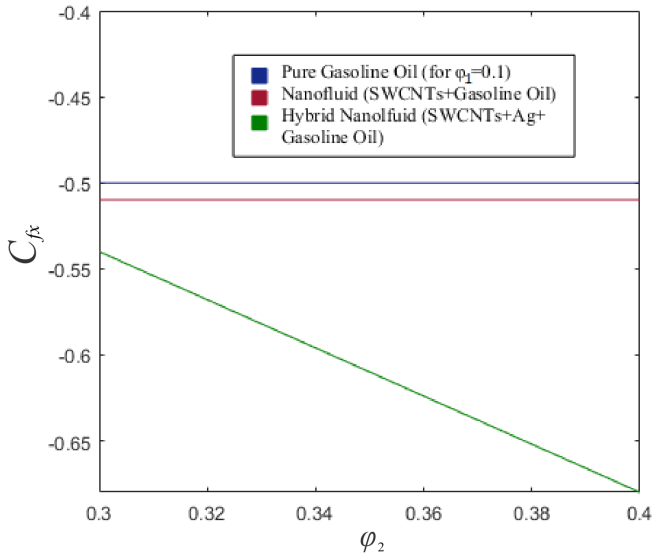

Fig. 4.25. Comparison of C_{fx} for φ_1 and φ_2.

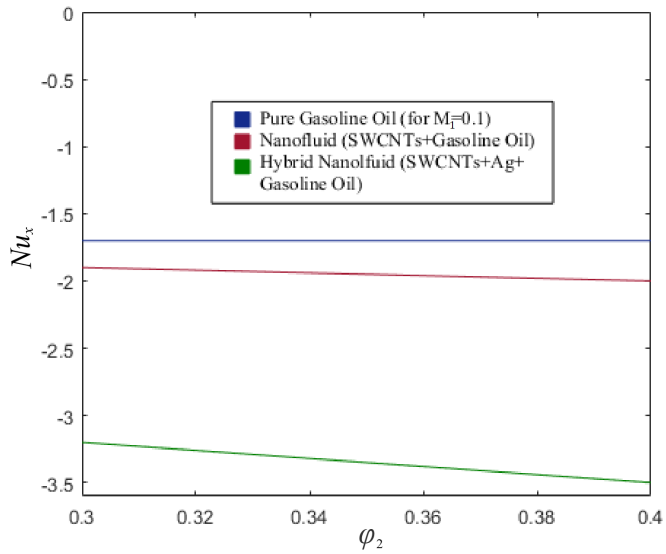

Fig. 4.26. Comparison of Nu_x for M_1 and φ_2.

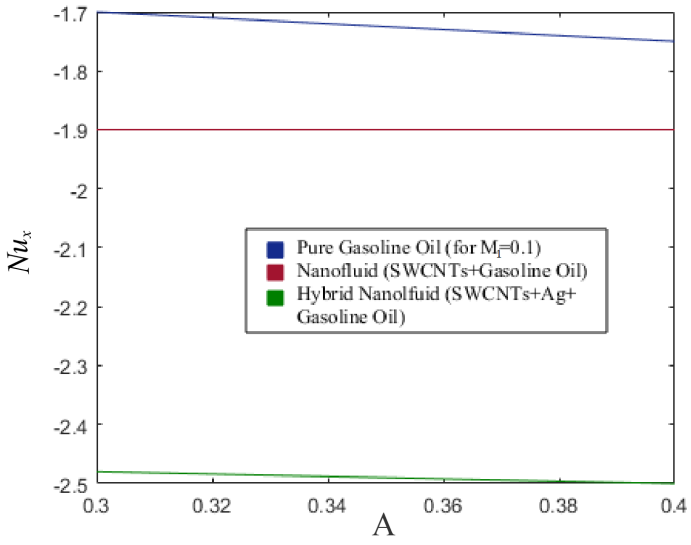

Fig. 4.27. Comparison of Nu_x for M_1 and A.

Chapter 5

The Magnetohydrodynamic Flow of Hybrid Nanofluid towards a Stretching Surface in the presence of Joule Heating and Melting Heat Transfer

This chapter focusses on the flow of a hybrid nanofluid (SWCNT, Ag and gasoline oil) near a stagnation point when magnetohydrodynamics is involved. The flow is induced by a stretching sheet with variable thickness and the effects of melting heat phenomenon, Joule heating, viscous dissipation and heat generation/absorption are also studied in the present flow model. The momentum and energy equations are reconstructed as ordinary differential equations by making use of appropriate similarity transformations. A numerical method, bvp4c is taken into account for the solution of the resulting equations and the variation in influential parameters for temperature and velocity alongwith Nusselt number and skin friction coefficient are explored graphically. The improved performance of hybrid nanofluid is exhibited through a graphical comparison of basefluid, nanofluid (SWCNTs and gasoline oil) and hybrid nanofluid (SWCNTs, Ag and gasoline oil).

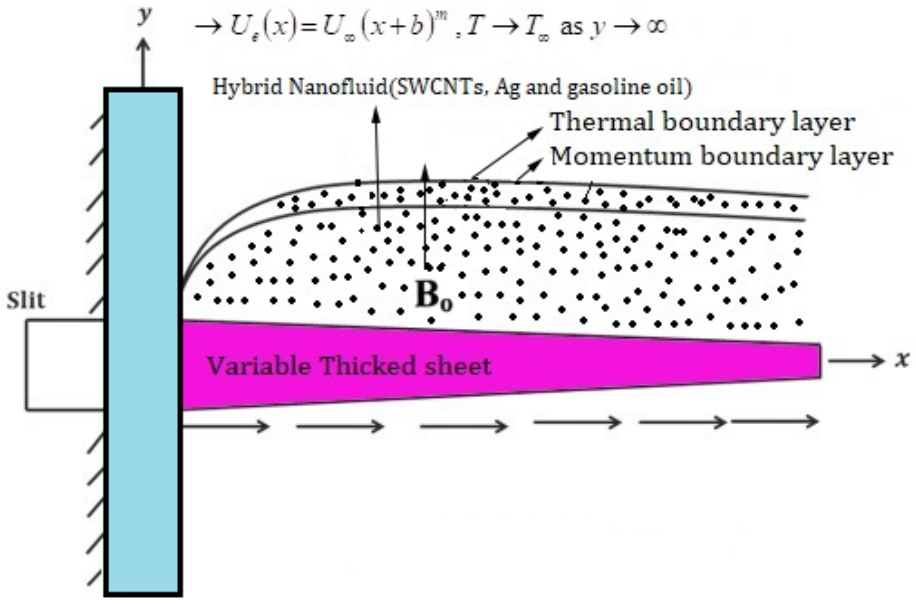

Fig. 5.1. Geometry of the problem.

5.1 Problem Formulation

A steady and magnetohydrodynamic flow involving hybrid nanofluid towards a variable thickened stretching sheet is examined for melting heat transfer. The sheet is stretching with a velocity given by $U_w = U_o(x+b)^m$ and $y = b^*(x+b)^{\frac{1-m}{2}}$ is the varying thickness of the sheet. The stretching sheet is placed in the direction orthogonal to y-axis. The flow is studied in stagnation point region and the significant effects of Joule heating alongwith viscous dissipation and heat generation/absorption affect the flow. The velocity of the sheet stretching is given by $U_w = U_o(x+b)^m$ while the thickness of the sheet is given by $y = b^*(x+b)^{\frac{1-m}{2}}$. In a position orthogonal to the y-axis, the stretching sheet is fixed. The flow is examined around the stagnation point, and the flow is significantly impacted by Joule heating, viscous dissipation, heat generation/absorption, and viscosity reduction.

We have considered the Cartesian coordinate system, so the velocity field is noted to be

$$\overrightarrow{\mathrm{V}} = [u(x,y),\ v(x,y),0], \tag{5.1}$$

The modeled equations can be exhibited as

$$\frac{\partial \rho}{\partial t} + \overrightarrow{\nabla}.\left(\rho\ \overrightarrow{\mathrm{V}}\right) = 0, \tag{5.2}$$

$$\rho_{hnf}\left(\frac{\partial \overrightarrow{\mathrm{V}}}{\partial t} + \left(\overrightarrow{\mathrm{V}}.\overrightarrow{\nabla}\right)\overrightarrow{\mathrm{V}}\right) = \overrightarrow{\nabla}.\overrightarrow{\tau} + \rho_{hnf}\ \overrightarrow{\mathrm{b}}, \tag{5.3}$$

$$(\rho C_p)_{hnf}\left(\frac{\partial T}{\partial t} + \left(\overrightarrow{\mathrm{V}}.\overrightarrow{\nabla}\right)T\right) = -\overrightarrow{\nabla}.\overrightarrow{\mathrm{q}} + Tr\left(\overrightarrow{\tau}.\overrightarrow{\mathrm{L}}\right), \tag{5.4}$$

$$\overrightarrow{\mathrm{q}} = -k\,\mathrm{grad}\,T.$$

Eq. 5.2 in the above written equations is introduced as the continuity equation. Mass conservation law serves as the basis for this equation. Newton's second law is the foundation for the momentum equation and in this equation, LHS stands for inertial forces, whereas the first term on the RHS is for surface forces and the second term is for body forces. The energy equation is obtained using the first law of thermodynamics. Here the LHS represents the total system's energy, whereas the 1st term given on the RHS is owing to Fourier's law of heat conduction and the 2nd term is brought on by dissipation.

In Eqs. 5.2 to 5.4, density is denoted as ρ, $\overrightarrow{\mathrm{V}}$ is introduced as velocity field, T represents fluids temperature, $\overrightarrow{\mathrm{q}}$ is the heat flux, $\overrightarrow{\mathrm{b}}$ is noted for body force, k for the thermal conductivity.

Assuming electric field $\overrightarrow{\mathrm{E}} = 0$, the electromagnetic force is indicated by

$$\overrightarrow{\mathrm{J}} \times \overrightarrow{\mathrm{B}} = -\sigma_{hnf} B_0^2(\mathrm{U}_e - \mathrm{u}), \tag{5.5}$$

where B_0 denotes the applied magnetic field in direction perpendicular to surface, σ stands for electrical conductivity and U_e for free stream velocity.

Further now with the help of boundary layer theory, the system of differential equations adopts following formation:

$$\frac{\partial u}{\partial x} + \frac{\partial v}{\partial y} = 0, \tag{5.6}$$

$$u\frac{\partial u}{\partial x}+v\frac{\partial u}{\partial y}=U_e\frac{dU_e}{dx}+\upsilon_{hnf}\frac{d^2u}{dy^2}-\frac{\sigma_{hnf}}{\rho_{hnf}}\beta_o^2(u-U_e), \tag{5.7}$$

$$u\frac{\partial T}{\partial x}+v\frac{\partial T}{\partial y}=\alpha_{hnf}\frac{\partial^2 T}{\partial y^2}+\frac{\mu_{hnf}}{(\rho c_p)_{hnf}}\left(\frac{\partial u}{\partial y}\right)^2+\frac{\sigma_{hnf}}{(\rho c_p)_{hnf}}\beta_o^2(u-U_e)^2+\frac{Q_0}{(\rho c_p)_{hnf}}(T-T_m), \tag{5.8}$$

The assumptions under consideration suggest the following boundary conditions.

$$\begin{aligned} u &= U_w(x)=U_0(x+b)^m,\quad v=0\ ,\ T=T_m \text{ at } y=b^*(x+b)^{\frac{1-m}{2}}\ , \\ u &\rightarrow U_e(x)=U_\infty(x+b)^m,\ T\rightarrow T_\infty \text{ as } y\rightarrow\infty, \end{aligned} \tag{5.9}$$

where u and v are noted to be orthogonal velocity components, U_0 , U_∞ are arbitrary constants, U_w is stretching velocity and T_m is surface temperature .

The melting heat transfer is given through:

$$\kappa_{hnf}\left(\frac{\partial T}{\partial y}\right)_{y=b^*(x+b)^{\frac{1-m}{2}}}=\rho_{hnf}\left[\lambda+C_s(T_m-T_0)\right]v_{\ y=b^*(x+b)^{\frac{1-m}{2}}}, \tag{5.10}$$

in which κ_{hnf} be the thermal conductivity represented for hybrid nanofluid, likewise ρ_{hnf} be the density of hybrid nanofluid, C_s be the heat capacity of solid surface, λ be the latent heat.

We consider the following transformations to change the partial differential equations to simplified differential equations.

$$\begin{aligned} \eta &= \sqrt{\frac{m+1}{2\upsilon_f}U_0(x+b)^{m-1}}y\ ,\ \Psi=\sqrt{\frac{2\upsilon_f}{m+1}U_0(x+b)^{m+1}}f^*(\eta)\ ,\ \theta^*(\eta)=\frac{T-T_m}{T_\infty-T_m}, \\ u &= U_0(x+b)^m f^{*'}(\eta),\quad v=\sqrt{\frac{(m+1)\upsilon_f}{2}U_0(x+b)^{m-1}}\left(f^*(\eta)+\eta f^{*'}(\eta)\frac{m-1}{m+1}\right). \end{aligned} \tag{5.11}$$

where f *represent non-dimentional velocity, θ^* be the temperature, m is flow behavior index parameter and υ_f is kinematic viscosity. Using these equations, we get

$$\frac{A_{11}}{(1-\varphi_1)^{2.5}(1-\varphi_2)^{2.5}}f^{*'''}+f^*f^{*''}-\frac{2m}{m+1}\left(f^{*'}\right)^2+\frac{2m}{m+1}A^2-\frac{1}{m+1}A_{12}A_{11}M(f^{*'}-A)=0, \tag{5.12}$$

$$\frac{\kappa_{hnf}}{\kappa_f}\theta^{*''} + B_{11}Prf^*\theta^{*'} + \frac{\Pr Ec}{(1-\varphi_1)^{2.5}(1-\varphi_2)^{2.5}}\left(f^{*''}\right)^2 + \frac{\sigma_{hnf}}{\sigma_f}\frac{1}{m+1}EcM\Pr(f^{*'}-A)^2$$

$$+Pr\delta B_{11}\theta^* = 0, \tag{5.13}$$

$$f^{*'}(\alpha) = 1,\ \ \theta^*(\alpha) = 0,$$

$$\frac{k_{hnf}}{k_f}M_1\ \theta^{*'}(\alpha) + \left(A_{11}Prf^*\ \ (\alpha) + \frac{m-1}{m+1}\alpha\right) = 0\ \ \text{at}\ \alpha = b^*\sqrt{\frac{m+1}{2v_f}U_0}, \tag{5.14}$$

$$f^{*'}(\infty) \to A\ ,\ \theta^*(\infty) \to 1\ \text{as}\ \alpha \to \infty.$$

where φ_1 and φ_2 represent volume fraction of SWCNT and Ag. Also we have

$$A_{11} = \frac{1}{(1-\varphi_2)(((1-\varphi_1) + \varphi_1\frac{\rho_{SWCNTs}}{\rho_f}) + \varphi_2\frac{\rho_{Ag}}{\rho_f}}, \tag{5.15}$$

$$A_{12} = 1 + \frac{3(\frac{\varphi_1\sigma_1+\varphi_2\sigma_2}{\sigma_f} - (\varphi_1+\varphi_2))}{2 + (\frac{\varphi_1\sigma_1+\varphi_2\sigma_2}{\varphi_1+\varphi_2)\sigma_f}) - (\frac{\varphi_1\sigma_1+\varphi_2\sigma_2}{\sigma_f} - (\varphi_1+\varphi_2))}, \tag{5.16}$$

$$B_{11} = (1-\varphi_2)\left((1-\varphi_1) + \varphi_1\frac{(\rho C_p)_{SWCNTs}}{(\rho C_P)_f}\right) + \varphi_2\frac{(\rho C_p)_{Ag}}{(\rho C_p)_f}. \tag{5.17}$$

In this case, prime indicates the derivative with reference to η and $\alpha = b^*\sqrt{\frac{m+1}{2\nu_f}U_0}$. Here $\alpha = \eta$ describes flat surface. Consider $f^*(\eta) = f(\eta-\alpha) = f(\xi)$

$$\frac{A_{11}}{(1-\varphi_1)^{2.5}(1-\varphi_2)^{2.5}}f^{'''} + ff'' - \frac{2m}{m+1}\left(f'\right)^2 + \frac{2m}{m+1}A^2 - \frac{1}{m+1}A_{12}A_{11}M(f'-A) = 0, \tag{5.18}$$

$$\frac{\kappa_{hnf}}{\kappa_f}\theta'' + B_{11}Prf\theta' + \frac{\Pr Ec}{(1-\varphi_1)^{2.5}(1-\varphi_2)^{2.5}}\left(f''\right) + \frac{\sigma_{hnf}}{\sigma_f}\frac{1}{m+1}EcM\Pr(f'-A)^2$$

$$+\frac{\sigma_{hnf}}{\sigma_f}\frac{1}{m+1}EcM\Pr(f'-A)^2 + Pr\delta B_{11}\theta\ \ = 0, \tag{5.19}$$

$$\begin{aligned} f^{'}(0) &= 1\ ,\ \theta(0)=0\ ,\ \frac{k_{hnf}}{k_f}M_1\ \theta^{'}(0)+\left(A_{11}Prf\ (0)+\frac{m-1}{m+1}\alpha\right)=0, \qquad (5.20)\\ f^{'}(\infty) &\rightarrow A\ ,\ \theta(\infty)\rightarrow 1 \text{ for } \xi\rightarrow\infty. \end{aligned}$$

The dimensionless quantities are defined as

$$A = \frac{U_\infty}{U_0}\ ,\ \alpha=b^*\sqrt{\frac{m+1}{2\upsilon_f}}U_0\ ,\ M_1=\frac{C_{\rho f}(T_\infty-T_m)}{\lambda+C_s\left(T_m-T_0\right)}, \qquad (5.21)$$

$$Pr = \frac{\nu_f}{\alpha_f},\ Ec=\frac{(U_w(x))^2\rho_f}{(\rho c_p)_f\left(T_\infty-T_m\right)},\ M=\frac{2\sigma_f B^2}{\rho_f U_o(x+b)^{m-1}}, \qquad (5.22)$$

$$\delta = \frac{2Q_o}{(\rho C_p)_{hnf}(m+1)U_o(x+b)^{m-1}}. \qquad (5.23)$$

In these terms, α is wall thickness parameter, M is magnetic parameter, Pr is Prandtl number, Ec is defined as Eckert number, M_1 is the melting parameter, δ is the heat generation/absorption parameter.Now we define the Surface friction coefficient (C_f) and Nusselt number (Nu_x) as follows:

$$C_f=\frac{\tau_w}{\rho_f\ U_w^2}, \qquad (5.24)$$

where

$$\tau_w=\mu_{hnf}\left(\frac{\partial u}{\partial y}\right)_{y=b^*\sqrt{\frac{m+1}{2\upsilon_f}U_0}}. \qquad (5.25)$$

Also

$$Nu_x=\frac{(x+b)\,q_w}{k\left(T_\infty-T_m\right)}, \qquad (5.26)$$

$$q_w=-k_{hnf}\left(\frac{\partial T}{\partial y}\right)_{y=b^*\sqrt{\frac{m+1}{2\upsilon_f}U_0}}. \qquad (5.27)$$

We acquire non-dimensional representations of C_f and Nu_x as

$$C_f\sqrt{\mathrm{Re}_x}=\frac{1}{(1-\varphi_1)^{2.5}(1-\varphi_2)^{2.5}}\sqrt{\frac{m+1}{2}}f''(0)\,, \qquad (5.28)$$

$$\frac{Nu_x}{\sqrt{\mathrm{Re}_x}}=-\frac{\kappa_{hnf}}{\kappa_f}\sqrt{\frac{m+1}{2}}\theta^{'}(0). \qquad (5.29)$$

where $\mathrm{Re}_x=\frac{U_0(x+b)}{\nu_f}$.

Table. 5.1. The thermophysical properties associated with the considered nanofluid. Muhammad *et al.* [139].

Properties	Nanofluid
Dynamic viscosity	$\mu_{nf} = \frac{\mu_f}{(1-\varphi_1)^{2.5}}$
Kinematic viscosity	$\nu_{nf} = \frac{\mu_{nf}}{\rho_{nf}}$
Heat capacitance	$(\rho c_p)_{nf} = (1-\varphi_1)(\rho c_p)_f + \varphi_1(\rho c_p)_{SWCNTs}$
Density	$\rho_{nf} = (1-\varphi_1)\rho_f + \varphi_1\rho_{SWCNTs}$
Thermal conductivity	$\frac{\kappa_{nf}}{\kappa_f} = \frac{\kappa_{SWCNTs}+(n-1)\kappa_f-(n-1)\varphi_1(\kappa_f-\kappa_{SWCNTs})}{\kappa_{SWCNTs}+(n-1)\kappa_f+\varphi_1(\kappa_f-\kappa_{SWCNTs})}$

Table. 5.2. For Hybrid nanofluid (SWCNTs, Ag and gasoline oil). Muhammad *et al.* [139].

Thermophysical properties	Hybrid nanofluid
Dynamic viscosity	$\frac{\mu_{hnf}}{\mu_f} = \frac{1}{(1-\varphi_1)^{2.5}(1-\varphi_2)^{2.5}}$
Density	$\frac{\rho_{hnf}}{\rho_f} = (1-\varphi_2)\left((1-\varphi_1)+\varphi_1\frac{\rho_{SWCNTs}}{\rho_f}\right)+\varphi_2\left(\frac{\rho_{Ag}}{\rho_f}\right)$
Electrical conductivity	$\frac{\sigma_{hnf}}{\sigma_f} = 1+\frac{3(\frac{\varphi_1\sigma_1+\varphi_2\sigma_2}{\sigma_f}-(\varphi_1+\varphi_2))}{2+(\frac{\varphi_1\sigma_1+\varphi_2\sigma_2}{(\varphi_1+\varphi_2)\sigma_f})-(\frac{\varphi_1\sigma_1+\varphi_2\sigma_2}{\sigma_f}-(\varphi_1+\varphi_2))}$
Heat capacitance	$\frac{(\rho c_p)_{hnf}}{(\rho c_p)_f} = (1-\varphi_2)\left[1-\varphi_1+\varphi_1(\frac{(\rho c_p)_{SWCNT}}{(\rho c_p)_f})\right]+\varphi_2(\frac{(\rho c_p)_{Ag}}{(\rho c_p)_f})$
Thermal conductivity	$\frac{\kappa_{hnf}}{\kappa_{nf}} = \frac{\kappa_{Ag}+(n-1)\kappa_{nf}-(n-1)\varphi_2(\kappa_{nf}-\kappa_{Ag})}{\kappa_{Ag}+(n-1)\kappa_{nf}+\varphi_2(\kappa_{nf}-\kappa_{Ag})}$ $\frac{\kappa_{nf}}{\kappa_f} = \frac{\kappa_{SWCNTs}+(n-1)\kappa_f-(n-1)\varphi_1(\kappa_f-\kappa_{SWCNTs})}{\kappa_{SWCNTs}+(n-1)\kappa_f+\varphi_1(\kappa_f-\kappa_{SWCNTs})}$

Table. 5.3. Important thermal features of (SWCNTs, Ag and gasoline oil). Muhammad *et al.* [139].

Nanoparticle	Properties				
Nanoparticle	$\rho\left(\frac{kg}{m^3}\right)$	Pr	$c_p(\frac{J}{kgK})$	$\kappa(\frac{W}{mK})$	$\sigma\left(\frac{s}{m}\right)$
Ag	10490	-	235	429	6.30×10^7
SWCNTs	1600	-	796	3000	10000
Gasoline oil	760	9.4	1.8691	0.114	25

5.2 Numerical Stratagem:

The fluid flow problems generally involve coupled and nonlinear equations, thus providing a challenge to the researcher for its solution. These problems can be handled through their numerical treatment which leads to effective solution of the problem. The bvp4c technique, a MATLAB built-in function is used to form solutions for the governed flow expressions (ODEs) numerically. This method employs first order differential equations solution to initiate the methodology.

$$f_1 = f, \tag{5.30}$$

$$f_2 = f_1^{'} = f^{'}, \tag{5.31}$$

$$f_3 = f_2^{'} = f^{''}, \tag{5.32}$$

$$f_5 = \theta, \quad f_6 = f_5^{'} = \theta^{'}, \tag{5.33}$$

$$f_4 = f_3^{'} = f^{'''} = -\frac{(1-\varphi_1)^{2.5}(1-\varphi_2)^{2.5}}{A_{11}} \begin{pmatrix} f_1 f_3 - \frac{2m}{m+1}(f_2)^2 + \frac{2m}{m+1}A^2 \\ -\frac{1}{m+1}A_{12}A_{11}M(f_2 - A) \end{pmatrix}, \tag{5.34}$$

$$f_7 = f_6^{'} = \theta^{''} = -\frac{1}{\frac{\kappa_{hnf}}{\kappa_f}} \begin{pmatrix} B_{11}\,\mathrm{Pr}\, f_1 f_6 + \frac{\mathrm{Pr}\, Ec}{(1-\varphi_1)^{2.5}(1-\varphi_2)^{2.5}}(f_3)^2 \\ +\frac{\sigma_{hnf}}{\sigma_f}\frac{1}{m+1}EcM\,\mathrm{Pr}(f_2 - A)^2 + \mathrm{Pr}\,\delta B_{11} f_5 \end{pmatrix}, \tag{5.35}$$

5.3 Graphical Results and Discussion

The graphical behavior of velocity and temperature owing to the diverse parameters are plotted and talked about. In addition to this, the results by varying important parameters with respect to skin friction coefficient and Nusselt number are also brought to light in this section. The analysis can help researchers and industrialists to understand the mechanism of hybrid nanofluid flow for the considered model and implement the model where required. To verify our current study, we have performed the relative examination of basefluid i.e., gasoline oil, nanofluid that includes SWCNT and gasoline oil and the hybrid nanofluid consisting of SWCNT, Ag and gasoline oil. Fig. 5.2. shows how SWCNTs volume fraction φ_1 influences the velocity profile. $f^{'}(\eta)$ experiences an increase for the larger values of φ_1, where hybrid nanofluid is observed to have greater influence than nanofluid. To investigate the dominance

of Ag volume fraction given by φ_2 for the velocity profile $f^{'}(\eta)$, Fig. 5.3. is shown. It is distinguishable that the velocity behavior improves with a rise of φ_2. The change in velocity profile $f^{'}(\eta)$ with increasing melting parameter M_1 is shown in Fig. 5.4. This figure portrays a larger $f^{'}(\eta)$ corresponds to higher M_1. For a higher M_1, the fluid particles tend to move towards the fluid from the surface due to the high temperature of the fluid and initiates a more rapid movement of fluid particles, resulting in an increased velocity distribution. Higher melting parameter values are associated with higher convective flow from heated fluid to the melting surface. The impact of flow behavior index parameter m on the velocity profile is plotted in Fig. 5.5. Velocity distribution reduces for increased m as wall thickness increases. Moreover, hybrid nanofluid showing stronger impact than nanofluid can be seen from the figure. The increasing values of wall thickness parameter α for the velocity distribution is displayed in Fig. 5.6. The increasing velocity profile can be seen in this figure. Fig. 5.7. is sketched to highlight the control of magnetohydrodynamics M on the velocity profile. As M rises, the velocity profile shortens down. This occurs as a result of Lorentz forces, which are resistance forces and prevent fluid particle motion. To discover the conduct of basefluid, nanofluid and hybrid nanofluid, Figs. 5.8. to 5.10. are plotted. The results support our present study and reveals that hybrid kind of nanofluid is ahead of basefluid and even the nanofluid. The analysis of $\theta(\eta)$ for rising values of SWCNTs volume fraction φ_1 is depicted in Fig. 5.11. There exist an inverse relation between temperature profile φ_1 i.e., higher values of φ_1 are associated to weak temperature profile. Fig. 5.12. demonstrates that the relationship between variable Ag volume fraction φ_2 and the temperature profile $\theta(\eta)$. A reduced temperature profile can be attained for higher φ_2 and this conclusion is quite obvious for hybrid nanofluid but if nanofluid is considered, the results seem to be not clear. This is in accordance to the expected facts. Fig. 5.13. illustrates that the Eckert number Ec affects the temperature profile. Due to more kinetic energy which raises the temperature. A rise in Eckert number causes an elevation in the temperature profile. Fig. 5.14. indicates that temperature profile increases as M increases. This is because of Lorentz forces which is a resistance force and resists the motion of fluid particles. The role of the heat generation or absorption parameter δ for the temperature distribution is delineated in Fig. 5.15. The fluid's thermal state is likely to rise as the heat generation parameter δ is increased. Through the thermal buoyancy effect, this rise in fluid temperature

induces additional flow toward the plate, thus temperature profile increases. This increase is prominent in both the hybrid nanofluid and the nanofluid. The impact of parameters like φ_1, φ_2 and M, A on skin friction coefficient is pictured in Figs. 5.16. and 5.17. The friction drag lessens with the elevated values of φ_1 and φ_2. Figs. 5.18. and 5.19. are drawn to estimate the impact of φ_1, φ_2 and Ec, A on the Nusselt number, which shows an increasing trend as the parameter φ_1 grows. It demonstrates how variations in φ_1,and φ_2, Ec and A is related to the Nusselt number. The discussion clearly takes the analysis to the level where reduced friction drag and enhanced heat transfer rate can be attained. Figs. 5.20. and 5.21. are sketched for the comparison of the considered fluids and the excellence of hybrid nanofluid can be proved from the images provided.

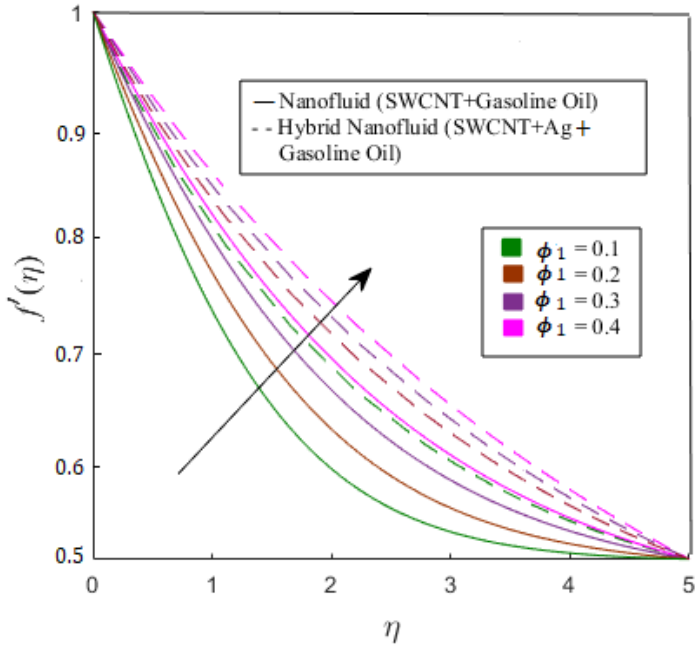

Fig. 5.2. Velocity distribution $f^{'}(\eta)$ for φ_1.

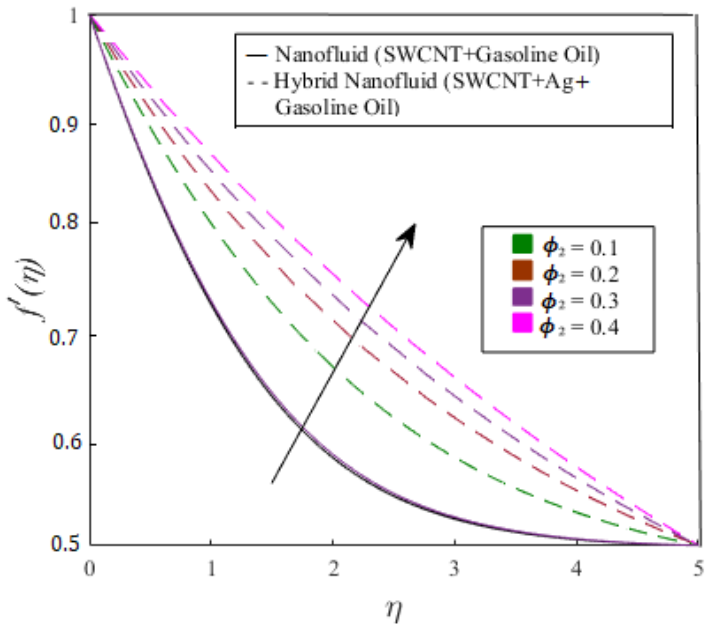

Fig. 5.3. Velocity distribution $f^{'}(\eta)$ for φ_2.

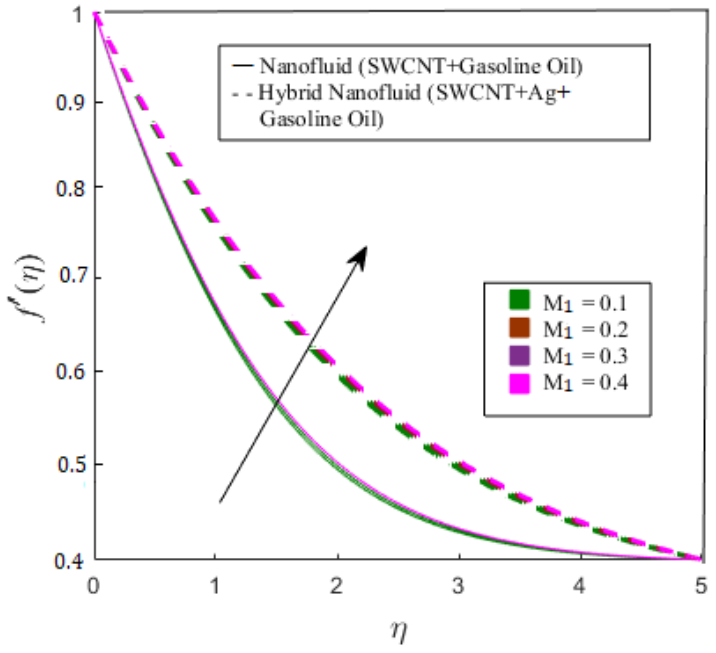

Fig. 5.4. Velocity distribution $f^{'}(\eta)$ for M_1.

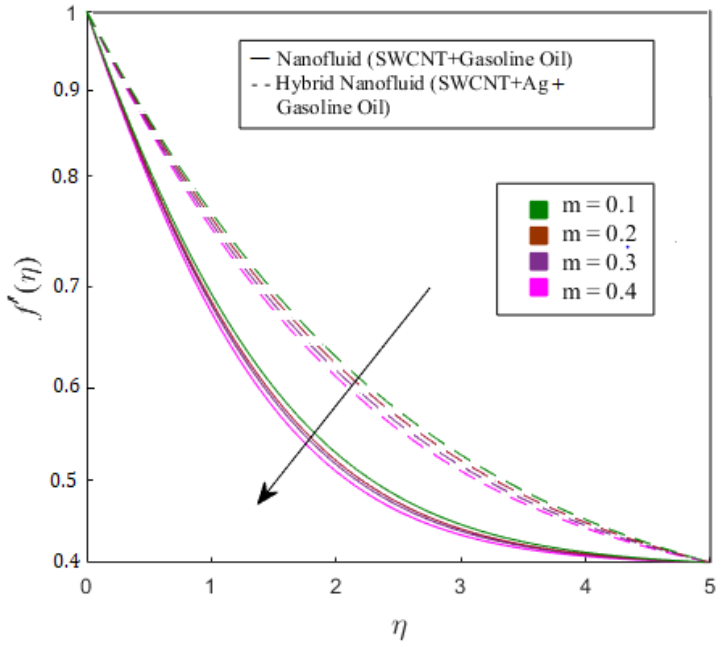

Fig. 5.5. Velocity distribution $f'(\eta)$ for m.

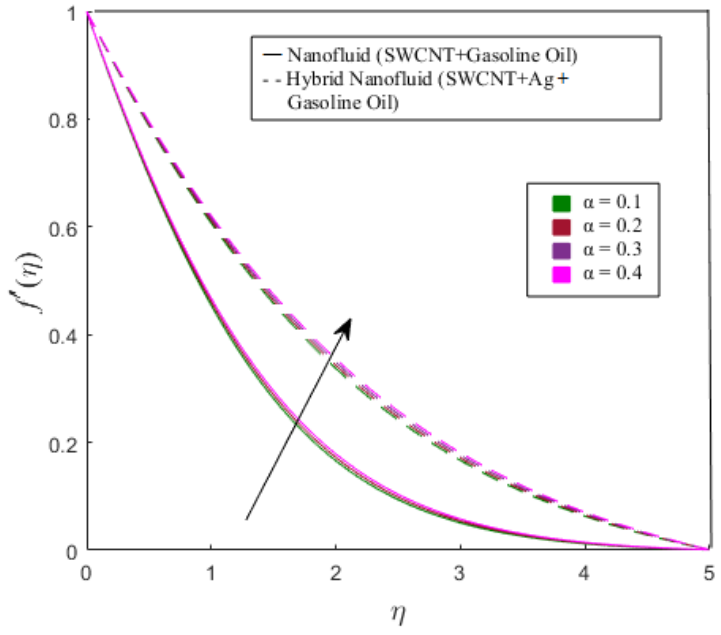

Fig. 5.6. Velocity distribution $f'(\eta)$ for α.

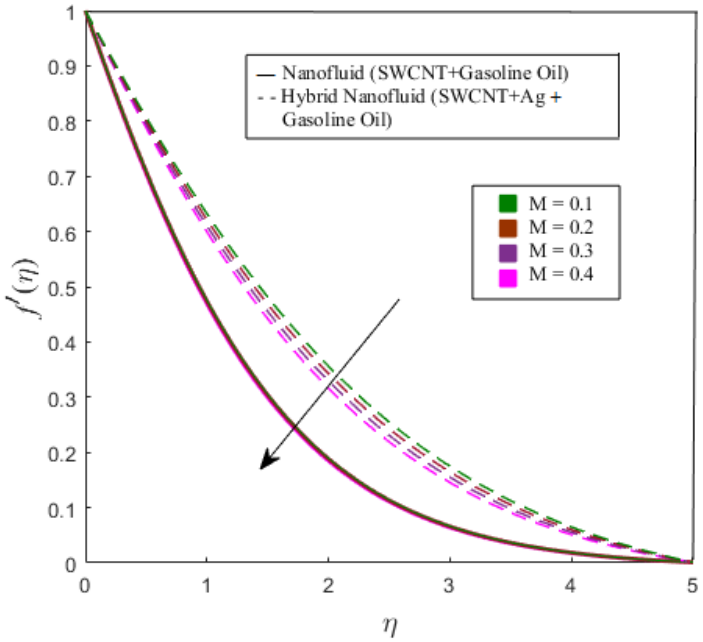

Fig. 5.7. Velocity distribution $f^{'}(\eta)$ for M.

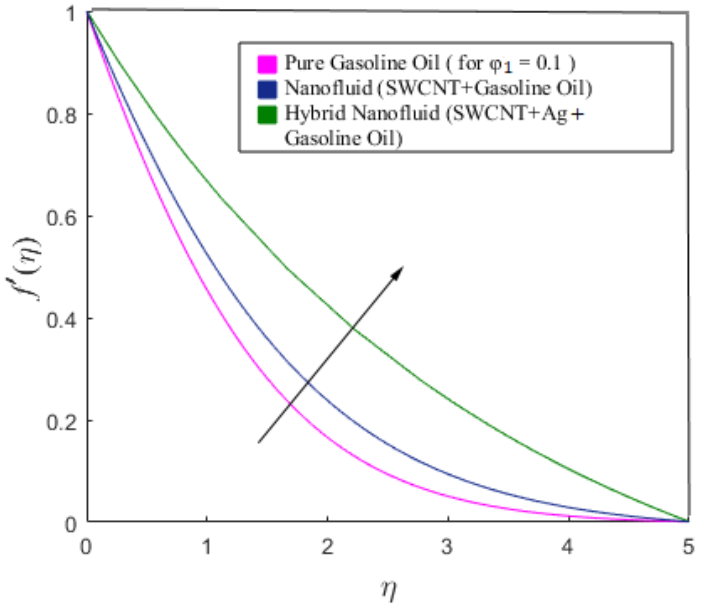

Fig. 5.8. Comparison of $f^{'}(\eta)$ for φ_1.

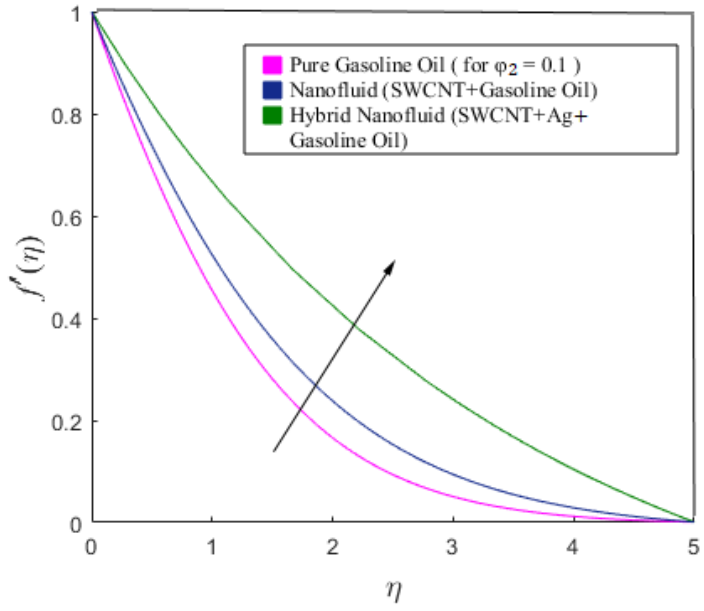

Fig. 5.9. Comparison of $f^{'}(\eta)$ for φ_2.

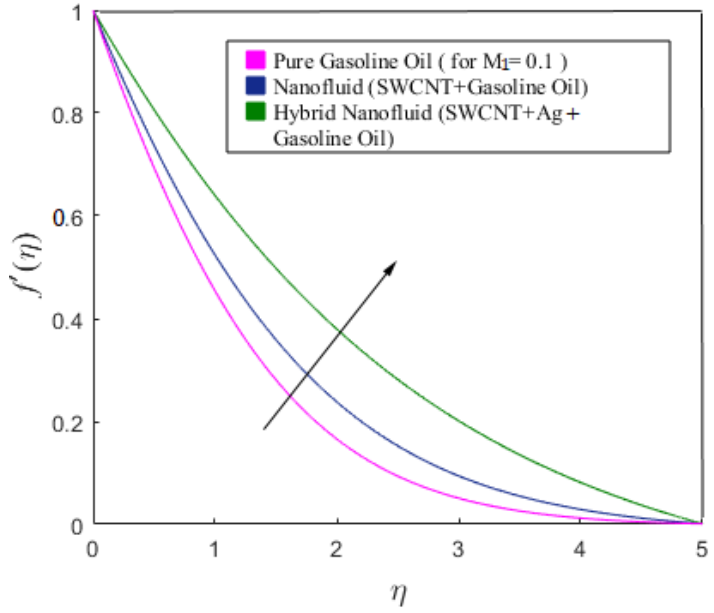

Fig. 5.10. Comparison of $f^{'}(\eta)$ for M_1.

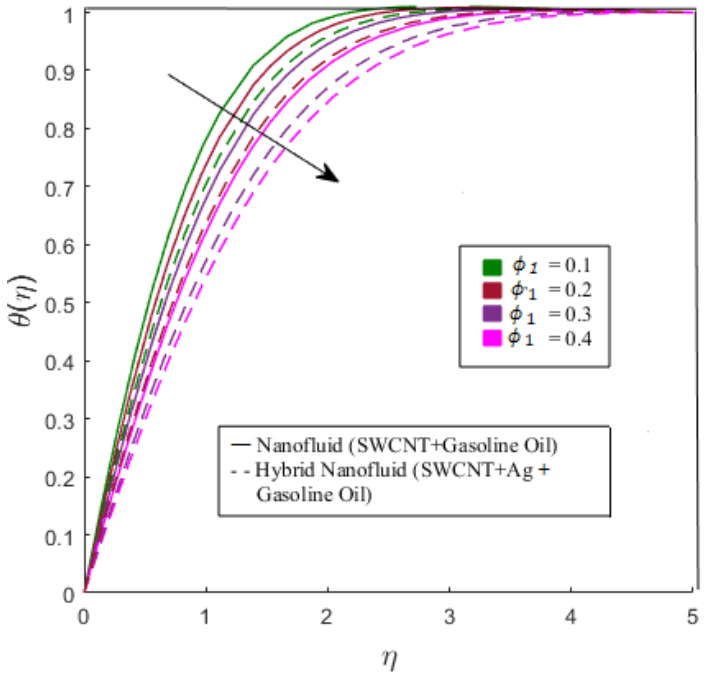

Fig. 5.11. Temperature distribution $\theta(\eta)$ for φ_1.

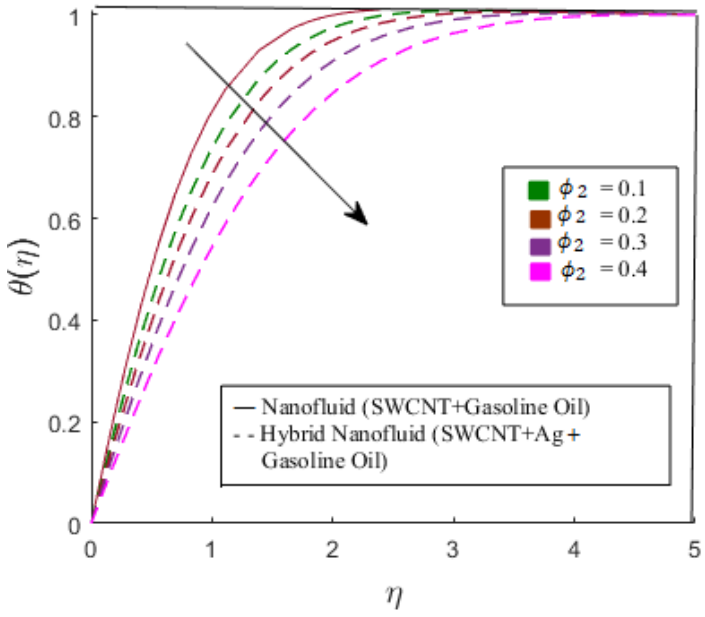

Fig. 5.12. Temperature distribution $\theta(\eta)$ for φ_2.

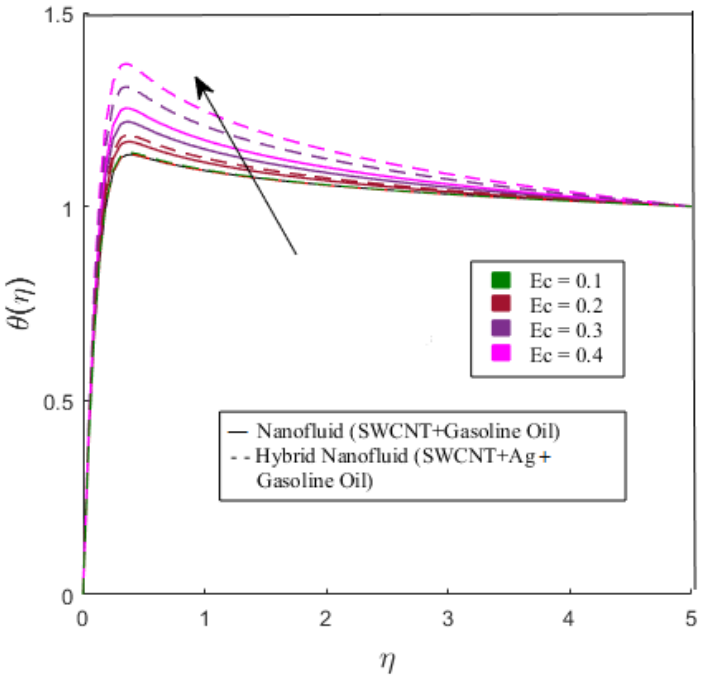

Fig. 5.13. Temperature distribution $\theta(\eta)$ for Ec.

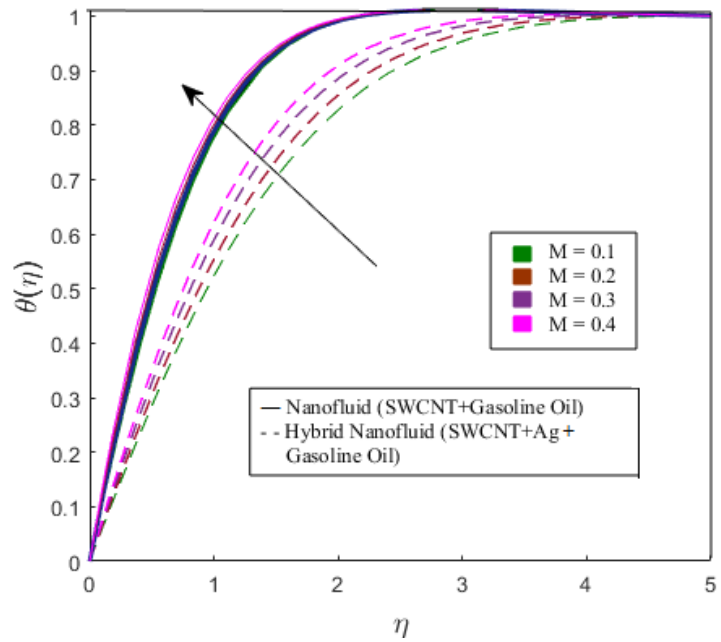

Fig. 5.14. Temperature distribution $\theta(\eta)$ for M.

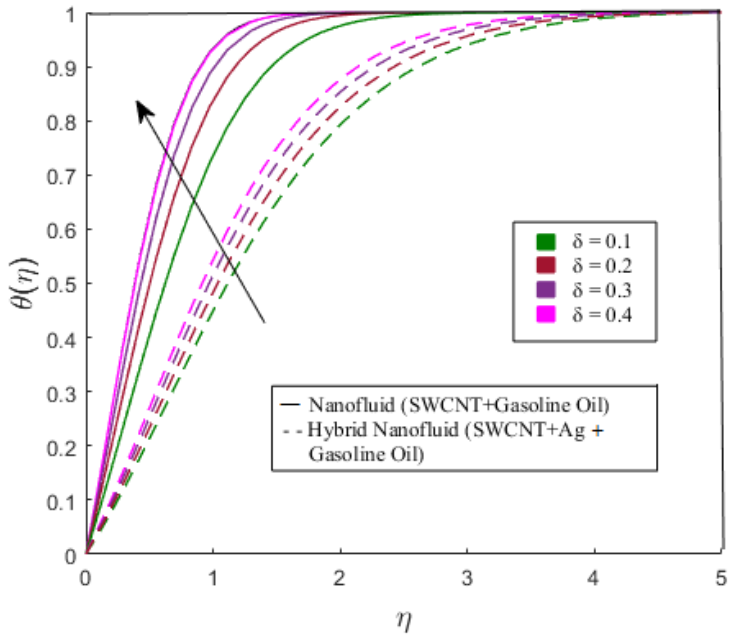

Fig. 5.15. Temperature distribution $\theta(\eta)$ for δ.

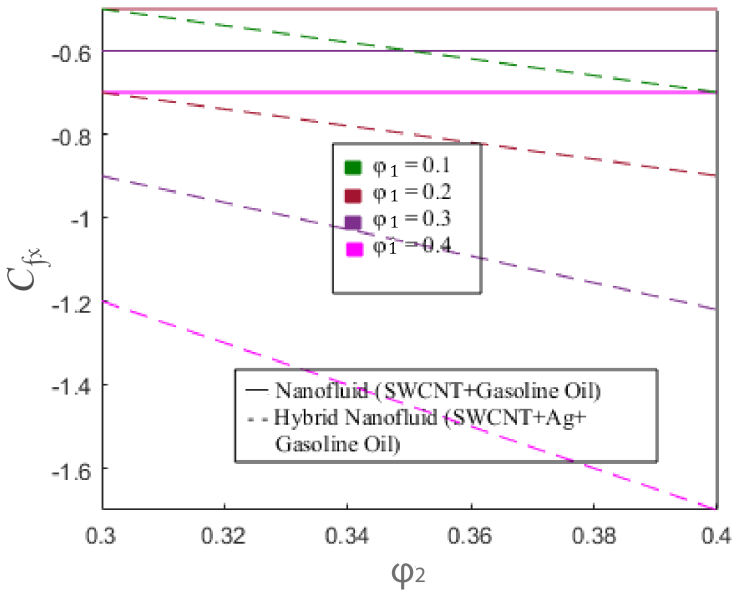

Fig. 5.16. Skin friction coefficient C_{fx} for φ_1 and φ_2.

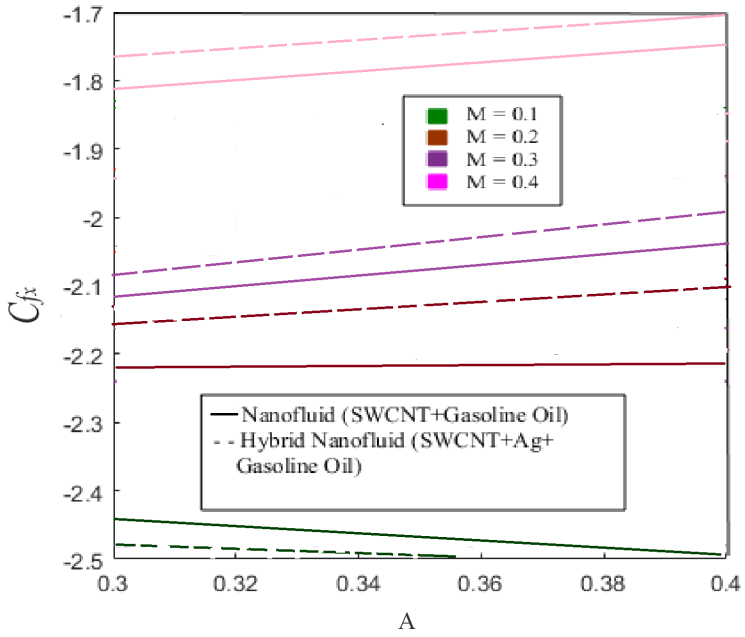

Fig. 5.17. Skin friction coefficient C_{fx} for M and A.

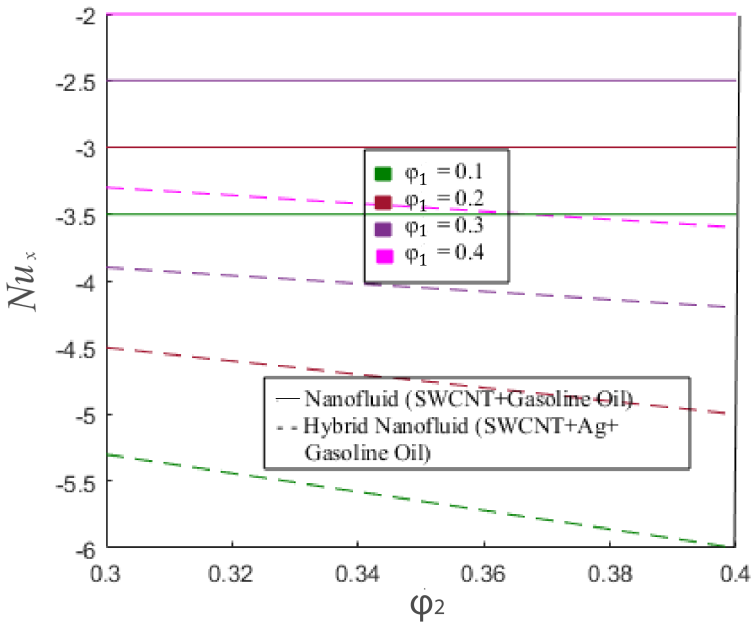

Fig. 5.18. Nusselt number Nu_x for φ_1 and φ_2.

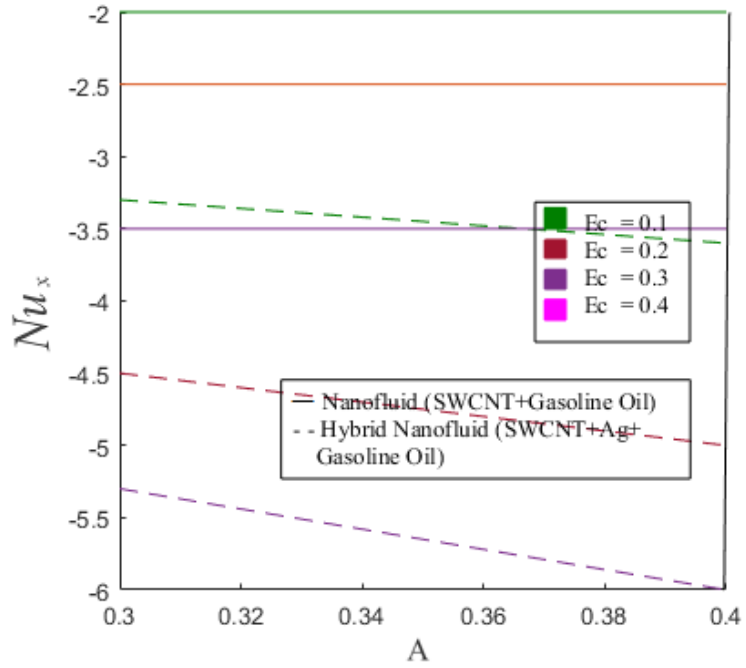

Fig. 5.19. Nusselt number Nu_x for Ec and A.

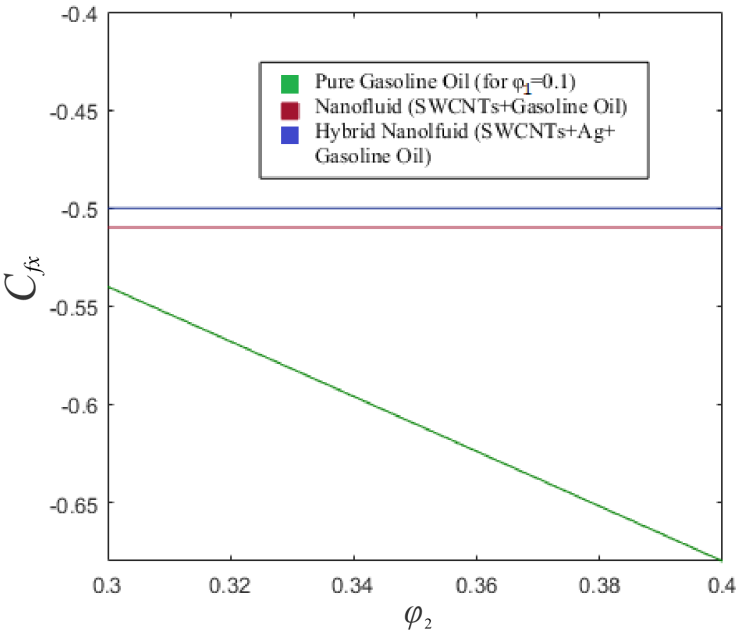

Fig. 5.20. Comparison of C_{fx} for φ_1 and φ_2.

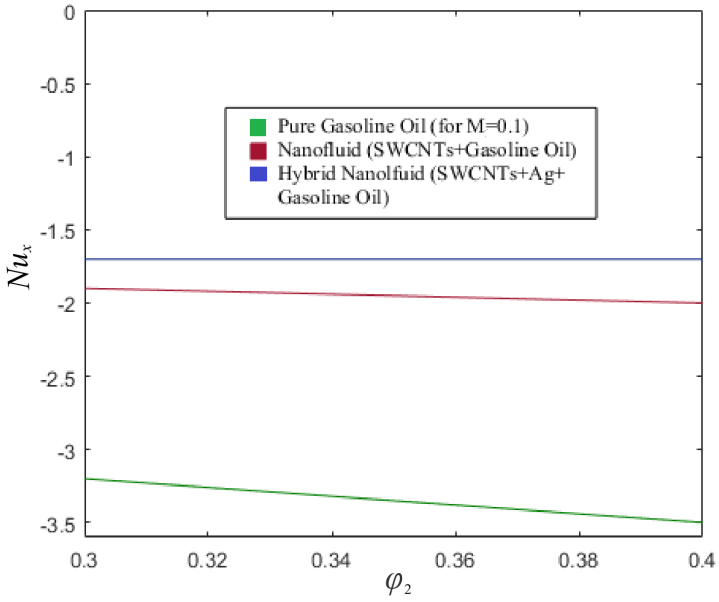

Fig. 5.21. Comparison of Nu_x for M and φ_2.

Chapter 6

Concluded and Future work

6.1 Conclusion remarks

In this research, the stagnation point flow of a hybrid nanofluid (SWCNT, Ag and gasoline oil) was investigated in relation to magnetohydrodynamics. Additionally elaborated are the effects of melting heat phenomenon and viscous dissipation. The system of equations are presented in term of PDEs which are then simplified into ODEs after applying transformation. The numerical investigation of the problem yields interesting results. The velocity distribution enhances for the rising values of φ_1 and also φ_2. Considering amplified values of M_1 and α, the velocity profile improves. The velocity profile reduces with the intensified value of m. Enhanced parameter A leads to an increase in the fluid's velocity for $A \succ 1$. The increment in values of M descends velocity distribution. The temperature distribution decreases if φ_1 and φ_2 are enhanced. Higher values of M_1 force the temperature profile to diminish. When magnetic parameter M is increased, the temperature distribution rises. The boost in the values of Eckert number Ec strengthens the temperature profile. When heat generation parameter increases, temperature profile reduces. For a better estimate of skin friction coefficient, the non dimensional velocity A at the melting parameter is minimized. Nu_x is strongly affected by increasing values of φ_1, φ_2, Ec and A. The heat transfer can be enhanced for smaller Ec. A comparative study is conducted between hybrid nanofluid (SWCNTs, Ag and gasoline oil), nanofluid (SWCNTs and gasoline oil) alongwith base fluid (gasoline oil) for rising values of involved parameters and the outcomes clearly point towards hybrid nanofluid excellence. In

addition, the results of hybrid nanofluid will reduced to ordinary nanofluid if $\varphi_2 = 0$.

6.2 Future Work

In this work the effects of melting heat transfer of hybrid nanofluid near a stagnation point towards a variable thicked sheet have been analyzed. However, there is still space to improve the existing work in order to address other different concerns. The following are some interesting possible studies that could be done in the future. The mixed convection flow for hybrid nanofluid due to irregular variably thicked moving surface with convex and concave effects. The investigation of MHD flow of hybrid nanofluid over a curved surface in the presence of thermal radiation and Arrhenius kinetics. The stagnation point flow and heat transfer modified hybrid nanofluid with Cattaneo-Christov heat flux model.

References

[1] S. U. S. Choi and J. A. Eastman, Enhancing thermal conductivity of fluids with nanoparticle.(1995). *International Mechanical Engineering Congress and Exposition*. 66, 99–105.

[2] Turcu. R., Darabont. A., Nan. A., Aldea. N., Macovei. D., Bica. D. and Koo. A. (2006). *New polypyrrole-multiwall carbon nanotubes hybrid materials. Journal of optoelectronics and advanced materials*. 8 (2), 643-647.

[3] Jana. S. Khojin. A. S. and Zhong. W. H. (2007). Enhancement of fluid thermal conductivity by the addition of single and hybrid nano-additives. *Thermochimica Acta*. 462 (1), 45-55.

[4] Suresh. S., Venkitaraj. K. P., Selvakumar. P., and Chandrasekar. M. (2012). Effect of /water hybrid nanofluid in heat transfer. *Experimental Thermal and Fluid Science*. 38, 54-60.

[5] Labib. M. N., Nine. M. J., Afrianto. H., Chung. H. and Jeong. H. (2013). Numerical investigation on effect of base fluids and hybrid nanofluid in forced convective heat transfer. *International Journal of Thermal Sciences*. 71, 163-171.

[6] Madhesh. D. and Kalaiselvam. S. (2014). Experimental analysis of hybrid nanofluid as a coolant. *Procedia engineering*. 97 , 1667-1675.

[7] Esfe. M. H., Alirezaie. A. and Toghraie. D. (2021). Thermal conductivity of ethylene glycol based nanofluids containing hybrid nanoparticles of SWCNT its price-performance analysis for energy management. *Journal of Materials Research and Technology*. 14, 1754-1760.

[8] Yaseen. M., Rawat. S. K., Shafiq. A., Kumar. M. and Nonlaopon. K. (2022). Analysis of heat transfer of mono and hybrid nanofluid flow between two parallel plates in a Darcy porous medium with thermal radiation and heat generation/absorption. *Symmetry.* 14(9), 1943.

[9] Huminic. G., Huminic. A., Dumitrache. F., Fleacă. C. and Morjan. I. (2020). Study of the thermal conductivity of hybrid nanofluids: Recent research and experimental study. *Powder Technology.* 367, 347-357.

[10] Li. Z., Shahsavar. A., Niazi. K., A. A., A. A. Al-Rashed. Sara Rostami. (2020). Numerical assessment on the hydrothermal behavior and irreversibility of hybrid nanofluid flow through a sinusoidal hairpin heat-exchanger. *International Communications in Heat and Mass Transfer.* 115, 104628.

[11] Rostami. Nademi. M., Dinarvand. S. and Pop.L., (2018) ."Dual solutions for mixed convective stagnation-point flow of an aqueous silica–alumina hybrid nanofluid." *Chinese journal of physics.* 56(5) , 2465-2478.

[12] Shoaib. M., Raja M. A. Z., Sabir. M. T., Nisar, K. S., Jamshed. W., Felemban. B. F. and Yahia. I. S. (2021). MHD hybrid nanofluid flow due to rotating disk with heat absorption and thermal slip effects: an application of intelligent computing. *Heat Transfer Asian Research.* 11(12), 1554.

[13] Basiri Parsa, Amir & Hayat, Tasawar. (2013). MHD Boundary-Layer Flow over a Stretching Surface with Internal Heat Generation or Absorption. *Heat Transfer Asian Research.* 42, 21054.

[14] Ata A. Servati V., Koroush Javaherdeh, Hamid Reza Ashorynejad. (2014). Magnetic field effects on force convection flow of a nanofluid in a channel partially filled with porous media using Lattice Boltzmann Method, *Advanced Powder Technology.* 25, 666-675,

[15] Waini. I., Ishak. A. and Pop. L. (2022). Symmetrical solutions of hybrid nanofluid stagnation-point flow in a porous medium. *International Communications in Heat and Mass Transfer.*130, 105804.

[16] Mabood. F., Ashwinkumar. G. P. and Sandeep. N. (2020). Effect of nonlinear radiation on 3D unsteady MHD stagnancy flow of hybrid nanofluid. *International Journal of Ambient Energy*. 56, 1-11.

[17] Naqvi. S. M. R. S., Muhammad. T., Saleem. S. and Kim. H. M. (2021). Significance of non-uniform heat generation/absorption in hydromagnetic flow of nanofluid due to stretching/shrinking disk. *Physica A: Statistical Mechanics and its Applications*. 553, 123970.

[18] Zainal. N. A., Nazar. R., Naganthran, K. and Po. I. (2020). Unsteady three-dimensional MHD non-axisymmetric Homann stagnation point flow of a hybrid nanofluid with stability analysis. *Mathematics*. 8(5), 784.

[19] Yashkun. U., Zaimi. K, Bakar. N. A. A., Ishak. A. and Pop. I. (2020). MHD hybrid nanofluid flow over a permeable stretching/shrinking sheet with thermal radiation effect. *International Journal of Numerical Methods for Heat & Fluid Flow*. 22, 8234.

[20] Khan. A. and Anwar. S. and Tassaddiq. A. and Gul. T. Bio-convective and Chemically Reactive Hybrid Nanofluid Flow Upon a Thin Stirring Needle with Viscous Dissipation (2021). *International Communications in Heat and Mass Transfer*. 131, 105843.

[21] Aziz. A., Jamshed. W., Aziz. T., Bahaidarah. H. and Rehman. K. (2021). Entropy analysis of Powell–Eyring hybrid nanofluid including effect of linear thermal radiation and viscous dissipation. *Journal of Thermal Analysis and Calorimetry*. 143(2), 1331-1343.

[22] Yan. L., Dero. S., Khan. I., Mari. I. A., Baleanu. D., Nisar. K. S. and Abdo H. S. (2020). Dual solutions and stability analysis of magnetized hybrid nanofluid with joule heating and multiple slip conditions. *Processes*. 8(3), 332.

[23] Khashi'ie. N. S., Arifin. N. M., Nazar.R., Hafidzuddin. E. H., Wahi. N. and Pop. I. (2020). Magnetohydrodynamics (MHD) axisymmetric flow and heat transfer of a hybrid nanofluid past a radially permeable stretching/shrinking sheet with Joule heating. *Chinese Journal of Physics*. 64, 251-263.

[24] Khan.U.„ Zaib.A., Bakar.S.B., Roy.N.A., Ishak. N.,(2021). Buoyancy effect on the stagnation point flow of a hybrid nanofluid toward a vertical plate in a saturated porous medium. *Case Studies in Thermal Engineering*. 27, 101342.

[25] Mustafa. J., Alqaed. S. and Sharifpur. M. (2022). Evaluation of energy efficiency, visualized energy, and production of environmental pollutants of a solar flat plate collector containing hybrid nanofluid. *Sustainable Energy Technologies and Assessments*. 53, 102399.

[26] Xia WF, Hafeez MU, Khan MI, Shah NA, Chung JD. Entropy optimized dissipative flow of hybrid nanofluid in the presence of non-linear thermal radiation and Joule heating. (2021). *Sustainable Energy Technologies and Assessments.* 23, 8352987.

[27] Hayat. T., Muhammad K.,. Alsaedi.A., Asghar.S., (2018). Numerical study for melting heat transfer and homogeneous-heterogeneous reactions in flow involving carbon nanotubes. *Results in Physics*. 8, 415-421.

[28] kumar, Pradhan & Misra, Ashok & Mishra, Saroj. (2021). Analysis of Heat and Mass Transfer on Nano Fluid over a Linear Stretching Sheet with the Effect of Electrification. 56, 102-399.

[29] Hayat.T.,Saif. R.S., Ellahi.R., Muhammad. T., Alsaedi. A., (2018). Simultaneous effects of melting heat and internal heat generation in stagnation point flow of Jeffrey fluid towards a nonlinear stretching surface with variable thicknes. *Int. J. Therm. Sci.* 132, 344–354.

[30] Hayat. T., Muhammad. T., Shehzad. S. A. and Alsaedi. A. (2017). An analytical solution for magnetohydrodynamic Oldroyd-B nanofluid flow induced by a stretching sheet with heat generation/absorption. *International Journal of Thermal Sciences.* 111, 274-288.

[31] Hussain. Z. (2022). Heat transfer through temperature dependent viscosity hybrid nanofluid subject to homogeneous-heterogeneous reactions and melting condition: A comparative study. *Physica Scripta.* 23, 23124.

[32] Yousefi. M., Dinarvan. S., Yazdi. M. E. and Po. I. (2018). Stagnation-point flow of an aqueous titania-copper hybrid nanofluid toward a wavy cylinder. *International Journal of Numerical Methods for Heat & Fluid Flow.* 23, 835-987.

[33] Nadeem. M., Siddique. I., Awrejcewicz. J., and Bilal. M., (2022). Numerical analysis of a second-grade fuzzy hybrid nanofluid flow and heat transfer over a permeable stretching/shrinking sheet. *Scientific Reports.* 12(1), 1-17.

[34] Rostami. Nademi. M., Dinarvand. S. and Pop.L., (2018) ."Dual solutions for mixed convective stagnation-point flow of an aqueous silica–alumina hybrid nanofluid." *Chinese journal of physics.* 56(5) , 2465-2478.

[35] Waini. I., Ishak. A. and Pop. L. (2022). Symmetrical solutions of hybrid nanofluid stagnation-point flow in a porous medium. *International Communications in Heat and Mass Transfer.*130, 105804.

[36] Megahed. A. M., Reddy. M. G. and Abbas. W. (2021). Modeling of MHD fluid flow over an unsteady stretching sheet with thermal radiation, variable fluid properties and heat flux. *Mathematics and Computers in Simulation.* 185, 583-593.

[37] Arafa. A. M., Sameh. E., Ahmed. M. and Allan. M. (2022). Peristaltic flow of non-homogeneous nanofluids through variable porosity and heat generating porous media with viscous dissipation: Entropy analyses. *Case Studies in Thermal Engineering.* 32, 101882.

[38] Sabi. Z., Akhtar. R., Zhiyu. Z., Umar. M., Imran A., Wahab.H. A. and Raja, M. A. Z. (2019). A computational analysis of two-phase casson nanofluid passing a stretching sheet using chemical reactions and gyrotactic microorganisms. *Mathematical Problems in Engineering.* (4), 1-12.

[39] Johnson. A. B. & Olajuwon. I., (2022). Impact of radiation and heat generation/absorption in a Walters' B fluid through a porous medium with thermal and thermo diffusion in the presence of chemical reaction. *International Journal of Modelling and Simulation.* 14, 8207-8220.

[40] Chu. Y. M., Bashir. S., Ramzan. M. and Malik. M. Y. (2022). Model-based comparative study of magnetohydrodynamics unsteady hybrid nanofluid flow between two infinite parallel plates with particle shape effects. *Mathematical Methods in the Applied Sciences.* 21(1), 101-220.

[41] Chu.Y. M., Khan, U., Zaib. A., Shah. S. H. A. M. and Marin. M. (2020). Numerical and computer simulations of cross-flow in the streamwise direction through a moving surface comprising the significant impacts of viscous dissipation and magnetic fields: stability analysis and dual solutions. *Mathematical Problems in Engineering.* 62(1), 1-11.

[42] Saleem. S., Nadeem.S., Rashidi, M. M. and Raju, C. S. K. (2019). An optimal analysis of radiated nanomaterial flow with viscous dissipation and heat source. *Microsystem Technologies.* 25(2), 683-689.

[43] Tahar. T., Hakan F., Öztop.A. and Ali J., Chamkha. (2020). Natural convection and entropy production in hybrid nanofluid filled-annular elliptical cavity with internal heat generation or absorption. *Thermal Science and Engineering Progress.* 19 ,100605.

[44] Muneerah A. N., Hafeez. A., Khalid. A., Aldhafeeri. A. (2022). Multiple solutions of melting heat transfer of MHD hybrid based nanofluid flow influenced by heat generation/absorption, *Case Studies in Thermal Engineering.* 35, 101-988.

[45] Safdar. R., Jawad. M., Hussain. S., Imran. M., Akgül. A. and Jamshed. W. (2022). Thermal radiative mixed convection flow of MHD Maxwell nanofluid: Implementation of buongiorno's model. *Chinese Journal of Physics.* 77, 1465-1478.

[46] Khan. A. and Anwar. S. and Tassaddiq. A. and Gul. T. Bio-convective and Chemically Reactive Hybrid Nanofluid Flow Upon a Thin Stirring Needle with Viscous Dissipation. (2021). *International Communications in Heat and Mass Transfer.* 131, 105843.

[47] Abbas. N., Nadeem. S, Saleem. A., Malik. M., Y. Issakhov. A. and Alharbi. F. M. (2021). Models base study of inclined MHD of hybrid nanofluid flow over nonlinear stretching cylinder. *Chinese Journal of Physics.* 69, 109-117.

[48] Muhammad. K., Abdelmohsen. S. A., Abdelbacki. A. M. and Ahmed. B. (2022). Darcy-Forchheimer flow of hybrid nanofluid subject to melting heat: A comparative numerical study via shooting method. *International Communications in Heat and Mass Transfer.* 135, 106160.

[49] Zainal. N. A., Nazar. R., Naganthran, K. and Po. I. (2020). Unsteady three-dimensional MHD non-axisymmetric Homann stagnation point flow of a hybrid nanofluid with stability analysis. *Mathematics.* 8(5), 784.

[50] Muneeshwaran. M., Srinivasan. G., Muthukumar. P. and Wang. C. C. (2021). Role of hybrid-nanofluid in heat transfer enhancement – A review. *International Communications in Heat and Mass Transfer.* 125 ,105341.

[51] Khan. M. R., Mao. S.. Deebani. W. and Elsiddie. A. M. (2022). Numerical analysis of heat transfer and friction drag relating to the effect of Joule heating, viscous dissipation and heat generation/absorption in aligned MHD slip flow of a nanofluid. *International Communications in Heat and Mass Transfer.* 131, 105843.

[52] Ali. B., Shafiq. A., Manan. A., Wakif. A and Hussain, S. (2022). Bioconvection: Significance of mixed convection and mhd on dynamics of Casson nanofluid in the stagnation point of rotating sphere via finite element simulation. *Mathematics and Computers in Simulation.* 194, 254-268.

[53] Chu. Y. M., Bashir. S., Ramzan. M. and Malik. M. Y. (2022). Model-based comparative study of magnetohydrodynamics unsteady hybrid nanofluid flow between two infinite parallel plates with particle shape effects. *Mathematical Methods in the Applied Sciences.* 21(1), 101-220.

[54] Waini. I., Ishak. A. and Pop. L. (2022). Symmetrical solutions of hybrid nanofluid stagnation-point flow in a porous medium. *International Communications in Heat and Mass Transfer.*130, 105804.

[55] Nadeem. M., Siddique. I., Awrejcewicz. J., and Bilal. M., (2022). Numerical analysis of a second-grade fuzzy hybrid nanofluid flow and heat transfer over a permeable stretching/shrinking sheet. *Scientific Reports.* 12(1), 1-17.

[56] Jyothi. A. M., Kumar. V. R. S. Madhukesh. J. K., Prasannakumara. B. C. and Ramesh. G. K. (2021). Squeezing flow of Casson hybrid nanofluid between parallel plates with a heat source or sink and thermophoretic particle deposition. *Heat Transfer*. 50(7), 7139-7156.

[57] Sulochana C., and Mahalaxmi. B. (2022). Thermophoresis and Brownian motion effects on Williamson nanofluid flow past a stretching surface with thermal radiation and chemical reaction. *Heat Transfer*. 51(3), 2761-2779.

[58] Salam. S. O., Fatunmbi. E. O. and Okoya. S. S., (2021). MHD heat and mass transport of Maxwell Arrhenius kinetic nanofluid flow over stretching surface with nonlinear variable properties. *Results in Chemistry*. 3, 100125.

[59] Rostami. Nademi. M., Dinarvand. S. and Pop.L., (2018) ."Dual solutions for mixed convective stagnation-point flow of an aqueous silica–alumina hybrid nanofluid." *Chinese journal of physics*. 56(5) , 2465-2478.

[60] Yaseen. M., Rawat. S. K., Shafiq. A., Kumar. M. and Nonlaopon. K. (2022). Analysis of heat transfer of mono and hybrid nanofluid flow between two parallel plates in a Darcy porous medium with thermal radiation and heat generation/absorption. Symmetry. 14(9), 1943.

[61] Hayat. T., Muhammad. T., Shehzad. S. A. and Alsaedi. A. (2017). An analytical solution for magnetohydrodynamic Oldroyd-B nanofluid flow induced by a stretching sheet with heat generation/absorption. *International Journal of Thermal Sciences*. 111, 274-288.

[62] Hussain. Z. (2022). Heat transfer through temperature dependent viscosity hybrid nanofluid subject to homogeneous-heterogeneous reactions and melting condition: A comparative study. *Physica Scripta.* 23, 23124.

[63] Neethu. T. S., Sabu. A. S., Mathew. A., Wakif. A. and Areekara. S. (2021). Multiple linear regression on bioconvective MHD hybrid nanofluid flow past an exponential stretching sheet with radiation and dissipation effects. *International Communications in Heat and Mass Transfer.* 135, 106115.

[64] Wahid. N. S., Arifin. N. M., Pop. I., Bachok. N. and Hafidzuddin. M. E. H. (2022). MHD stagnation-point flow of nanofluid due to a shrinking sheet with melting, viscous dissipation and Joule heating effects. *Alexandria Engineering Journal.* 61(12), 12661-12672.

[65] Salami. S. O., Fatunmbi. E. O. and Okoya. S. S., (2021). MHD heat and mass transport of Maxwell Arrhenius kinetic nanofluid flow over stretching surface with nonlinear variable properties. Results in Chemistry. 3, 100125.

[66] Mahdi. D. and Kalaiselvam. S. (2014). Experimental analysis of hybrid nanofluid as a coolant. Procedia engineering. 97 , 1667-1675.

[67] Kayalvizhi. J. and Kumar. V. A. G. (2022). Entropy Analysis of EMHD Hybrid Nanofluid Stagnation Point Flow over a Porous Stretching Sheet with Melting Heat Transfer in the Presence of Thermal Radiation. 15, 8317.

[68] Naqvi.N., Muhammad. T., Saleem. S. and Kim. H. M., (2020). Significance of non-uniform heat generation/absorption in hydromagnetic flow of nanofluid due to stretching/shrinking disk. *Physica A: Statistical Mechanics and its Applications.* 553, 123970.

[69] Vijatha. M., and Reddy. A.S., (2022). Comparative analysis on magnetohydrodynamic flow of non-Newtonian hybrid nanofluid over a stretching cylinder: Entropy generation. *Proceedings of the Institution of Mechanical Engineer. Part E: Journal of Process Mechanical Engineering.* 23, 33-23.

[70] Azam. M., Mabood. F., Xu. T., Waly. M. and Tlili. I. (2020). Entropy optimized radiative heat transportation in axisymmetric flow of Williamson nanofluid with activation energy. *Results in Physics.* 19, 103576.

[71] Johnson. A. B. & Olajuwon. I., (2022). Impact of radiation and heat generation/absorption in a Walters' B fluid through a porous medium with thermal and thermo diffusion in the presence of chemical reaction. International Journal of Modelling and Simulation. 14, 8207-8220.

[72] Sulochana C., and Mahalaxmi. B. (2022). Thermophoresis and Brownian motion effects on Williamson nanofluid flow past a stretching surface with thermal radiation and chemical reaction. *Heat Transfer.* 51(3), 2761-2779.

[73] Soomro. F. A., Usman. M., El-Sapa. S., Hamid. M. and Haq. R. U. (2022). Numerical study of heat transfer performance of MHD hybrid nanofluid flow over inclined surface. *Archive of Applied Mechanics.* 92(9), 2757-2765.

[74] Khan. A. and Anwar. S. and Tassaddiq. A. and Gul. T. Bio-convective and Chemically Reactive Hybrid Nanofluid Flow Upon a Thin Stirring Needle with Viscous Dissipation (2021). *International Communications in Heat and Mass Transfer.* 131, 105843.

[75] Gangadhar. K., Subba. R. M. V., Surekha. P. and Kannan. T. (2022). Shape effects on 3D MHD micropolar hybrid nanofluid with Joule Heating. *International Journal of Ambient Energy.* 43(1), 8428-8437.

[76] Zainal. N. A., Nazar. R., Naganthran, K. and Po. I. (2020). Unsteady three-dimensional MHD non-axisymmetric Homann stagnation point flow of a hybrid nanofluid with stability analysis. *Mathematics.* 8(5), 784.

[77] Jyoth. A. M., Kumar. V. R. S. Madhukesh. J. K., Prasannakumara. B. C. and Ramesh. G. K. (2021). Squeezing flow of Casson hybrid nanofluid between parallel plates with a heat source or sink and thermophoretic particle deposition. *Heat Transfer.* 50(7), 7139-7156.

[78] Sulochana C., and Mahalaxmi. B. (2022). Thermophoresis and Brownian motion effects on Williamson nanofluid flow past a stretching surface with thermal radiation and chemical reaction. *Heat Transfer.* 51(3), 2761-2779.

[79] Khan.U.„ Zaib.A., Bakar.S.B., Roy.N.A., Ishak. N.,(2021). Buoyancy effect on the stagnation point flow of a hybrid nanofluid toward a vertical plate in a saturated porous medium. *Case Studies in Thermal Engineering.* 27, 101342.

[80] Mustafa. J., Alqaed. S. and Sharifpur. M. (2022). Evaluation of energy efficiency, visualized energy, and production of environmental pollutants of a solar flat plate collec-

tor containing hybrid nanofluid. *Sustainable Energy Technologies and Assessments*. 53, 102399.

[81] Ali. R, Khan. M. R., Abidi. A., Rasheed, S. and Galal. A. M. (2021). Application of PEST and PEHF in magneto-Williamson nanofluid depending on the suction/injection. *Case Studies in Thermal Engineering*. 27, 101329.

[82] Yang. L. Ji. W., Mao, M. and Huang, J. N. (2020). An updated review on the properties, fabrication and application of hybrid-nanofluids along with their environmental effects. *Journal of Cleaner Production*. 257, 120408.

[83] Khashi'ie. N. S., Arifin. N. M., Nazar.R., Hafidzuddin. E. H., Wahi. N. and Pop. I. (2020). Magnetohydrodynamics (MHD) axisymmetric flow and heat transfer of a hybrid nanofluid past a radially permeable stretching/shrinking sheet with Joule heating. *Chinese Journal of Physics*. 64, 251-263.

[84] Wahid. N. S., Arifin. N. M., Pop. I., Bachok. N. and Hafidzuddin. M. E. H. (2022). MHD stagnation-point flow of nanofluid due to a shrinking sheet with melting, viscous dissipation and Joule heating effects. *Alexandria Engineering Journal.* 61(12), 12661-12672.

[85] Wahid.., Pop. I., Bachok. N. and Hafidzuddin. M. E. H. (2021). Nanofluid due to a shrinking sheet with melting, viscous dissipation. *Alexandria Engineering Journal.* 61(12), 12661-12662.

[86] Khan. A. and Anwar. S. and Tassaddiq. A. and Gul. T. Bio-convective and Chemically Reactive Hybrid Nanofluid Flow Upon a Thin Stirring Needle with Viscous Dissipation (2022). International Communications in Heat and Mass Transfer. 131, 105843.

[87] Eid. M. R. and Nafe. M. A. (2022). Thermal conductivity variation and heat generation effects on magneto-hybrid nanofluid flow in a porous medium with slip condition. *Waves in Random and Complex Media*. 32(3), 1103-1127.

[88] Arshad. M, Hussain. A, Hassan. A., Shah. S. A. G. A., Elkotb. M. A., Gouadria. S. and Galal. A. M. (2022). Heat and mass transfer analysis above an unsteady infinite porous surface with chemical reaction. *Case Studies in Thermal Engineering.* 36, 102140.

[89] Hayat. T., Muhammad K.,. Alsaedi.A., Asghar.S., (2018). Numerical study for melting heat transfer and homogeneous-heterogeneous reactions in flow involving carbon nanotubes. *Results in Physics.* 8, 415-421.

[90] Song. Y. Q., Hamid. A., Sun. T. C., Kha. M. I., Qayyum. S., Kumar. R. N. and Chinram. R. (2022). Unsteady mixed convection flow of magneto-Williamson nanofluid due to stretched cylinder with significant non-uniform heat source/sink features. *Alexandria Engineering Journal.* 61(1), 195-206.

[91] Kakar.N., Khalid.M., Amnah S., Johani.A., Nawa Alshammari and Ilyas Khan. (2022). Melting heat transfer of a magnetized water-based hybrid nanofluid flow past over a stretching/shrinking wedge. *Case Studies in Thermal Engineering.* 30, 101-674.

[92] Kayalvizhi. J. and Kumar. V. A. G. (2022). Entropy Analysis of EMHD Hybrid Nanofluid Stagnation Point Flow over a Porous Stretching Sheet with Melting Heat Transfer in the Presence of Thermal Radiation. 15, 8317.

[93] Labib. M. N., Nine. M. J., Afrianto. H., Chung. H. and Jeong. H. (2013). Numerical investigation on effect of base fluids and hybrid nanofluid in forced convective heat transfer. *International Journal of Thermal Sciences.* 71, 163-171.

[94] Muhammad. K., Abdelmohsen. S. A., Abdelbacki. A. M. and Ahmed. B. (2022). Darcy-Forchheimer flow of hybrid nanofluid subject to melting heat: A comparative numerical study via shooting method. *International Communications in Heat and Mass Transfer.* 135, 106160.

[95] Huminic. G., Huminic. A., Dumitrache. F., Fleacă. C. and Morjan. I. (2020). Study of the thermal conductivity of hybrid nanofluids: Recent research and experimental study. *Powder Technology.* 367, 347-357.

[96] Nalivela. N. R., Vempati. S. R., Ravindra R. B. and Reddy. Y. D. (2022). Viscous dissipation and thermal radiation impact on MHD mass transfer natural convective flow over a stretching sheet. *Journal of Materials Research and Technology.* 9(1), 421-432.

[97] Mah. D. and Kalaiselvam. S. (2014). Experimental analysis of hybrid nanofluid as a coolant. *Procedia engineering.* 97 , 1667-1675.

[98] Yousefi. M., Dinarvan. S., Yazdi. M. E. and Po. I. (2018). Stagnation-point flow of an aqueous titania-copper hybrid nanofluid toward a wavy cylinder. *International Journal of Numerical Methods for Heat & Fluid Flow.* 71, 163-173.

[99] Nadeem. M., Siddique. I., Awrejcewicz. J., and Bilal. M., (2022). Numerical analysis of a second-grade fuzzy hybrid nanofluid flow and heat transfer over a permeable stretching/shrinking sheet. *Scientific Reports.* 12(1), 1-17.

[100] Rostami. Nademi. M., Dinarvand. S. and Pop.L., (2018) ."Dual solutions for mixed convective stagnation-point flow of an aqueous silica–alumina hybrid nanofluid." *Chinese journal of physics.* 56(5) , 2465-2478.

[101] Zainal. N. A., Nazar. R., Naganthran, K. and Po. I. (2021). Unsteady three-dimensional MHD non-axisymmetric Homann stagnation point flow of a hybrid nanofluid with stability analysis. *Mathematics.* 8(5), 784.

[102] Emad. M. H., Alirezaie. A. and Toghraie. D. (2021). Thermal conductivity of ethylene glycol based nanofluids containing hybrid nanoparticles its price-performance analysis for energy management. *Journal of Materials Research and Technology.* 14, 1754-1760.

[103] Waini. I., Ishak. A. and Pop. L. (2022). Symmetrical solutions of hybrid nanofluid stagnation-point flow in a porous medium. *International Communications in Heat and Mass Transfer.*130, 105804.

[104] Adigun. J. A., Adeniyan. A., and Abiala. I. O. (2021). Stagnation point MHD slip-flow of viscoelastic nanomaterial over a stretched inclined cylindrical surface in a porous medium with dual stratification. *International Communications in Heat and Mass Transfer.* 126, 105479.

[105] Adigun. N., Mohyud-Din. S. T. and Hassan. S. M. (2016). Flow and heat transfer of nanofluid in an asymmetric channel with expanding and contracting walls suspended by carbon nanotubes: a numerical investigation. *Aerospace Science and Technology*. 48, 53-60.

[106] Zainal. T. A., Mabood. F., Prasannakumara.B. C. and Sarris. I. E. (2021). Magneto-bioconvection flow of Williamson nanofluid over an inclined plate with gyrotactic microorganisms and entropy generation. *Fluids.* 6(3), 109.

[107] Alphonsa. R, Khan. M. R., Abidi. A., Rasheed, S. and Galal. A. M. (2021). Application of PEST and PEHF in magneto-Williamson nanofluid depending on the suction/injection. *Case Studies in Thermal Engineering*. 27, 101329.

[108] Abbas. N., Nadeem. S, Saleem. A., Malik. M., Y. Issakhov. A. and Alharbi. F. M. (2021). Models base study of inclined MHD of hybrid nanofluid flow over nonlinear stretching cylinder. *Chinese Journal of Physics*. 69, 109-117.

[109] Zainal. N. A., Nazar. R., Naganthran, K. and Po. I. (2020). steady MHD non-axisymmetric Homann stagnation point flow of a hybrid nanofluid with stability analysis. *Mathematics*. 8(5), 876.

[110] Yahaya. R. I., Arifin. N. M., Pop. I., Ali. F. M. and Isa. S. S. P. M. (2022). Dual solutions for MHD hybrid nanofluid stagnation point flow due to a radially shrinking disk with convective boundary condition. *International Journal of Numerical Methods for Heat and Fluid Flow.* 33, 66-80.

[111] Abbas., Bhuvaneswari. M., Sivasankaran. S. and Saravanan. K. (2022). Nanofluid flow with activation energy and heat generation under slip boundary condition with convective heat and mass transfer. Materials. 5, 959-967.

[112] Zainal. L., Dero. S., Khan. I., Mari. I. A., Baleanu. D., Nisar. K. S. and Abdo H. S. (2020). Dual solutions and stability analysis of magnetized hybrid nanofluid with joule heating and multiple slip conditions. 8(3), 332.

[113] Farooq. M., Doostani. A., Izadpanahi. E. and Chamkha. A. J. (2020). Conjugate natural convection flow of hybrid nanofluid in a square cavity. *Journal of Thermal Analysis and Calorimetry.* 139(3), 2321-2336.

[114] Emad .M. H., Alirezaie. A. and Toghraie. D. (2021). Thermal conductivity of ethylene glycol based nanofluids containing hybrid nanoparticles its price-performance analysis for energy management. *Journal of Materials Research and Technology.* 14, 1754-1760.

[115] Roy. N. C. and Pop. I. (2022). Heat and mass transfer of a hybrid nanofluid flow with binary chemical reaction over a permeable shrinking surface. *Chinese Journal of Physics.* 76, 283-298.

[116] Yaseen. M., Rawat. S. K., Shafiq. A., Kumar. M. and Nonlaopon. K. (2022). Analysis of heat transfer of mono and hybrid nanofluid flow between two parallel plates in a Darcy porous medium with thermal radiation and heat generation/absorption. *Symmetry.* 14(9), 1943.

[117] Aziz. A. S., Ramesh. K., Oudina. F. M. and Abidi, A. (2021). Numerical investigation of the stagnation point flow of radiative magnetomicropolar liquid past a heated porous stretching sheet. *Journal of Thermal Analysis and Calorimetry.* 126, 105479.

[118] Venkateswarlu.A., Bhumavarapu.S. and Narayana. S.,W(2021).Cu-Al2O3/H2O hybrid nanofluid flow past a porous stretching sheet due to temperatue-dependent viscosity and viscous dissipation. *Heat Transfer.* 50(1), 432-449.

[119] Zainal. N. S., Arifin. N. M., Pop. I., Bachok. N. and Hafidzuddin. M. E. H. (2022). MHD stagnation-point flow of nanofluid due to a shrinking sheet with melting, viscous dissipation and Joule heating effects. *Alexandria Engineering Journal.* 61(12), 12661-12672.

[120] Lund. L. A., Omar. Z., Khan. I., Seikh, A. H., Sherif. E. S. M., and Nisar. K. S. (2020). Stability analysis and multiple solution nanofluid contains hybrid nanomaterials over a shrinking surface in the presence of viscous dissipation. *Journal of Materials Research and Technology.* 9(1), 421-432.

[121] Famakinwa. A. and Malik. M. Y. (2021). MHD nanofluid flow over stretching cylinder with convective boundary conditions and Nield conditions in the presence of gyrotactic swimming microorganism: A biomathematical model. *International Communications in Heat and Mass Transfer*. 126, 105425.

[122] Hayat. R., Jawad. M., Hussain. S., Imran. M., Akgül. A. and Jamshed. W. (2022). Thermal radiative mixed convection flow of MHD Maxwell nanofluid: Implementation of buongiorno's model. *Chinese Journal of Physics*. 77, 1465-1478.

[123] Tayebi. T., Hakan F., Öztop.A. and Ali J., Chamkha. (2020) Natural convection and entropy production in hybrid nanofluid filled-annular elliptical cavity with internal heat generation or absorption. *Thermal Science and Engineering Progress*. 19 ,100605.

[124] Yaseen. M., Rawat. S. K., Shafiq. A., Kumar. M. and Nonlaopon. K. (2022). Analysis of heat transfer of mono and hybrid nanofluid flow between two parallel plates in a Darcy porous medium with thermal radiation and heat generation/absorption. *Symmetry*. 14(9), 1943.

[125] Naqvi.N., Muhammad. T., Saleem. S. and Kim. H. M., (2020). Significance of non-uniform heat generation/absorption in hydromagnetic flow of nanofluid due to stretching/shrinking disk. *Physica A: Statistical Mechanics and its Applications*. 553, 123970.

[126] Shoaib. M., Raja M. A. Z., Sabir. M. T., Nisar, K. S., Jamshed. W., Felemban. B. F. and Yahia. I. S. (2021). MHD hybrid nanofluid flow due to rotating disk with heat absorption and thermal slip effects: an application of intelligent computing. *Coatings*, 11(12). 1554.

[127] Zainal. L., Dero. S., Khan. I., Mari. I. A., Baleanu. D., Nisar. K. S. and Abdo H. S. (2020). Dual solutions and stability analysis of magnetized hybrid nanofluid with joule heating and multiple slip conditions. *Processes*. 8(3), 332.

[128] Jyoth. A. M., Kumar. V. R. S. Madhukesh. J. K., Prasannakumara. B. C. and Ramesh. G. K. (2021). Squeezing flow of Casson hybrid nanofluid between parallel plates with a heat source or sink and thermophoretic particle deposition. *Heat Transfer*. 50(7), 7139-7156.

[129] Sulochana. R., Jawad. M., Hussain. S., Imran. M., Akgül. A. and Jamshed. W. (2022). Thermal radiative mixed convection flow of MHD Maxwell nanofluid: Implementation of buongiorno's model. *Chinese Journal of Physics*. 77, 1465-1478.

[130] Khan.U.„ Zaib.A., Bakar.S.B., Roy.N.A. and Ishak. N.,(2021). Buoyancy effect on the stagnation point flow of a hybrid nanofluid toward a vertical plate in a saturated porous medium. *Case Studies in Thermal Engineering.* 27, 101342.

[131] Krishna. M. V. (2022). Chemical reaction, heat absorption and Newtonian heating on MHD free convective Casson hybrid nanofluids past an infinite oscillating vertical porous plate. *International Communications in Heat and Mass Transfe*r. 138, 106-327.

[132] Hameed. N., Noeiaghdam. S., Khan. W., Pimpunchat. B., Fernandez-Gamiz. U., Khan. M. S. and Rehman. A. (2022). Analytical analysis of the magnetic field, heat generation and absorption, viscous dissipation on couple stress casson hybrid nano fluid over a nonlinear stretching surface. *Results in Engineering.* 16, 100601.

[133] Krishna. M. V. (2022). Newtonian heating on MHD free convective Casson hybrid nanofluids past an infinite oscillating vertical porous plate. *International Communications in Heat and Mass Transfer.* 138, 106-327.

[134] Unyong. B., Vadivel. R., Govindaraju. M., Anbuvithya. R. and Gunasekaran. N. (2022). Entropy analysis for ethylene glycol hybrid nanofluid flow with elastic deformation, radiation, non-uniform heat generation/absorption. and inclined Lorentz force effects. *Case Studies in Thermal Engineering.* 30, 101639.

[135] Whitaker, S. (1977). *Fundamental Principles of Heat Transfer.* (1st ed.) United Kingdom.: Elsevier Science and Technology Books.

[136] Durst, F. (2008). *Fluid Mechanics: An Introduction to the Theory of Fluid flows.* (3rd ed.) Germany.: Springer Berlin Heidelberg.

[137] McDonald, A. T., Fox, R. W., and Pritchard, P. J. (2009). *Introduction to fluid mechanics.* (8th ed.) India.: Wiley

[138] Musharafa (2021). *Lie group study of some non-newtanion fluid flow with heat transfer anaylsis.* MS Thesis pages 30-34, University of Engineering and Technology, Lahore.

[139] Muhammad, T. Hayat, A. Alsaedi, (2021), Numerical study for melting heat in dissipative flow of hybrid nanofluid over a variable thicked surface. *International Communications in Heat and Mass Transfer.* 121, 10735-1933.